Salt/Gila River Sediment Transport Modeling

Maricopa County

Technical Support Data Notebook

Contract Number: FCD 2012C020 WA3

Prepared for:

Flood Control District of Maricopa County
2801 W. Durango Street
Phoenix, AZ 85009

Prepared by:

WEST Consultants, Inc.
8950 S. 52nd Street, Suite 210
Tempe, Arizona 85284

February 2016

Registered Professional Engineer (Civil)
CERTIFICATE NO.
41980
BRIAN THOMAS
WAHLIN
Date Signed 02-03-2016
ARIZONA, U.S.A.

Expires 3/31/2017

Table of Contents

List of Figures v

List of Tables viii

List of Appendices ix

1 Introduction 1

1.1 Purpose of the Study 1

1.2 Authority for the Study 1

1.3 Location of the Study Reach 2

1.4 Methodology used for Hydrology, Hydraulics, and Sediment Transport 4

1.5 Acknowledgments 4

1.6 Study Results 5

2 FEMA Forms 6

3 Surveying and Mapping Information 7

3.1 Digital Projection Information 8

3.2 Field Survey Information 8

4 Hydrology 9

4.1 Effective Hydrology for Base Hydraulic Model 9

4.2 Historic Flow Records 9

4.2.1 Historic Flows on the Lower Salt River at the Upstream End of the Study Reach 13

4.2.2 Historic Flows on the Upper Gila River at the Confluence with the Lower Salt River 13

4.2.3 Historic Flows on the Agua Fria River at the Confluence with the Lower Gila River 14

4.2.4 Historic Flows on Waterman Wash at the Confluence with the Lower Gila River 16

4.3 1% Annual Chance Flood Hydrographs 17

5 Hydraulics 20

5.1 Method Description for HEC-RAS Base Hydraulic Model 20

5.1.1 Lower Salt FDS (RM 203.08 – RM 217.71) 20

5.1.2 Tres Rios North Levee PMR (RM 197.92 – RM 203.08) 20

5.1.3 Gap area from 2008 Gillespie Topography (RM 195.16 - RM 197.9) 21

5.1.4 Lower Gila FDS (RM 147.44 - RM 195.09) 21

5.1.5 Assembling the Base Hydraulics Model for Existing Conditions 22

5.1.6 Assembling the Base Hydraulics Model for Proposed Conditions 23

5.2 Work Study Maps 23
5.3 Parameter Estimation 24
5.3.1 Roughness Coefficients 24
5.3.2 Expansion and Contraction Coefficients 25
5.4 Cross-Section Descriptions 26
5.5 Modeling Considerations 26
5.5.1 Hydraulic Jump and Drop Analysis 26
5.5.2 Bridges and Culverts 27
5.5.3 Levees and Dikes 27
5.5.4 Non-Levee Embankments 28
5.5.5 Islands and Flow Splits 29
5.5.6 Ineffective Flow Areas 29
5.5.7 Supercritical Flow 29
5.5.8 Sand and Gravel Operations 29
5.6 Floodway Modeling 29
5.7 Hydraulic Issues Encountered During the Study 30
5.7.1 Special Issues and Solutions 30
5.7.2 Modeling Warning and Error Messages 30
5.8 HEC-6T Base Hydraulic Model 30
5.9 Calibration 32
5.10 Final Results 32
5.10.1 Hydraulic Analysis Results 32
5.10.2 Verification or Comparison of Results 33
6 Erosion, Sediment Transport, and Geomorphic Analysis 36
6.1 Previous Sediment Transport Modeling Studies 36
6.1.1 Rio Salado Low Flow Channel Design (RM 210.64 – RM 217.95) 36
6.1.2 Rio Salado Oeste Sediment Transport Study (RM 202.09 – RM 211.21) 37
6.1.3 Tres Rios North Levee PED (RM 195.16 – RM 203.48) 38
6.1.4 El Rio Watercourse Master Plan (RM 178.61 – 199.07) 39
6.1.5 Gila River Sediment Program (115th Ave – SR85) 40
6.1.6 Agua Fria River Sediment Trend Analysis 41
6.1.7 Waterman Wash Sediment Transport Analysis 42

6.2 Sediment Transport Modeling Data 42
6.2.1 Sediment Transport Model Hydrology 42
6.2.2 Bed Material Sediment Gradations 43
6.2.3 Moveable Bed Boundary Limits 47
6.2.4 Inflow Sediment Loads 47
6.2.5 Selection of the Sediment Transport Function 49
6.3 Development of the Existing Conditions HEC-RAS Sediment Transport Model 49
6.4 Development of the Proposed Conditions HEC-RAS Sediment Transport Model 49
6.5 Calibration of the Existing Conditions HEC-RAS Sediment Transport Model 50
6.5.1 The Calibration Reach 50
6.5.2 Geometric Data for the Calibration Reach 51
6.5.3 Calibration Runs 51
6.5.4 Hydrology and Inflowing Sediment Load for the Calibration Runs 52
6.5.5 Calibration Process 54
6.5.6 Calibration Results for HEC-6T Model 54
6.5.7 Calibration Results for HEC-RAS Sediment Transport Model 58
6.5.8 Spatial Pattern for the Calibration Runs 59
6.5.9 Conclusions from Calibration Runs 60
6.6 Creation of the HEC-6T Sediment Transport Models (Existing and Proposed Conditions) 61
6.7 Sediment Transport Modeling Results 63
6.7.1 Existing Condition Model with Historic Flow Series 63
6.7.2 Proposed Condition Model with Historic Flow Series 74
6.7.3 Existing Condition Model for the 1% Annual Chance Flood Hydrograph 84
6.7.4 Proposed Conditions Model for the 1% Annual Chance Flood Hydrograph 94
6.7.5 Sediment Issues Encountered During the Study 104
6.7.6 Comparison with Previous Sediment Transport Studies 106
7 Draft FIS Data 111
8 References 112

List of Figures

Figure 1-1. Vicinity map for the Salt/Gila sediment transport model 3
Figure 4-1. Locations of flow and sediment inflows (marked by an arrow and number) in the sediment model: 1) Lower Salt at I-10, 2) Upper Gila, 3) Agua Fria, and 4) Waterman Wash 12
Figure 4-2. Historic flow hydrograph for the Lower Salt River and the Upper Gila River (WEST Consultants, Inc., 2002a) 13
Figure 4-3. Original Agua Fria River 1% annual chance flood hydrograph and re-sample hydrograph (note that volume is conserved) 15
Figure 4-4. Historic flow hydrograph for Agua Fria River 15
Figure 4-5. Flood hydrograph series for URS's sediment transport study of Waterman Wash (URS, 2011) 16
Figure 4-6. Historic flow hydrograph for Waterman Wash 17
Figure 4-7. 1% annual chance flood hydrograph for the Agua Fria River downstream of the New River confluence (Kimley-Horn and Associates, 2001) 19
Figure 4-8. 1% annual chance flood hydrograph for Waterman Wash (URS, 2011) 19
Figure 5-1. Project location map showing the two study reaches for Gila River FDS (Stantec, 2014) 22
Figure 5-2. Comparison between the base hydraulic model water surface elevations (1% annual chance) for a portion of the study reach for HEC-RAS and the final adjusted HEC-6T model 31
Figure 5-3. Comparison of 1% annual chance flood water surface elevation profiles between Salt/Gila existing conditions hydraulic model and the original hydraulic models from various past studies 34
Figure 5-4. Comparison of 1% annual chance flood water surface elevation profiles between Salt/Gila existing conditions hydraulic model before IFA/blocked obstruction adjustments at the sand and gravel mines and the original hydraulic models from various past studies 35
Figure 6-1. Sediment sample locations for the Rio Salado Low Flow Channel Design (WEST Consultants, Inc., 2000) 37
Figure 6-2. Sediment sample locations for Rio Salado Oeste (WEST Consultants, Inc., 2002b) 38
Figure 6-3. Summary of gradations for the sediment samples collected on the Lower Gila River (Stantec, 2006) 39
Figure 6-4. Source of bed material samples for Gila River Sediment Program (Stantec, 2009) 40
Figure 6-5. Sediment sample locations for Tres Rios North Levee PED (WEST Consultants, Inc., 2002a), the El Rio Watercourse Master Plan (Stantec, 2006), and the Gila River Sediment Program (Stantec, 2009) 41
Figure 6-6. Bed gradation data for cross-sections between RM 211.64 and RM 217.1 44
Figure 6-7. Bed gradation data for cross-sections between RM 204.87 and RM 211.44 45
Figure 6-8. Bed gradation data for cross-sections between RM 178.61 and RM 204.42 46
Figure 6-9. Locations of sediment inflow (marked by an arrow and number) in the study reach: (1) I-10 Bridge, (2) Upper Gila, (3) Agua Fria and (4) Waterman Wash 48
Figure 6-10. Thalweg profile for the initial and final geometry of the calibration reach 51
Figure 6-11. Upstream boundary (RM 217.95) discharge time series developed using observed data at the Priest Drive gage 53
Figure 6-12. Inflow sediment rating curve at the upstream boundary for the calibration model 53

Figure 6-13. Average bed elevation profile of HEC-6T runs using TMPM and Yang sediment transport function 56
Figure 6-14. Thalweg profile plot for 2000 and 2013 geometries, and for HEC-6T runs using TMPM and Yang functions 56
Figure 6-15. Observed thalweg elevation difference between 2013 and 2000 conditions along the calibration reach 59
Figure 6-16. Erosional-depositional pattern for HEC-6T/HEC-RAS runs using TMPM and Yang transport functions 60
Figure 6-17. Invert profile change at the end of the simulation for the existing conditions HEC-RAS model with historic flow series 66
Figure 6-18. Change in average bed for the cross-section for the existing conditions HEC-RAS model with historic flow series 67
Figure 6-19. Change in average bed for the main channel for the existing conditions HEC-RAS model with historic flow series 68
Figure 6-20. Cumulative total sediment outflow for existing conditions HEC-RAS model with historic flow series 69
Figure 6-21. Invert profile change at the end of the simulation for the existing conditions HEC-6T model with historic flow series 70
Figure 6-22. Change in average bed elevation for the cross-section for the existing conditions HEC-6T model with historic flow series 71
Figure 6-23. Change in average bed elevation for the main channel for the existing conditions HEC-6T model with historic flow series 72
Figure 6-24. Cumulative total sediment outflow for existing conditions HEC-6T model with historic flow series 73
Figure 6-25. Invert profile change at the end of the simulation for the proposed conditions HEC-RAS model with historic flow series 76
Figure 6-26. Change in average bed elevation for the cross-section for the proposed conditions HEC-RAS model with historic flow series 77
Figure 6-27. Change in average bed elevation for the main channel for the proposed conditions HEC-RAS model with historic flow series 78
Figure 6-28. Cumulative total sediment outflow for proposed conditions HEC-RAS model with historic flow series 79
Figure 6-29. Invert profile change at the end of the simulation for the proposed conditions HEC-6T model with historic flow series 80
Figure 6-30. Change in average bed elevation for cross-section for the proposed conditions HEC-6T model with historic flow series 81
Figure 6-31. Change in average bed elevation for main channel for the proposed conditions HEC-6T model with historic flow series 82
Figure 6-32. Cumulative total sediment outflow for proposed conditions HEC-6T model with historic flow series 83
Figure 6-33. Maximum invert profile change for existing conditions HEC-RAS model with 1% annual chance flow series 86

Figure 6-34. Change in the average bed elevation for the entire cross-section for existing conditions HEC-RAS model with 1% annual chance flow series 87
Figure 6-35. Change in the average bed elevation for the main channel for existing conditions HEC-RAS model with 1% annual chance flow series 88
Figure 6-36. Cumulative total sediment outflow for existing conditions HEC-RAS model with 1% annual chance flood hydrograph 89
Figure 6-37. Maximum invert profile change for existing conditions HEC-6T model with 1% annual chance flow series 90
Figure 6-38. Change in the average bed elevation for the entire cross-section for existing conditions HEC-6T model with 1% annual chance flow series 91
Figure 6-39. Change in the average bed elevation for the main channel for existing conditions HEC-6T model with 1% annual chance flow series 92
Figure 6-40. Cumulative total sediment outflow for existing conditions HEC-6T model with 1% annual chance flood hydrograph 93
Figure 6-41. Maximum invert profile change for proposed conditions HEC-RAS model with 1% annual chance flow series 96
Figure 6-42. Change in average bed elevation of the cross-section for proposed conditions HEC-RAS model with 1% annual chance flow series 97
Figure 6-43. Change in average bed elevation of the main channel for proposed conditions HEC-RAS model with 1% annual chance flow series 98
Figure 6-44. Cumulative total sediment outflow for proposed conditions HEC-RAS model with 1% annual chance flood hydrograph 99
Figure 6-45. Maximum invert profile change for proposed conditions HEC-6T model with 1% annual chance flow series 100
Figure 6-46. Change in average bed elevation for cross-section for proposed conditions HEC-6T model with 1% annual chance flow series 101
Figure 6-47. Change in average bed elevation for main channel for proposed conditions HEC-6T model with 1% annual chance flow series 102
Figure 6-48. Cumulative total sediment outflow for proposed conditions HEC-6T model with 1% annual chance flood hydrograph 103
Figure 6-49. Plan view of first set of multiple pits located just downstream of 51st Avenue 105
Figure 6-50. Plan view of second set of multiple pits located downstream of Avondale Boulevard 105
Figure 6-51. Initial and final average bed elevations for the El Rio sediment transport study (Stantec, 2006) 107
Figure 6-52. HEC-6T average bed elevations (main channel) for current study and the Rio Salado Oeste study 108
Figure 6-53. HEC-6T average bed elevations (main channel) for current study and the Tres Rios PED study (downstream end of the reach) 109
Figure 6-54. HEC-6T average bed elevations (main channel) for current study and the Tres Rios PED study (upstream end of the reach) 110

List of Tables

Table 1-1. Summary of sediment transport model results for 1% annual chance flow hydrograph 5
Table 1-2. Summary of sediment transport model results for historic series of flows 5
Table 4-1. 1% annual chance discharges for the Salt/Gila River system 9
Table 4-2. Stream gage information in the study reach 10
Table 4-3. Sequence of flow events and peak flows used to generate historic flood series for both the Agua Fria River and Waterman Wash 14
Table 4-4. Peak flows on the Agua Fria River for various flood events and ratio to the SPF 15
Table 4-5. 1% annual chance flood hydrograph for Lower Salt River and Upper Gila River (Stantec, 2006) 18
Table 5-1. Summary of pit modifications for proposed condition model 24
Table 5-2. Summary of the Manning's *n*-value categories identified in the Lower Salt River FDS (WEST Consultants, Inc., 2015) 25
Table 5-3. Summary of the Manning's *n*-value categories identified in the Lower Gila River FDS (Stantec, 2014) 25
Table 5-4. Bridge data source 28
Table 6-1. Upstream sediment inflow boundary condition (WEST, 2000) 48
Table 6-2. Sediment inflow rating curve for the Upper Gila River (WEST, 2011) 48
Table 6-3. Sediment inflow rating curve for the Agua Fria River (Kimley-Horn, 2001) 48
Table 6-4. Sediment inflow rating curve for the Waterman Wash 48
Table 6-5. Sediment transport functions used in the HEC-6T calibration runs 55
Table 6-6. Root mean square error (feet) for HEC-6T calibration runs with varying Manning's roughness values 57
Table 6-7. Root mean square error (feet) for calibration runs using different upstream sediment loading condition 58
Table 6-8. Root mean square errors (feet) for HEC-RAS calibration runs 59

List of Appendices

Appendix A – Data Collection Report

Appendix B – As-Built Drawings

Appendix C – CHECKRAS Results

Appendix D – General Correspondence

Appendix E – Comments and Responses

1 Introduction

1.1 Purpose of the Study

Recently, there have been several projects on the Salt/Gila River system that have led to new hydraulic models:

- Lower Salt River Floodplain Delineation Study (FDS) completed in 2015 (WEST Consultants, Inc., 2015);
- Tres Rios North Levee (TRNL) Physical Map Revision (PMR) completed in 2012 (WEST Consultants, Inc., 2012);
- El Rio Watercourse Master Plan completed in 2006 (Stantec, 2006); and
- Lower Gila River FDS, which is ongoing but a draft report was produced in 2014 (Stantec, 2014).

All of the models listed above concentrate on hydraulics and not sediment transport. While there are existing sediment transport models of these areas, these sediment transport models are older and have not been updated using the newer topographic data and Manning's roughness coefficients utilized by the newer hydraulic models. Thus, there is a need to update/develop sediment transport models on the Salt River and the Gila River. The overall purpose of this study is to create both HEC-6T and HEC-RAS sediment transport models of the Salt/Gila River system from the upstream limit of detailed study for the Lower Salt River Floodplain Delineation Study (FDS), which was upstream of the I-10 Bridge, downstream to SR-85. See Figure 1-1 for more detail regarding the study reach extents.

A total of seven different models were developed as part of this scope of work as summarized below. The existing conditions models utilized the newest available topography and Manning's roughness coefficients. The proposed conditions models added proposed sand and gravel pits to the existing conditions topography. The models created for this project are:

1. Calibration model for the Rio Salado study reach (beginning with historic conditions geometry and utilizing the most recent topography for calibration);
2. Existing conditions HEC-RAS model using the record of historic flows;
3. Existing conditions HEC-RAS model using the 1% annual chance flood hydrograph;
4. Proposed conditions HEC-RAS model using the 1% annual chance flood hydrograph;
5. Existing conditions HEC-6T model using the record of historic flows;
6. Existing conditions HEC-6T model using the 1% annual chance flood hydrograph; and
7. Proposed conditions HEC-6T model using the 1% annual chance hydrograph.

1.2 Authority for the Study

WEST Consultants, Inc. (WEST) prepared these sediment transport models of the Salt/Gila River system under contract with the District. This study was commissioned under contract FCD 2012C020 Work Assignment #3 (WA3). District personnel affiliated with the project include Dr. Bing Zhao, P.E., (Project

Manager), Mr. Raj Shrestha, P.E., CFM; Ms. Pramita Chitrakar, CFM; and Mr. Shimin Li. WEST personnel involved included Dr. Brian Wahlin, Ph.D., P.E., D.WRE (Project Manager, Engineer of Record); Mr. Chris Bahner, P.E., D.WRE; Mr. Gyan Basyal; and Mr. Jesse Piotrowski, P.E., CFM. The project began in February 2015. WEST would also like to acknowledge the work done by our internal quality assurance team; and the review performed internally by District staff for the study.

This Technical Support Data Notebook (TSDN) has been prepared according to the standards as specified in the Arizona Department of Water Resources (ADWR) State Standard SS1-12 (Arizona Department of Water Resources, 2012).

1.3 Location of the Study Reach

The study covers sections of the Lower Salt River and the Lower Gila River, located in central Maricopa County. The upstream limit of the study is approximately 7,500 feet upstream of the I-10 Bridge and the downstream limit is SR-85. Major tributary inflows to the system come from the Agua Fria River, the Upper Gila River, and Waterman Wash. A vicinity map showing the study reach is shown in Figure 1-1.

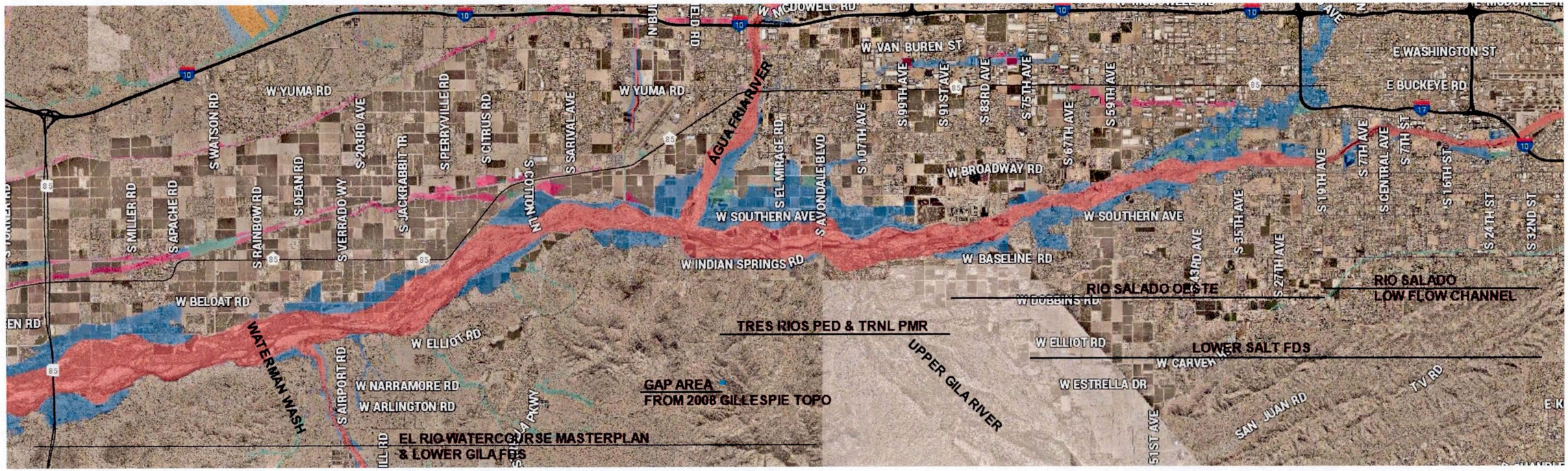

Figure 1-1. Vicinity map for the Salt/Gila sediment transport model

1.4 Methodology used for Hydrology, Hydraulics, and Sediment Transport

Two different hydrologic events were considered for this project. The first hydrologic event considered historic flows for the river and tributaries. The second hydrologic event considered the 1% annual chance flood hydrograph for the river and tributaries. New hydrologic analyses were not included as part of this study. Instead, hydrologic analyses from previous studies and existing stream gages were used to generate the necessary hydrologic input for the sediment transport models. Details of the hydrologic data used are found in Section 4 below.

HEC-RAS versions 4.1.0 and 5.0 beta were utilized to develop a base hydraulic model from the previous study models (Hydrologic Engineering Center, 2010). The details of the hydraulic analysis are described further in Section 5 below.

HEC-RAS versions 4.1.0 and 5.0 beta were also utilized to perform the sediment transport analyses (Hydrologic Engineering Center, 2010). In addition, HEC-6T version 5.13.22_08T was utilized (MBH Software, 2006) for the HEC-6T sediment transport models. The HEC-RAS beta version used in this study was the August 2015 release. The sediment transport models were initially developed using HEC-RAS and then they were converted into HEC-6T format. The details of the sediment transport analyses are described further in Section 6 below.

A Data Collection Report was prepared as part of this study. This report is divided into five sections. First, data from gage records in the study reach that were used to generate the historic hydrologic event are presented. Second, sources of structure data for structures modeled in HEC-RAS or HEC-6T such as bridges and grade control structures are discussed. The sources of topographic data, geometric data, and sediment data that were used for the current modeling effort were also included in the Data Collection Report. The final section of this report describes the plans for sand and gravel mining pits in the study reach in their final built-out condition that will be used for the current modeling effort to model effects of future conditions of these pits. A copy of the Data Collection Report can be found in Appendix A.1.

1.5 Acknowledgments

The District was the primary supplier of the data needed for this study and provided technical guidance for the final product. The bulk of this study can be attributed to the ready communication with and input from the District. In addition, the project team would also like to acknowledge Mr. Tony Beuche, P.E., of the District for his invaluable input regarding the mining operations in the reach, both current and future.

1.6 Study Results

The study results are discussed in detail in the remainder of the report. A summary of the results is shown in Table 1-1 and Table 1-2. Overall, eight different scenarios were run with HEC-RAS and HEC-6T. Two different geometry files were used: one for existing conditions and one for a proposed condition with all the sand and gravel pits built out to their fullest extent. There were also two different hydrologic events that were simulated: one with the 1% annual chance flood hydrograph and one with a historic series of flows. In general, the sediment transport models showed degradation downstream of 51st Avenue and aggradation upstream of 51st Avenue. While both the HEC-RAS sediment transport models and the HEC-6T sediment transport models had similar results, the HEC-6T model tended to have more aggradation than the HEC-RAS models. For most scenarios, the simulations indicated that the bed of the river would drop on average (i.e., a negative average of the change in the average main channel bed elevation). Also, the HEC-6T runs produced less degradation than, on average, than the HEC-RAS runs.

The HEC-6T average bed results for the historic hydrograph was compared to previous studies completed in the study area. The new and old sediment transport models had many different factors such as different initial conditions geometry, different historic flow hydrographs, different sediment inflow hydrographs, etc. Despite these differences in the models, the average bed results were similar.

Table 1-1. Summary of sediment transport model results for 1% annual chance flow hydrograph

Model	Scenario	Average change in minimum bed elevation (ft)	Average change in average main channel bed elevation (ft)
HEC-RAS	Existing, 1% annual	-1.1	-0.6
HEC-RAS	Proposed, 1% annual	-1.5	-0.7
HEC-6T	Existing, 1% annual	-0.9	-0.1
HEC-6T	Proposed, 1% annual	-1.2	-0.2

Table 1-2. Summary of sediment transport model results for historic series of flows

Model	Scenario	Average change in final bed elevation (ft)	Average change in average main channel bed elevation (ft)
HEC-RAS	Existing, historic	-1.4	-1.2
HEC-RAS	Proposed, historic	-0.1	-1.5
HEC-6T	Existing, historic	0.2	0.1
HEC-6T	Proposed, historic	2.1	0.0

2 FEMA Forms

FEMA MT-2 Forms are not required for this study.

3 Surveying and Mapping Information

The final geometry for the combined hydraulic and sediment transport models for the Salt/Gila River system was based on three different existing models:

1. Lower Salt FDS;
2. Tres Rios North Levee PMR; and
3. Lower Gila FDS.

The final topography used for floodplain mapping in these studies was obtained from a number of sources as discussed below.

The primary source of topography for the Lower Salt FDS (WEST Consultants, Inc., 2015) portion of the study reach was 2-foot contour topographic survey data developed specifically for the Lower Salt FDS.

Topography for the TRNL PMR portion of the study reach was taken from four different sources as summarized below (WEST Consultants, Inc., 2012):

1. The main portion of the Salt/Gila River system upstream of El Mirage Road was mapped using 1-foot contour interval topography developed in 2001 by Towill, Inc. for the US Army Corps of Engineers, Los Angeles District (LACOE).
2. The main Salt/Gila River channel and overbanks downstream of El Mirage Road were mapped using 2-foot contour interval topography developed in 2008 as part of the Gillespie Area Drainage Master Study (ADMS) (Stantec, 2013).
3. The north overbanks of the Salt/Gila River system on the landward side of the TRNL were mapped using 2-foot contour interval topography developed in 1994 as part of the District's Maryvale ADMS (Wood, Patel and Associates, 1997).
4. The rest of the overbank areas were mapped using 4-foot contour interval topography developed in 1991 as part of the effective Salt River FDS (Michael Baker, Jr., Inc., 1999).

The topography for the Lower Gila FDS portion of the study reach was obtained from three different sources (Stantec, 2014):

1. The main Gila River channel and overbanks were mapped using 2-foot contour interval topography developed in 2008 as part of the Gillespie ADMS.
2. A portion of the right overbank in the Buckeye Slough area was mapped using 2-foot contour interval topography developed in 2013 specifically for the Lower Gila FDS.
3. A portion of the right overbank downstream of the Buckeye Slough area was mapped using 2-foot contour interval topography developed in 2002 as part of the Buckeye/Sun Valley ADMS.

3.1 Digital Projection Information

The vertical datum used for this study is the North American Vertical Datum of 1988 (NAVD88). The horizontal datum used for this study is the North American Datum of 1983 (NAD83) projected in the Arizona State Plane Central Zone coordinates. All data sources used in this study reference this horizontal projection using a High Accuracy Reference Network (HARN) with units of international feet.

3.2 Field Survey Information

No field surveys were performed as part of this project.

4 Hydrology

Hydrologic modeling was not performed as part of this study; existing hydrologic studies and data were used instead. As mentioned earlier, two different hydrologic events were considered for this project. The first hydrologic event considered historic flows for the river and tributaries while the second hydrologic event considered the 1% annual chance flood hydrograph for the river and tributaries. In addition, a base hydraulic model was developed prior to the sediment transport models that utilized the effective FEMA 1% annual chance hydrology.

4.1 Effective Hydrology for Base Hydraulic Model

The current Flood Insurance Study (FIS) hydrology for the Salt/Gila River hydraulic model is based on Baker's analysis of the 1% annual chance flood for the Salt/Gila River system (Michael Baker, Jr., Inc., 1999), which relies on an older LACOE report titled *Section 7 Study for Modified Roosevelt Dam, Arizona: Hydrologic Evaluation of Water Control Plans, Salt River Project to Gila River at Gillespie Dam* as the basis for the hydrology (U.S. Army Corps of Engineers, 1996). The Lower Salt River FDS (WEST Consultants, Inc., 2015) and the Tres Rios North Levee PMR (WEST Consultants, Inc., 2012) both discuss a slight discrepancy between the FIS hydrology and the hydrology reported in the LACOE's Section 7 report. Table 4-1 lists the 1% annual chance discharges for the Salt/Gila River system that were used for the base hydraulic model.

Table 4-1. 1% annual chance discharges for the Salt/Gila River system

Flow Change Location (HEC-RAS Cross-Section ID Number)	1% Annual Chance Discharge (cfs)
203.08 (River: Salt, Reach: Salt)	162,000
199.44 (River: Gila, Reach: Lower Gila)	227,000

4.2 Historic Flow Records

Gage records by the United States Geological Survey (USGS) and the District in the study reach and tributaries were used to determine the historic flow records entering the Salt/Gila study reach. Historic flow and stage data were available for the gages shown in Table 4-2.

Table 4-2. Stream gage information in the study reach

Agency	Gage Number	Name	Dates	Data
USGS	09512165	Salt River at Priest Drive near Phoenix, AZ	12/7/1993 – present	stage, flow
District	4523	Salt River @ Priest Drive	12/7/1993 – present	stage, flow
USGS	09512190	Salt River at 24th Street at Phoenix	10/1/1989 – 1/7/1993	flow
District	4763	Salt River @ 7th Avenue	1/25/2015 – present	stage, flow
USGS	09512405	Salt R at 35th Ave at Phoenix, AZ	1/5/1979 – 9/30/1979	flow
USGS	09512406	Salt River at 51st Avenue, Phoenix, AZ	10/1/2002 – 9/30/2005	flow
USGS	09512407	Salt River at 91st Ave.	10/1/1995 – 4/30/1998	flow
District	4753	Salt R. @ 51st Ave.	4/27/2011 – present	stage, flow
District	4758	Salt River @ 67th Ave.	7/14/2008 – present	stage, flow
District	6848	Gila R. @ 116th Ave.	1/26/1989 – present	stage, flow
USGS	09479500	Gila River near Laveen, Ariz.	1/1/1940 – 6/18/1995	flow
USGS	09479501	Gila River near Laveen (Main Channel)	10/1/1992 – 6/18/1995	flow
USGS	09479502	Gila River near Laveen (Overflow Channel)	10/1/1983 – 6/18/1995	flow
USGS	09479350	Gila River near Maricopa, AZ.	5/19/1995 – 9/30/2005	flow
District	778	Gila River @ Maricopa Rd.	4/6/1995 – present	stage, flow
District	6848	Gila R. @ 116th Ave.	1/26/1989 – present	stage, flow
USGS	09513970	Agua Fria River at Avondale, Ariz.	10/1/1967 – 9/30/1982	flow
District	5403	Agua Fria R. @ Buckeye Rd.	10/6/1998 – present	stage, flow
USGS	09514100	Gila River at Estrella Parkway, near Goodyear, AZ.	10/1/1992 – 9/30/2005	flow
District	6853	Gila R. @ Estrella Pkwy.	2/28/1989 – present	stage, flow
District	6833	Waterman Wash @ Rainbow Valley Rd.	3/18/1999 – present	stage, flow
USGS	09514300	Gila R at State Hwy 82, NR Buckeye, AZ	5/1/1979 – 9/30/1992	flow

Flows enter the Salt/Gila study reach from the following locations:

1. Lower Salt River at the upstream end of the study reach;
2. Upper Gila River at the confluence with the Lower Salt River;
3. Agua Fria River at the confluence with the Lower Gila River; and
4. Waterman Wash at the confluence with the Lower Gila River.

It was assumed that all other inflow locations (include Cave Creek) were minor inflows that did not significantly contribute to the sediment loading on the Salt/Gila River system.

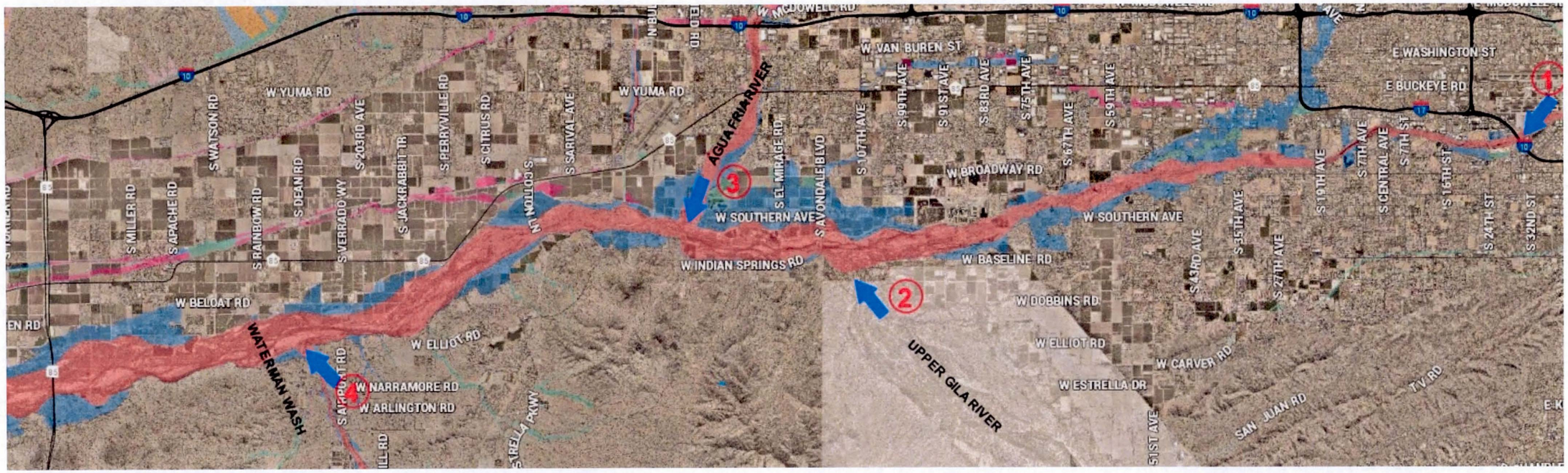

Figure 4-1. Locations of flow and sediment inflows (marked by an arrow and number) in the sediment model: 1) Lower Salt at I-10, 2) Upper Gila, 3) Agua Fria, and 4) Waterman Wash

4.2.1 Historic Flows on the Lower Salt River at the Upstream End of the Study Reach

A long-term flow series was developed for the Lower Salt River using the gage data shown in Table 4-2 in the Tres Rios North Levee PED study (WEST Consultants, Inc., 2002a). This time series was used as inflow boundary at the upstream end of the sediment transport model. The flow series primarily consists of 72-hour duration hydrographs with values given at every six hours for the period 1889-1993 (see Figure 4-2).

4.2.2 Historic Flows on the Upper Gila River at the Confluence with the Lower Salt River

A long-term flow series was also developed for the Upper Gila River in the Tres Rios North Levee PED study (WEST Consultants, Inc., 2002a). This time series was used as inflow for the Upper Gila River into the Salt/Gila River confluence. The flow series primarily consists of 72-hour duration hydrographs with values given at every six hours for the period 1889-1993 (see Figure 4-2).

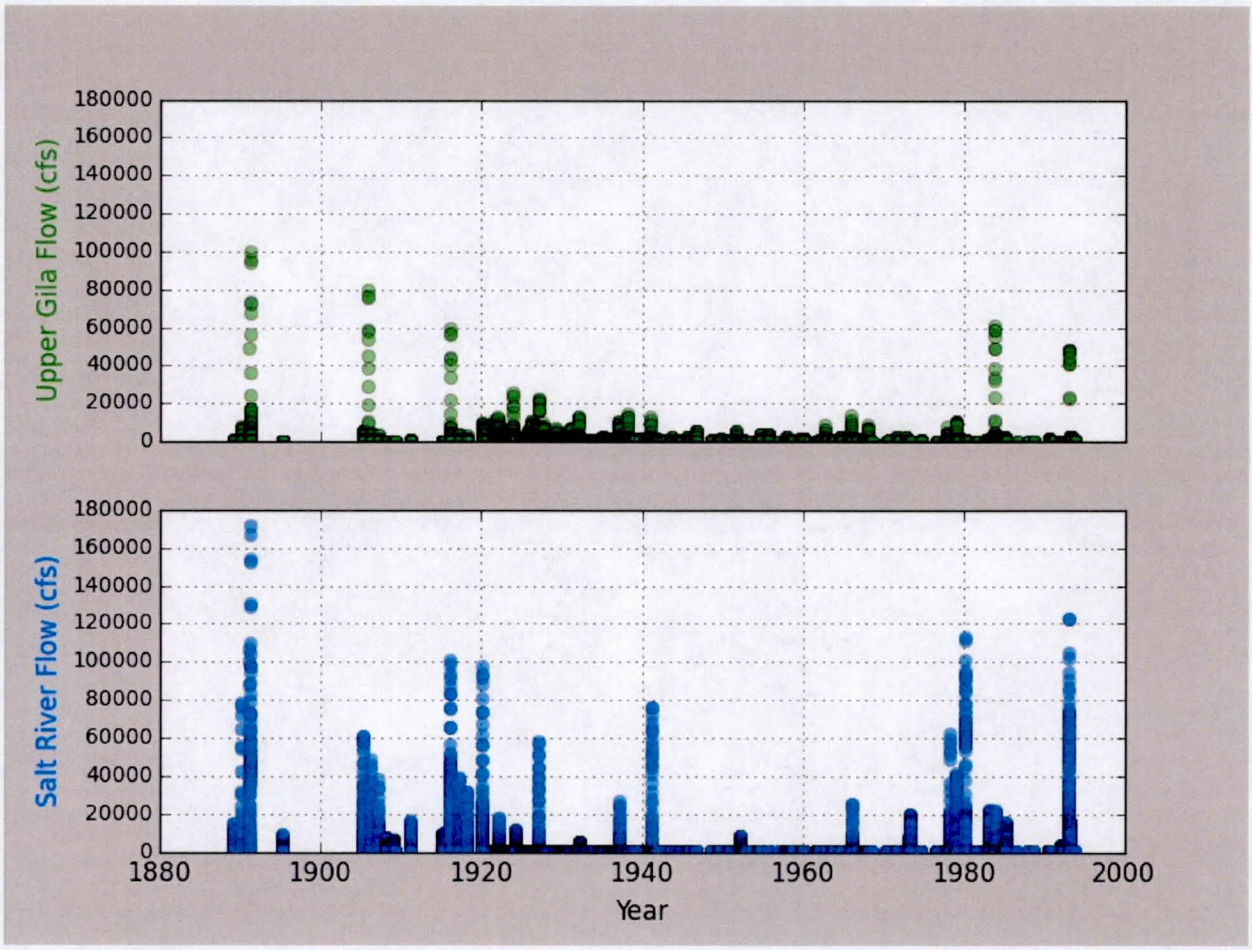

Figure 4-2. Historic flow hydrograph for the Lower Salt River and the Upper Gila River (WEST Consultants, Inc., 2002a)

4.2.3 Historic Flows on the Agua Fria River at the Confluence with the Lower Gila River

A long-term flow series was developed for the Agua Fria River by combining 10%, 4%, 2%, and 1% annual chance flood events as described in the District's Hydraulics Manual (Flood Control District of Maricopa County, 2013). The historic flow series was composed of six 10% annual chance flood events, two 4% annual chance flood events, one 2% annual chance flood event, and one 1% annual chance flood event. The order of the individual events is subject to engineering judgement. For this study, the order was chosen to be the same order as was used in the Waterman Wash study (URS, 2010) as described in Table 4-3. For consistency with the historic flows on the Upper Gila and Lower Salt, the individual flood event hydrographs were resampled at 6-hour intervals and were placed at regular intervals in the normalized time axis of Salt and Upper Gila historical flow series. The total flow volume of each event was conserved although the peak flow was reduced because of resampling at the 6-hour interval. The original 1% annual chance flood hydrograph and the re-sampled hydrograph are shown in Figure 4-3. The final historic flow series used for the Agua Fria River is shown in Figure 4-4. Note that the x-axis in this figure distorts the hydrographs and they appear as individual spikes instead of as hydrographs.

The 1% annual chance flood hydrograph was available from Kimley-Horn and Associates' (KHA) Sediment Trend Analysis of the Agua Fria River (Kimley-Horn and Associates, 2001). According to KHA, the Standard Project Hydrograph (SPF) for the Agua Fria River downstream of New River was available from the LACOE, which yielded a peak flow of 94,000 cfs. The ratio of the SPF to the 1% annual chance flood event of 0.58 was applied to the SPF to develop the 1% annual chance flood hydrograph for Agua Fria River. In similar fashion, in the present study, the ratio of SPF to peak flow of corresponding flood events were used to develop the 10%, 4%, and 2% annual chance flood hydrographs for Agua Fria River. The peak flows for the various events are reported in KHA's Sediment Trend Analysis report (Kimley-Horn and Associates, 2001) and are shown in Table 4-4. The ratio between the peak SPF flow of 94,000 cfs and the peak flow for a given event is also shown in Table 4-4. Note that the peak flows shown in Table 4-4 were reduced due to the re-sampling process. However, the total volume for each event was conserved.

Table 4-3. Sequence of flow events and peak flows used to generate historic flood series for both the Agua Fria River and Waterman Wash

Order	Event
1	10% annual chance flood hydrograph
2	10% annual chance flood hydrograph
3	4% annual chance flood hydrograph
4	10% annual chance flood hydrograph
5	2% annual chance flood hydrograph
6	10% annual chance flood hydrograph
7	1% annual chance flood hydrograph
8	10% annual chance flood hydrograph
9	4% annual chance flood hydrograph
10	10% annual chance flood hydrograph

Table 4-4. Peak flows on the Agua Fria River for various flood events and ratio to the SPF

Event	Peak Flow (cfs)	Ratio to SPF
10% annual chance flood hydrograph	16,100	0.17
4% annual chance flood hydrograph	26,000	0.28
2% annual chance flood hydrograph	39,000	0.41
1% annual chance flood hydrograph	54,400	0.58

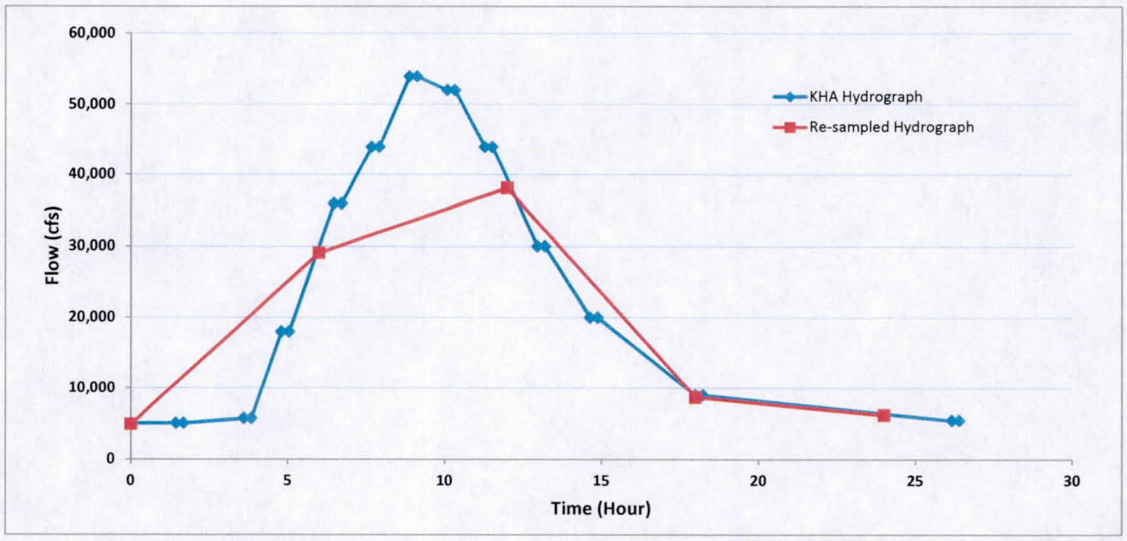

Figure 4-3. Original Agua Fria River 1% annual chance flood hydrograph and re-sample hydrograph (note that volume is conserved)

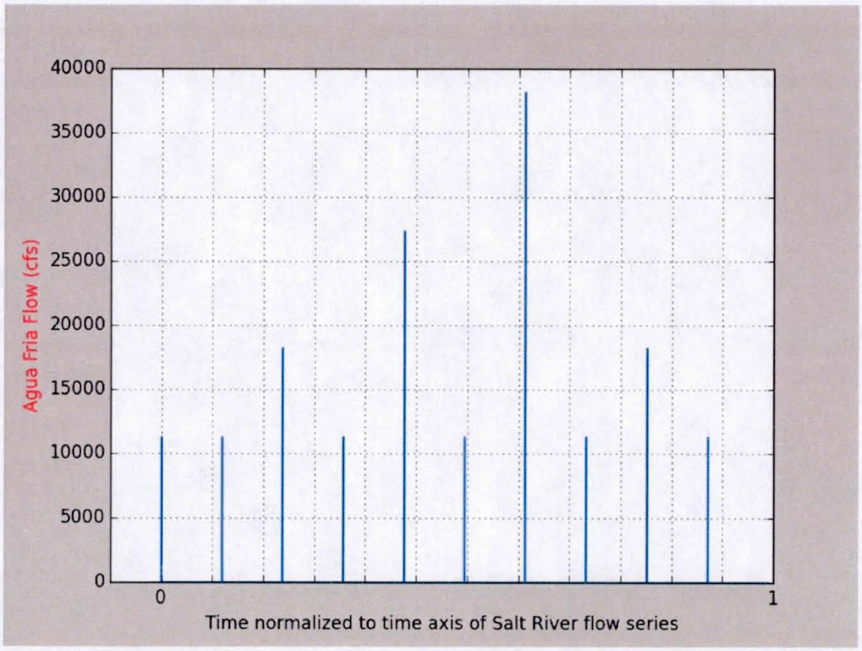

Figure 4-4. Historic flow hydrograph for Agua Fria River

4.2.4 Historic Flows on Waterman Wash at the Confluence with the Lower Gila River

The historic flow series for Waterman Wash was based on URS's sediment transport analysis of Waterman Wash (URS, 2011). URS presented a sediment transport analysis of Waterman Wash that was conducted by using continuous series of 10%, 4%, 2%, and 1% annual chance flood hydrographs at 1-hour time intervals (see Figure 4-5). Note that these flows are the flows in Waterman Wash at the confluence with the Lower Gila River. The order of the various flood event hydrographs shown in Figure 4-5 is the same as was used for the Agua Fria River (see Table 4-3). In this current study, the individual flood events or hydrographs were resampled at 6-hour intervals and the flows were scaled to conserve the total flow volume for each hydrograph. Then the series of hydrographs were normalized with the time axis of Salt and Upper Gila historical flow series as shown in Figure 4-6. Note that the x-axis in this figure distorts the hydrographs and they appear as individual spikes instead of a hydrograph. Because of resampling of the flow interval, the peaks for hydrographs have been reduced but the hydrographs have same total flow volumes.

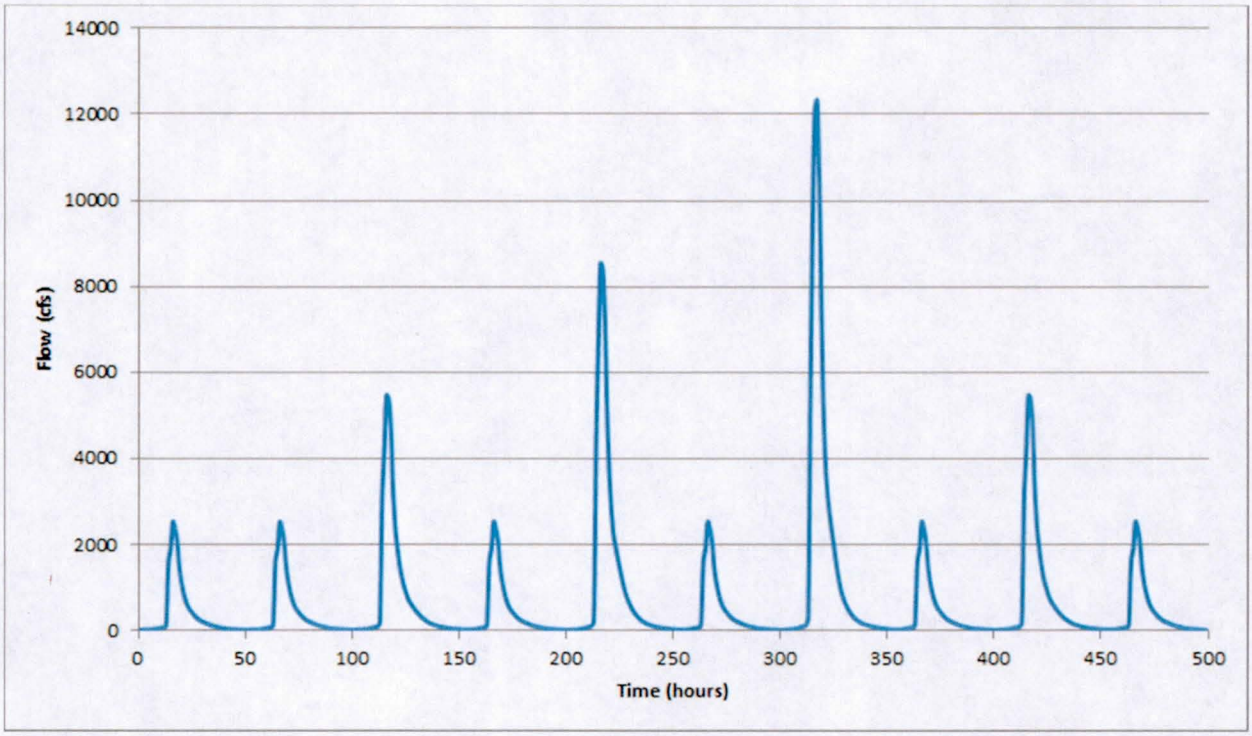

Figure 4-5. Flood hydrograph series for URS's sediment transport study of Waterman Wash (URS, 2011)

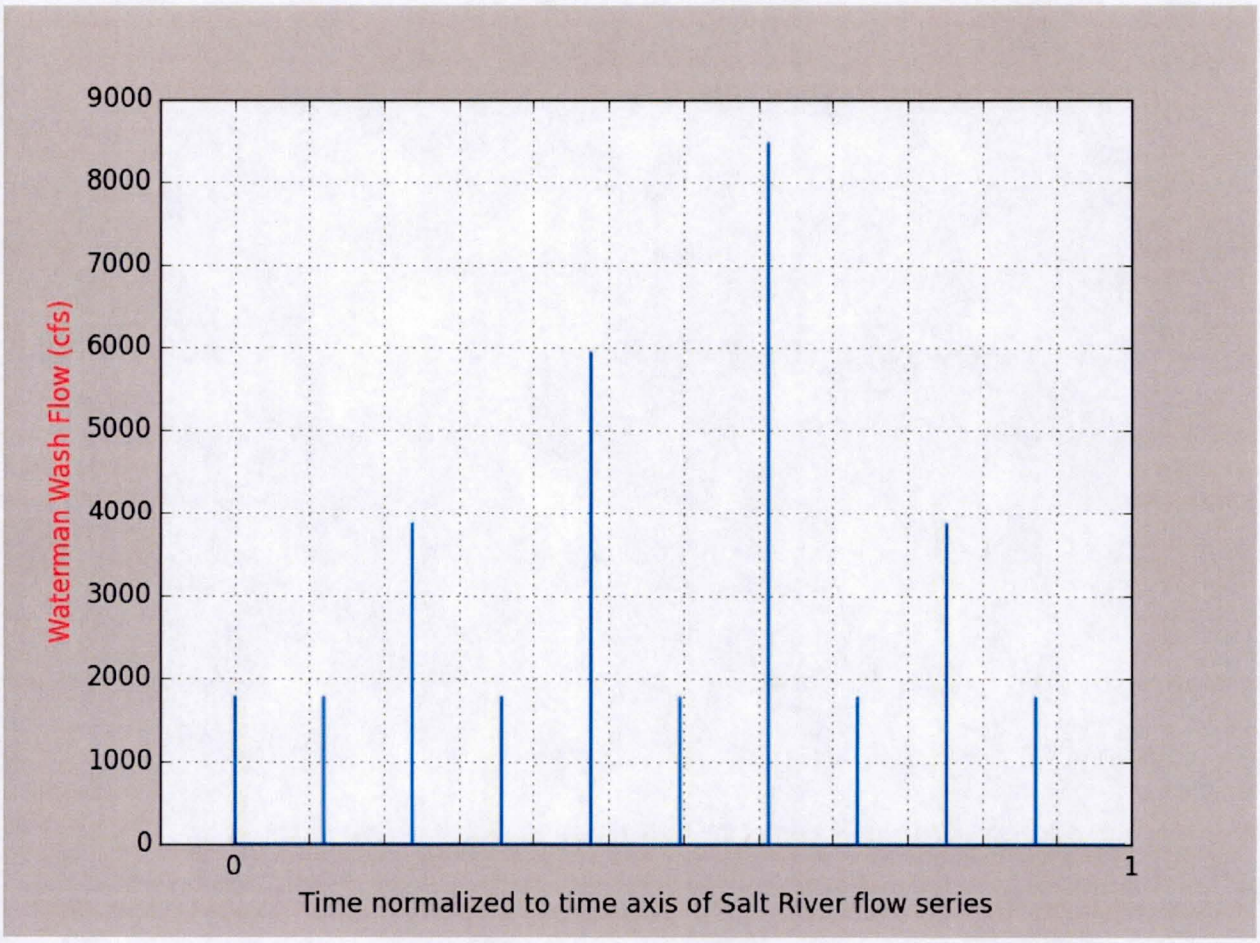

Figure 4-6. Historic flow hydrograph for Waterman Wash

4.3 1% Annual Chance Flood Hydrographs

As mentioned earlier, the sediment transport models were also run with 1% annual chance flood hydrographs in addition to the historic flow records. Flows enter the model from the following locations:

1. Lower Salt River at the upstream end of the study reach;
2. Upper Gila River at the confluence with the Lower Salt River;
3. Agua Fria River at the confluence with the Lower Gila River; and
4. Waterman Wash at the confluence with the Lower Gila River.

It was assumed that all other inflow locations (including Cave Creek) consisted of minor inflows that did not significantly contribute to the sediment loading on the Salt/Gila River system. Hydrographs for the 1% annual chance floods were already determined for the four inflow locations in previous studies.

The 1% annual chance flood inputs for the Lower Salt River at the upstream end and the Upper Gila at the confluence were obtained from Stantec's El Rio Sedimentation Analysis, which is part of the El Rio Watercourse Master Plan (Stantec, 2006). The discretized hydrographs are provided in Table 4-5.

Table 4-5. 1% annual chance flood hydrograph for Lower Salt River and Upper Gila River (Stantec, 2006)

Day	Lower Salt River Flow (cfs)	Upper Gila River Flow (cfs)
1	31,000	9,000
2	154,000	46,000
3	127,000	38,000
4	108,000	32,000
5	92,000	28,000
6	79,000	24,000
7	69,000	21,000
8	61,000	18,000
9	52,000	16,000
10	45,000	13,000
11	38,000	11,000
12	31,000	9,000

The 1% annual chance flood hydrograph for the Agua Fria River was obtained from KHA's sediment trend analysis of Agua Fria River (Kimley-Horn and Associates, 2001). The 1% annual chance flood hydrograph is shown in Figure 4-7. This hydrograph was re-sampled at a 30-minute time interval to generate the quasi-unsteady flow series to represent the 1% annual chance flood hydrograph. The volume between the original and re-sample hydrographs was conserved.

Similarly, the 1% annual chance flood hydrograph for Waterman Wash was obtained for URS's sediment transport analysis of Waterman Wash (URS, 2011). The 1% annual chance flood hydrograph is shown in Figure 4-8.

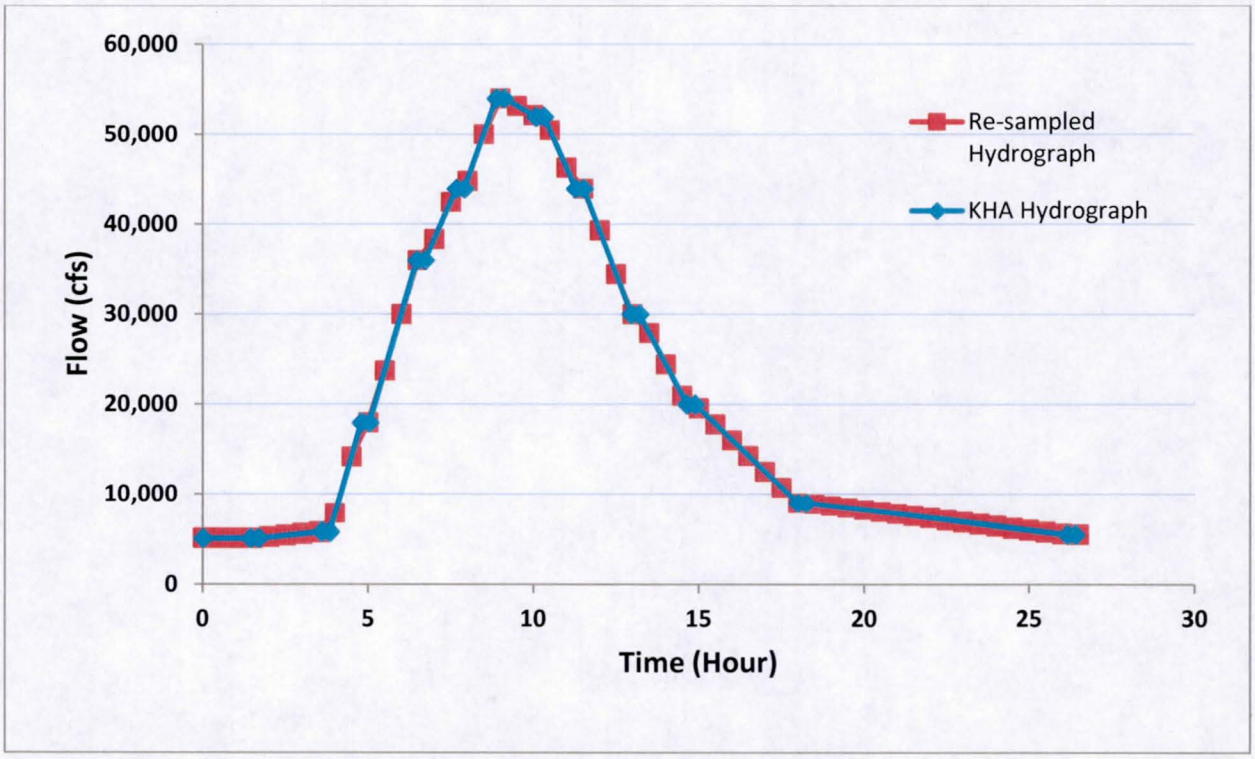

Figure 4-7. 1% annual chance flood hydrograph for the Agua Fria River downstream of the New River confluence (Kimley-Horn and Associates, 2001)

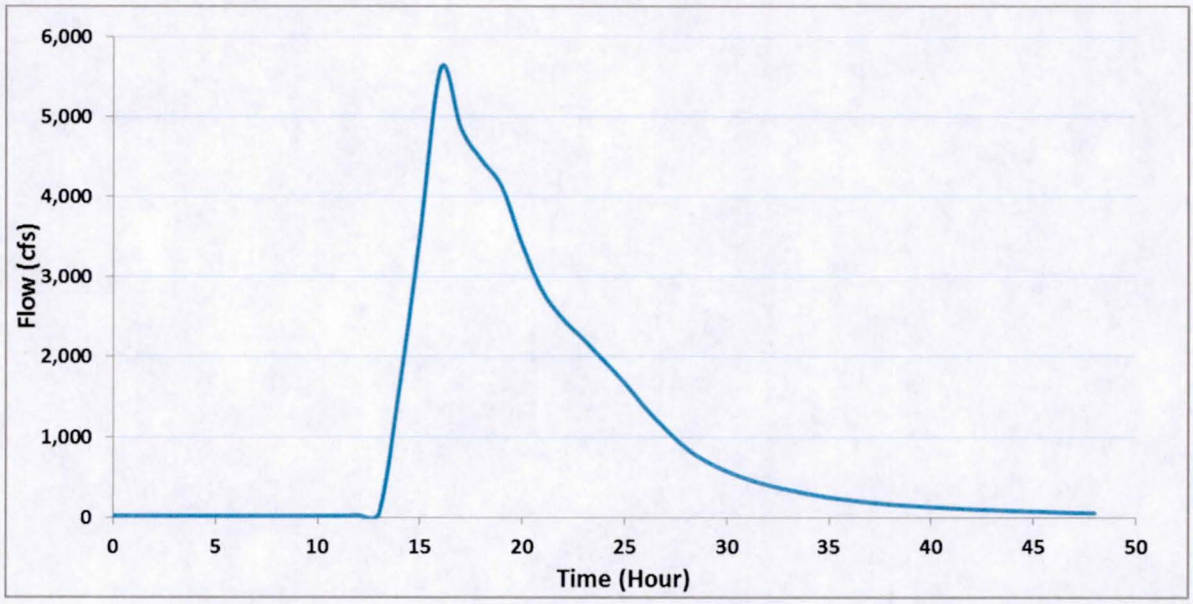

Figure 4-8. 1% annual chance flood hydrograph for Waterman Wash (URS, 2011)

5 Hydraulics

5.1 Method Description for HEC-RAS Base Hydraulic Model

The USACE's Hydrologic Engineering Center's River Analysis System (HEC-RAS) version 4.1.0 and 5.0 beta (Hydrologic Engineering Center, 2010) was the software used to perform the one-dimensional hydraulic modeling for the study reach to determine the base hydraulic conditions. HEC-RAS is a one-dimensional hydraulics model, and the steady-state module of the software was used to compute flood profiles in the study reach for the 1% annual chance flood hydrologic events for the base hydraulic conditions.

Existing cross-sections from the Lower Gila FDS, Lower Salt FDS, and Tres Rios North Levee projects were used as the starting point for the cross-section geometric data in the base hydraulic model (and also the sediment transport models). The geometry files from these three studies were stitched together to create a single geometry file from the upstream study limit (approximately 7,500 feet upstream of the I-10 Bridge) downstream to SR-85. As such, base geometry model parameters from each individual model used to create the existing conditions models (e.g., Manning's roughness coefficients, reach lengths, ineffective flow areas, blocked obstructions, etc.) were taken directly from the original model geometry data without modification.

Note that an HEC-6T base hydraulic model was also created. This model is discussed in Section 5.8.

A summary of the hydraulic models used to create the HEC-RAS base hydraulic model follows.

5.1.1 Lower Salt FDS (RM 203.08 – RM 217.71)

The Lower Salt River FDS is a recently completed study by WEST (WEST Consultants, Inc., 2015) for the District. The purpose of this study was to determine approximately 15 miles of Zone AE floodplain and floodway along the Salt River in the metropolitan Phoenix area. The study reach stretched from just upstream of the I-10 Bridge down to just upstream of 91st Avenue in Phoenix. Tributary tie-ins, such as Cave Creek, were also located in this reach. This study was necessary to account for the significant change in the channel and overbanks along the study reach due to active sand and gravel mining operations since the previous study by Baker (Michael Baker, Jr., Inc., 1999). In the study, HEC-RAS version 4.1.0 was used for hydraulic modeling. The latest 2013 topographic data was used to delineate the 1% annual chance floodplain. The flows used in this study agree with Tres Rios North Levee PMR study (WEST Consultants, Inc., 2012). The hydrologic data for the project was obtained from LACOE report titled *Section 7 Study for Modified Roosevelt Dam, Arizona: Hydrologic Evaluation of Water Control Plans, Salt River Project to Gila River at Gillespie Dam* (U.S. Army Corps of Engineers, 1996).

5.1.2 Tres Rios North Levee PMR (RM 197.92 – RM 203.08)

This report was part of a Physical Map Revision (PMR) for FEMA along a reach of the Salt and Gila Rivers in Phoenix and Avondale. This floodplain re-delineation study was done by WEST (WEST Consultants, Inc., 2012) for the District with the support of the LACOE. The study was done to update the changes in floodplain and floodway resulting from the construction of 2.3 mile long levee on the north bank of the river from approximately 105th Avenue to 123rd Avenue. The 5.2-mile study reach along the Salt River extended from approximately 1,500 feet downstream from 83rd Avenue to approximately 2,000 feet

downstream of the El Mirage Road (123rd Avenue) crossing of the Salt River. The hydrologic data for the project was obtained from LACOE report titled *Section 7 Study for Modified Roosevelt Dam, Arizona: Hydrologic Evaluation of Water Control Plans, Salt River Project to Gila River at Gillespie Dam* (U.S. Army Corps of Engineers, 1996).

5.1.3 Gap area from 2008 Gillespie Topography (RM 195.16 - RM 197.9)

There is a gap in the existing hydraulic models between RS 195.09 at the upstream end of Stantec's Lower Gila FDS and RS 197.92 at the downstream end of WEST's Tres Rios North Levee PMR. There were three possible choices for a previous model in the gap area:

1. The hydraulic model created as part of the Pre-construction Engineering and Design (PED) for the Tres Rios North Levee (WEST Consultants, Inc., 2002a), which extends downstream to RS 195.16 and covers the gap area, one cross-section upstream of the upstream end of the Lower Gila FDS (Bullard Ave Bridge is in this model at RS 195.21);
2. The hydraulic model that was created as part of the El Rio Watercourse Master Plan (Stantec, 2006), which extends all the way upstream to RS 199.07 to cover the gap area; and
3. An intermediate model from the Tres Rios North Levee PMR (WEST Consultants, Inc., 2012), which covers the gap area.

The Tres Rios North Levee PED model (WEST Consultants, Inc., 2002a) was based on the 2001 Towill topography that was also used in the Tres Rios North Levee PMR (WEST Consultants, Inc., 2012). The El Rio Watercourse Master Plan model (Stantec, 2006), on the other hand, was based on the topography used for the effective model (circa 1993). Therefore, it would appear that using the original Tres Rios North Levee PED cross-sections in the gap area would be the best choice.

However, during the Tres Rios North Levee PMR project (WEST Consultants, Inc., 2012), an intermediate model (one not used in the final results because of FEMA tie-in issues) was developed that re-cut the Tres Rios North Levee PED cross-sections in the gap area using the 2008 Gillespie ADMS 2-foot contour interval topography (Stantec, 2013). While much of this area was deleted from the final Tres Rios North Levee PMR model because of FEMA tie-issues, this intermediate model represents the most up-to-date topographic information for the gap area. Note that the Tres Rios North Levee PMR intermediate model was cut in NGVD29, even though the Gillespie 2-foot topography was developed in NAVD88. Since the remainder of the PMR study was completed in NGVD29, WEST shifted the Gillespie topography from NAVD88 into NGVD29 before re-cutting the intermediate PMR cross-sections in the gap reach. Therefore, these draft cross-sections from the PMR in the gap reach were shifted back to NAVD88 before inclusion in the final hydraulics and sediment transport models. Note that for NGVD29 to NAVD88 datum conversion, datum conversion factor of +2.1 feet is used.

5.1.4 Lower Gila FDS (RM 147.44 - RM 195.09)

Stantec is currently delineating the floodplain and floodway for the Lower Gila River from Bullard Avenue downstream to Painted Rock Dam (Stantec, 2014). The project is located within the Town of Gila Bend, City of Buckeye, City of Goodyear, and Unincorporated Maricopa County. For the hydraulic modeling portion, the study reach was subdivided into two sub reaches: Reach 1 and Reach 2 (see

Figure 5-1). Reach 1 extends from the Painted Rock reservoir impoundment area to Gillespie Dam. Reach 2 extends from Gillespie Dam to approximately Bullard Avenue. While the project is not officially complete at the time of this report, the models have been developed. Most of the topography from this study was taken from the 2-foot contour data collected for the Gillespie ADMS.

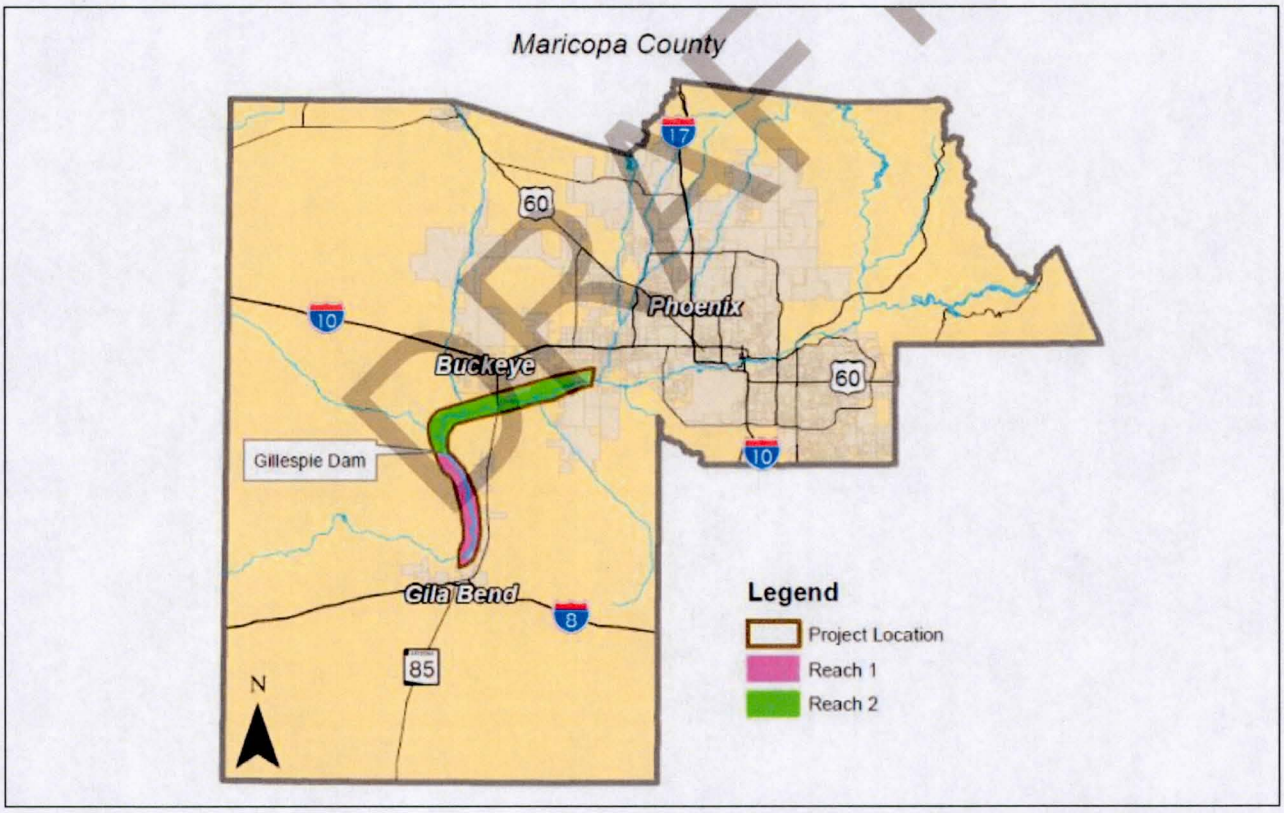

Figure 5-1. Project location map showing the two study reaches for Gila River FDS (Stantec, 2014)

5.1.5 Assembling the Base Hydraulics Model for Existing Conditions

The four different hydraulic models mentioned above (Lower Salt FDS, Tres Rios North Levee PMR, Intermediate Tres Rios North Levee, and Lower Gila FDS) were stitched together to create a single model of the entire study reach. No changes were made to Manning's *n*-values, expansion/contraction coefficients, bank stations, and ineffective flow areas (except as described below) so that the combined model retains the overall hydraulic characteristics of the original models. At the downstream boundary of the base hydraulic model, a normal depth boundary was assigned with the calculated average slope of 0.00147.

The only changes to the base hydraulics geometry of the combined model were near the sand and gravel mining pits that are located throughout the main channel and overbanks in the Salt/Gila River system. Because the main goal of the project was sediment transport modeling, it was decided between WEST and District staff that the modeling approach around the sand and gravel mines should be modified to reflect what would happen in the pits from a sediment transport perspective. In the physical system, pits located in the main channel could contribute to upstream and downstream

degradation/erosion. In order to reflect this phenomenon in the numerical sediment transport modeling, the pit areas in the main channel must be available as active flow area to simulate velocity changes that lead to upstream and downstream degradation/erosion processes in the model. Therefore, in the entire combined model geometry, for pits in the main channel, the following guidelines were applied:

- the pits in the main channel are included in the geometry as ground points; and
- the blocked obstructions in the main channel pits from previous models were removed.

Additional modifications were considered for the pits located in the overbanks of the Salt/Gila River system. For most of the sand and gravel pits in the overbank, there was some sort of protective berm around the perimeter of the pit. For some of the sand and gravel pits, this berm was engineered and designed. For other pits, the berm simply consisted of pushed up dirt (sometimes referred to as sugar dikes as they would dissolve or fail under a significant flow event). If a sand and gravel pit had an engineered berm around the pit, then it was assumed that the berm would remain in place during a flood event. In these cases, the ineffective flow areas in the pit were changed to become blocked obstructions. If the sand and gravel pit did not have an engineered berm, then the protective berm was assumed to fail and the ineffective flow areas were removed from the pit.

After an extensive data collection effort and coordination with the District, all the plans and permits for the sand and gravel pits were assembled and reviewed to determine whether or not the berms protecting the pits were engineered. Summary information regarding the various sand and gravel pits can be found in the Data Collection Report in Appendix A.

5.1.6 Assembling the Base Hydraulics Model for Proposed Conditions

For the proposed conditions base hydraulic model, it was assumed that all the permitted sand and gravel pits were built out to their maximum limit. The sand and gravel pit plans and permits were reviewed for the ultimate pit dimensions. A summary of the modifications to the proposed conditions geometry as a result of the built-out pits is shown in Table 5-1 while more detailed information regarding these pits can be found in the Data Collection Report in Appendix A. For the proposed conditions geometry, the cross-sections were modified to reflect the ultimate pit dimensions.

5.2 Work Study Maps

Work study maps were not generated as part of this study.

Table 5-1. Summary of pit modifications for proposed condition model

S.N.	Permit Number	Remark
1	SG13-003 (formerly FA88-039)	Same as Existing Condition Model (Blocked obstruction)
2	FA87-035R	
3	FA94-072	Second pit that is within FW has invert elevation 952.1 feet (NAVD88)
4	SG05-003	Same as Existing Condition Model (Blocked obstruction)
5	SGA03-005	Same as Existing Condition Model (Blocked obstruction)
6	FA83-012 (new permit SG15-005)	Pit was filled to elevation of 995 feet
7	SG15-001 (formerly SG08-006)	Same as Existing Condition Model (Blocked obstruction)
8	SG07-003	Pit invert elevation of 880 feet
9	SG14-004 (formerly SG08-004)	Same as Existing Condition Model (Blocked obstruction)
10	SG04-002	
11	FA01-043 (permit closed)	Same as Existing Condition Model (Mining closed, ultimate pit condition same as existing condition)
12	SG14-003 (formerly SG04-005)	
13	SG13-001	Same as Existing Condition Model (Blocked obstruction)
14	SG14-001 (formerly SG06-008)	Same as Existing Condition Model (Blocked obstruction)
15	SG04-001	Depth of pit 8 feet
16	SG05-007	Pit invert elevation of 806 feet
17	SG15-002 (formerly SG05-001)	Pit invert elevation 774.1 feet
18	SG04-006	Pit invert elevation of 774.1 feet
19	SG03-004A	Multiple pits. Pit invert elevation 960 – 970 feet

5.3 Parameter Estimation

5.3.1 Roughness Coefficients

Manning's roughness values were not modified as part of this study in an effort to keep the hydraulic characteristics the same between the individual models and the combined model. A summary of the Manning's roughness coefficients used in for the Lower Salt River FDS is shown in Table 5-2.

The roughness coefficients for the Tres Rios North Levee PMR were developed during Phase 3 of the Tres Rios Environmental Restoration Project [(JE Fuller Hydrology and Geomorphology, Inc., 2010) and (HNTB, December 15, 2010)]. In addition, it was assumed that a reduction in flow resistance would occur as flow depth increased. Therefore, the HEC-RAS "Vertical Variation in Manning's *n*-Values" option was utilized based on a change in flow rate (JE Fuller Hydrology and Geomorphology, Inc., 2010). This study did not modify the final Manning's roughness coefficients used for the Tres Rios North Levee PMR.

A summary of the Manning's roughness coefficients used in for the Lower Gila River FDS is shown in Table 5-3.

Table 5-2. Summary of the Manning's *n*-value categories identified in the Lower Salt River FDS (WEST Consultants, Inc., 2015)

Category	Manning's *n*-value
Bare Land	0.031
Heavy Vegetation	0.081
Medium Vegetation	0.053
Light Vegetation	0.037
Mining Areas	0.043
Industrial/Commercial	0.059
Residential (High Density)	0.080
Residential (Low Density)	0.064
Agricultural Areas	0.045

Table 5-3. Summary of the Manning's *n*-value categories identified in the Lower Gila River FDS (Stantec, 2014)

Category	Manning's *n*-value
Riverine	0.015 – 0.130
Agricultural	0.030 – 0.155
Residential	0.040 – 0.155
Sand and Gravel	0.065 – 0.145
Industrial	0.030 – 0.090
Undisturbed Desert	0.045

5.3.2 Expansion and Contraction Coefficients

The expansion and contraction coefficients for the combined model were not changed from the values used in the individual models. As recommended by HEC's *Hydraulic Reference Manual* (Hydrologic Engineering Center, 2010), the expansion and contraction coefficients were set equal to 0.1 and 0.3, respectively, along the entire study reach due to the small variation in velocity and cross-sectional area from one cross-section to the next throughout the modeled reach. HEC recommends increasing the contraction and expansion coefficients to 0.3 and 0.5, respectively, for two cross-sections upstream of bridges and one cross-section downstream of the bridge. These increased values account for the energy loss as the top width of the river is often significantly reduced at bridge entrances and enlarged at bridge exits. However, in the study reach, very little contraction and expansion occurs at the following bridges:

- 24th Street Bridge (RM 215.815)
- 16th Street Bridge (RM 214.785)
- 7th Street Bridge (RM 213.745)
- Central Avenue Bridge (RM 213.255)
- 7th Avenue Bridge (RM 212.675)

- 19th Avenue Bridge (RM 211.525)
- 27th Avenue Conveyor Belt Bridge (RM 210.435)

At the two cross-sections immediately upstream of these bridges and the one cross-section immediately downstream, the contraction and expansion coefficients were set to 0.15 and 0.35, respectively. Significant contraction and expansion occurs at the 35th Avenue Bridge (RM 209.535) and the 51st Avenue Bridge (RM 207.485). At these two bridges, the contraction and expansion coefficients were set to 0.3 and 0.5, respectively.

In the Tres Rios North Levee PMR, there is only one bridge: the 115th Avenue Bridge. There is essentially no contraction or expansion of the flow through this bridge, so the contraction and expansion coefficients were left at 0.1 and 0.3, respectively.

For bridges in the Lower Gila River FDS portion of the study, the contraction and expansion coefficients were raised to 0.3 and 0.5, respectively, for all bridges in the study reach.

5.4 Cross-Section Descriptions

Typical convention was used for cross-section horizontal stationing for all HEC-RAS modeling in this study (i.e., cross-section stationing is from left to right when looking in the downstream direction). Cross-section spacing varies throughout the study area on a reach-by-reach basis depending on cross-sectional channel geometry, bed slope breaks, and location of bridges.

For the base hydraulics model, the same cross-sections were used in the combined model as for the individual models.

5.5 Modeling Considerations

5.5.1 Hydraulic Jump and Drop Analysis

Grade control structures are very important to model in sediment transport modeling. For the Salt/Gila River system, there are five grade control structures. These structures are located in the upper end of the study reach between 19th Avenue and the I-10 Bridge:

1. One grade control structure downstream of the I-10 Bridge at RM 216.23;
2. One grade control structure downstream of the 24th Street Bridge at RM 215.81;
3. One grade control structure downstream of 16th Street at RM 214.61;
4. One grade control structure downstream of Central Avenue at RM 213.25; and
5. One grade control structure downstream of 19th Avenue at RM 211.51.

The as-built plans for these structures (except the one downstream of 19th Avenue) were obtained from Rio Salado Low Flow Channel Design study (WEST Consultants, Inc., 2000). As-built plans for the grade control structure downstream of 19th Avenue were obtained from the 19th Avenue Landfill

Environmental Cleanup project (Simons Li and Associates, 1995). The as-built plans were used to code in the correct location and elevation of the grade control structure in both the base hydraulics model and the sediment transport models.

For all the profiles, the hydraulic model defaulted to critical depth at the grade control structure downstream of 19th Avenue. In addition, the model defaulted to critical depth just downstream of the 51st Avenue Bridge near the broken pipeline. WEST examined these locations in detail as part of the Lower Salt River FDS and determined it was justifiable to allow these defaults to critical depth to remain (WEST Consultants, Inc., 2015).

The 10% annual chance flood also defaulted to critical depth at a few additional locations near RM 205.4, 202.65, 201.12, and 199.52. Adjusting the geometry in these areas (i.e., adding new cross-sections, moving ineffective flow areas, etc.) may have eliminated these defaults to critical. However, the only changes to be implemented to the geometry from the previous studies focused on the ineffective flow areas and blocked obstructions near sand and gravel pits. Thus, these default-to-critical-depths remain.

5.5.2 Bridges and Culverts

Sixteen bridges are located within the study reach as shown in Table 5-4. The District provided WEST with plans and as-built plans for most of the bridges within the study reach. These files were provided by the District, except for the 51st Avenue Bridge plans which were provided by the Maricopa County Department of Transportation. As part of the Lower Salt River FDS (WEST Consultants, Inc., 2015), DEA surveyed the 16th Street Bridge, 7th Street Bridge, and the 27th Avenue conveyor belt bridge. The as-built plans for the bridges are provided in Appendix B. Survey information for the three surveyed bridges is provided in Appendix B.

5.5.3 Levees and Dikes

From RM 217.76 upstream to RM 216.77 (the upstream limit of the study), there is a levee on the left bank of the Lower Salt River. In 2011, the City of Phoenix submitted a LOMR (TY Lin International, 2011a) and a levee certification package (TY Lin International, 2011b) to FEMA for review. The certification package was approved by FEMA on August 26, 2011, and the levee was accredited.

From RM 198.34 to RS 200.48, there is a levee on the right bank of the Salt/Gila River (i.e., the Tres Rios North Levee). The LACOE prepared a Design Document Report (DDR) in support of the levee certification (US Army Corps of Engineers, 2012) while WEST performed the hydraulic modeling and floodplain mapping (WEST Consultants, Inc., 2012). The certification package was approved by FEMA on December 4, 2012, and the levee was accredited (note that the updated floodplains in the area will not become effective until November 4, 2015).

Table 5-4. Bridge data source

Bridge Name	Data Source
Interstate 10 (RM 216.505)	Bridge as-built plans provided by the District, dated 1987
24th Street (RM 215.815)	Bridge as-built plans provided by the District, dated 1982
16th Street (RM 214.785)	Surveyed by DEA for the Lower Salt River FDS
7th Street (RM 213.745)	Surveyed by DEA for the Lower Salt River FDS
Central Avenue (RM 213.255)	Bridge as-built plans provided by the District, dated 1974
7th Avenue (RM 212.675)	Surveyed by DEA for the Lower Salt River FDS
19th Avenue (RM 211.525)	Bridge as-built plans provided by the District, dated 1985
27th Avenue Conveyor Belt (RM 210.435)	Surveyed by DEA for the Lower Salt River FDS
35th Avenue (RM 209.535)	Bridge as-built plans provided by the District, dated 2006
51st Avenue (RM 207.485)	Bridge as-built plans provided by Maricopa County Department of Transportation, dated 2001
115th Avenue Bridge or the Avondale Boulevard Bridge (RM 199.19)	Bridge as-built plans provided by the District, dated 1997
Bullard Bridge (RM 195.21)	Bridge as-built plans provided by the District, dated 1982
Estrella Parkway (RM 194.26)	Bridge as-built plans provided by the District, dated 1987
Cotton Lane (RM 192.42)	Bridge as-built plans provided by the District, dated 2006
Tuthill Road (RM 188.04)	Bridge as-built plans provided by the District, dated 1980
State Route 85 (RM 179.90)	Bridge as-built plans provided by the District, dated 1998

5.5.4 Non-Levee Embankments

During the study data collection phase, it was noted that there are numerous embankments in or near the main channel, separating the channel from lower-lying lands such as mining pits. The handling of these embankments is different than what was done for the floodplain delineation studies because the goal of the modeling was different. As mentioned earlier, some of these embankments have been engineered while others have not. If a sand and gravel pit had an engineered berm around the pit, then then it was assumed that the berm would remain in place during a flood event. In these cases, blocked obstruction was applied over the sand and gravel pit. If the sand and gravel pit did not have an engineered berm, then the berm was assumed to fail and the ineffective flow areas were removed from the pit.

Below the Rio Salado environmental restoration portion of the study reach (ending approximately one-half mile downstream of 7th Avenue) and near the 19th Avenue Bridge, large embankments were built to separate the river from two former landfill sites (one on the north side of the river and one on the south side of the river) as part of the 19th Avenue Landfill Environmental Cleanup project (Simons Li and Associates, 1995). These embankments have not been certified by FEMA. These non-levee embankments were modeled as ground points for this study.

In the Lower Gila portion of the study reach, there are spur dikes and one engineered non-levee embankments along the left bank downstream of Estrella Parkway between RM 193.85 and RM 194.25 (Stantec, 2014). The non-levee embankment was modeled as ground points for this study.

5.5.5 Islands and Flow Splits

The study reach does not contain any significant islands or flow splits.

5.5.6 Ineffective Flow Areas

For the most part, the Ineffective Flow Areas (IFAs) defined for the Lower Salt River FDS, the Tres Rios North Levee PMR, and the Lower Gila FDS were not changed for the combined model. The one exception was for the numerous gravel pits and mines that exist within the study area. When performing the floodplain delineation studies, it was assumed that the majority of these areas do not actively convey flow and IFAs were used to indicate that no water is conveyed through the sand and gravel mining pits. In addition, in-channel pits and pits that are hydraulically connected to the main channel were defined using blocked obstructions in the bottom of the pits to account for the likelihood they would fill up with sediment during a flood event.

As mentioned earlier, this modeling approach was not used for the sediment transport modeling. Some of the embankments around the pits have been engineered while others have not. If a sand and gravel pit had an engineered berm around the pit, then then it was assumed that the berm would remain in place during a flood event. In these cases, blocked obstructions were put in place of the pit. If the sand and gravel pit did not have an engineered berm, then the berm was assumed to fail and the ineffective flow areas were removed from the pit.

In addition, for in-channel pits and pits that are hydraulically connected to the main channel, the blocked obstructions in the bottom of the pits were removed in an attempt to model the pits filling up with sediment.

5.5.7 Supercritical Flow

Extended reaches of supercritical flow was not anticipated in the study reach, so the subcritical flow regime was defined in the Salt / Gila River HEC-RAS model for this study.

5.5.8 Sand and Gravel Operations

There are various sand and gravel mining operations in the study reach. The District provided WEST with mining plans and location maps (shape file) for most of the mining operations during a meeting held on March 25, 2015. Plans that were not located during that meeting were eventually found and provided to WEST. The Data Collection Report in Appendix A provides the summary of data for these sand and gravel mining operations along with figures showing the locations of the sand and gravel mining operations.

5.6 Floodway Modeling

Floodway modeling was not a part of this study.

5.7 Hydraulic Issues Encountered During the Study

5.7.1 Special Issues and Solutions

As previously discussed, the handing of the IFAs and blocked obstructions around the sand and gravel pits was different than what was used in the floodplain delineation studies because the goal of the modeling is different. This topic is discussed in Section 5.5.6.

5.7.2 Modeling Warning and Error Messages

The CHECKRAS results for the HEC-RAS base hydraulic model (existing and proposed conditions) are provided in Appendix C.

5.8 HEC-6T Base Hydraulic Model

Because HEC-6T sediment transport models were created in addition to the HEC-RAS sediment transport model, a base hydraulics model was created using HEC-6T. To create the HEC-6T base hydraulics model, the HEC-RAS hydraulics model was converted from HEC-RAS to HEC-6T. The process used in the conversion routine is described in Section 6.6. Once the base hydraulics HEC-6T model was created, the results were compared to the results from the HEC-RAS base hydraulics model. While some areas had good agreement between the HEC-RAS and HEC-6T hydraulic models, there were many areas within the study reach that had significant differences in results between the two models. After discussions with the District, it was decided that both base hydraulics models should yield similar results and that the results from the HEC-RAS base hydraulics model would be considered correct. Thus, the Manning's roughness values in the base hydraulics HEC-6T model were modified to improvement its agreement with the HEC-RAS base hydraulics model. This "calibration" of the HEC-6T base hydraulics model was accomplished by changing the Manning's roughness values in the HEC-6T base hydraulics model until its computed water surface elevations were within 1 foot of the water surface elevations computed by the HEC-RAS base hydraulics model for the 1%, 2%, and 10% annual change flows. A plot of a portion of the study reach comparing the HEC-RAS water surface elevations and the final HEC-6T water surface elevations for the base hydraulics model for the 1% annual chance flow is shown in Figure 5-2.

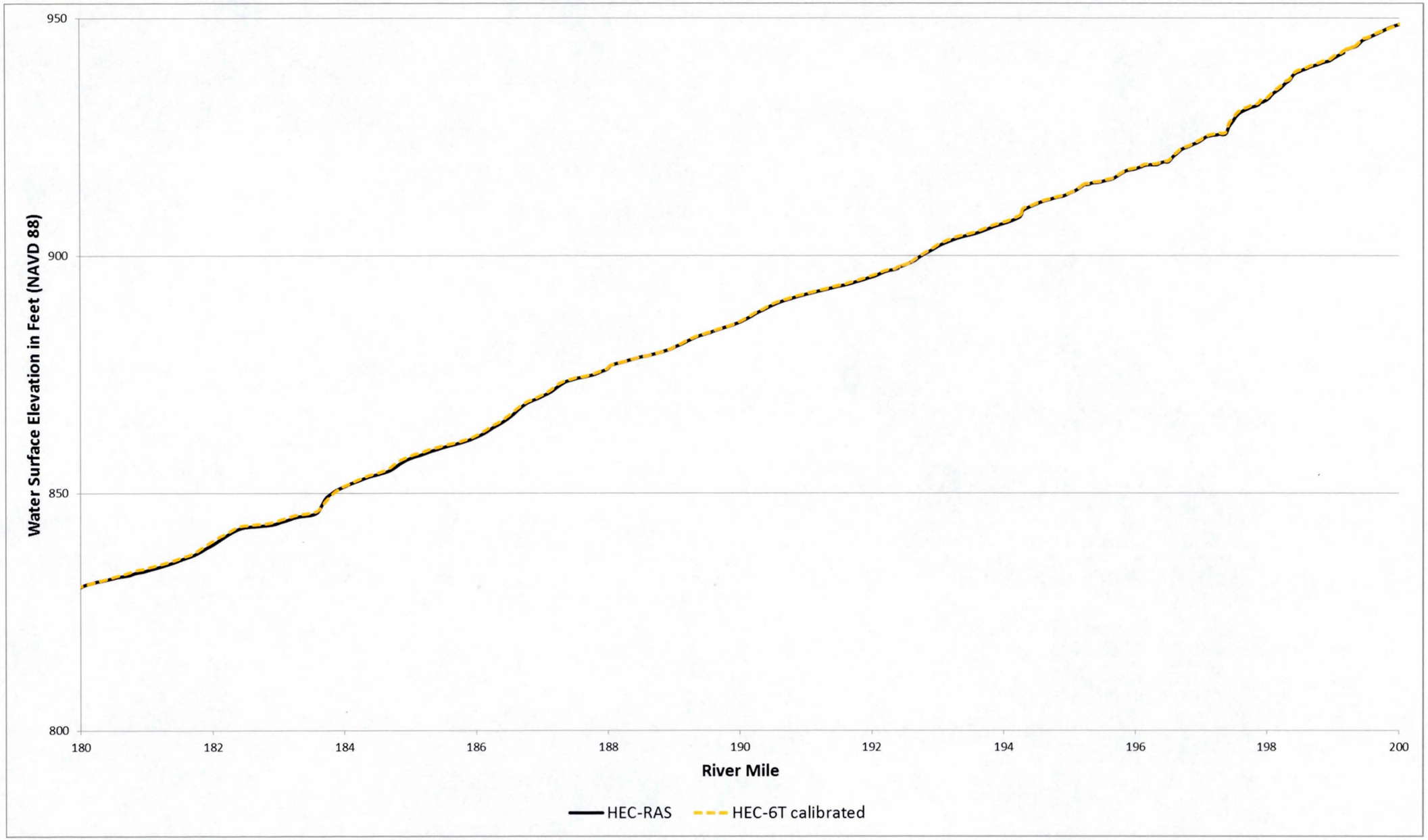

Figure 5-2. Comparison between the base hydraulic model water surface elevations (1% annual chance) for a portion of the study reach for HEC-RAS and the final adjusted HEC-6T model

5.9 Calibration

No measured field data was available for model calibration of the base hydraulic HEC-RAS model. However, a simplified calibration method was used for the sediment transport model as discussed in Section 6.

While not a true calibration, the base hydraulic HEC-6T model was modified by changing the Manning's roughness coefficients so that it agreed with the base hydraulic HEC-RAS model. A discussion of this process can be found in Section 5.8.

5.10 Final Results

5.10.1 Hydraulic Analysis Results

The existing conditions hydraulic model was created by stitching the HEC-RAS geometry files from Lower Gila FDS, Tres Rios PMR and Lower Salt FDS studies, and making few changes as described earlier in the report. Some of the changes included filling in the gap area with topography; removing ineffective flow areas and removing (or adding) blocked obstruction at sand and gravel pits; and modifying the downstream boundary condition. As few changes as possible were made to the models in order to retain their original results. In order to check the impact the changes made to the model had on the results, the 1% annual chance flood water surface elevations for the combined Salt/Gila River system were compared to the 1% annual chance flood water surface elevations for the original hydraulic models (see Figure 5-3).

The blue dashed line and the black line in the Figure 5-3 represents the 1% annual chance flood water surface elevations for the exiting conditions hydraulic model and the original hydraulic models, respectively. At the scale shown in Figure 5-3, very little difference can be seen between the two water surface profiles. Thus, the difference in water surface elevations between the existing conditions hydraulic model and the original models was also plotted in Figure 5-3 as red dots. The location of the sand and gravel mining operations are identified as yellow triangles at the top of the figure. Finally, there is a blank area in the middle of Figure 5-3. This is the gap area where there was no existing hydraulic model. For the most part, the differences between the existing conditions model and the original models are small (with most values under 0.5 feet). However, the deviation of water surface elevations was larger near the locations of sand and gravel mines (e.g., near 51st Avenue and Tuthill Road). The behavior was expected as the infective flow areas at sand and gravel pits had been altered in the existing conditions hydraulic model. The deviations near the end of the Tres Rios North Levee reach (i.e., around 115th Avenue) are due to changes in boundary conditions. Near 115th Avenue, the downstream boundary condition for the Tres Rios North Levee PMR study was set at a known water surface elevation for tie-in purposes for the floodplain study (WEST Consultants, Inc., 2012). Thus, deviations in the hydraulic model results at this location are not surprising.

To better examine the effect that modifying the ineffective flow areas and blocked obstruction areas around the sand and gravel mines had on the hydraulic results, a similar figure was prepared that compared the combined Salt/Gila River system hydraulic model without the pits alteration to the original hydraulic model results. The results shown in Figure 5-4 indicates that no observable deviations in water surface elevations are observed except near the downstream ends of the Lower Salt River FDS and the TRNL PMR. As explained above, these deviations are most likely due to changes in boundary conditions between the two models.

5.10.2 Verification or Comparison of Results

The input parameters for each of the HEC-RAS models were applied in a manner consistent with standard engineering practices for floodplain delineation and sediment transport modeling studies.

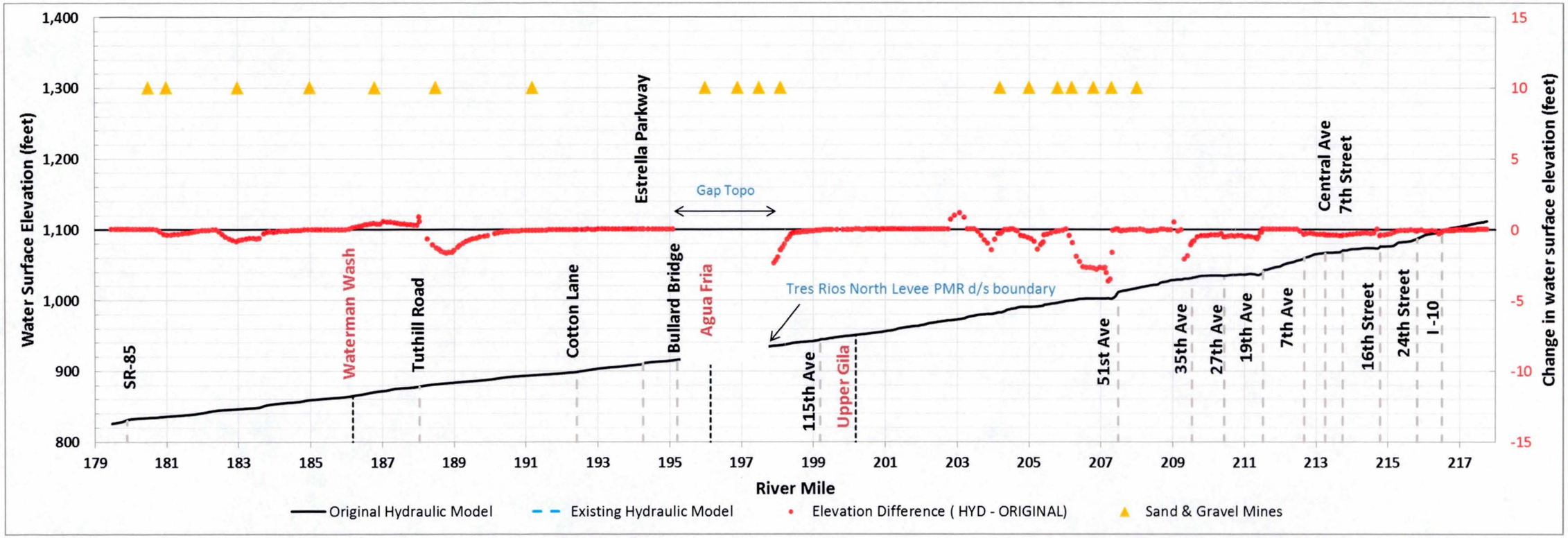

Figure 5-3. Comparison of 1% annual chance flood water surface elevation profiles between Salt/Gila existing conditions hydraulic model and the original hydraulic models from various past studies

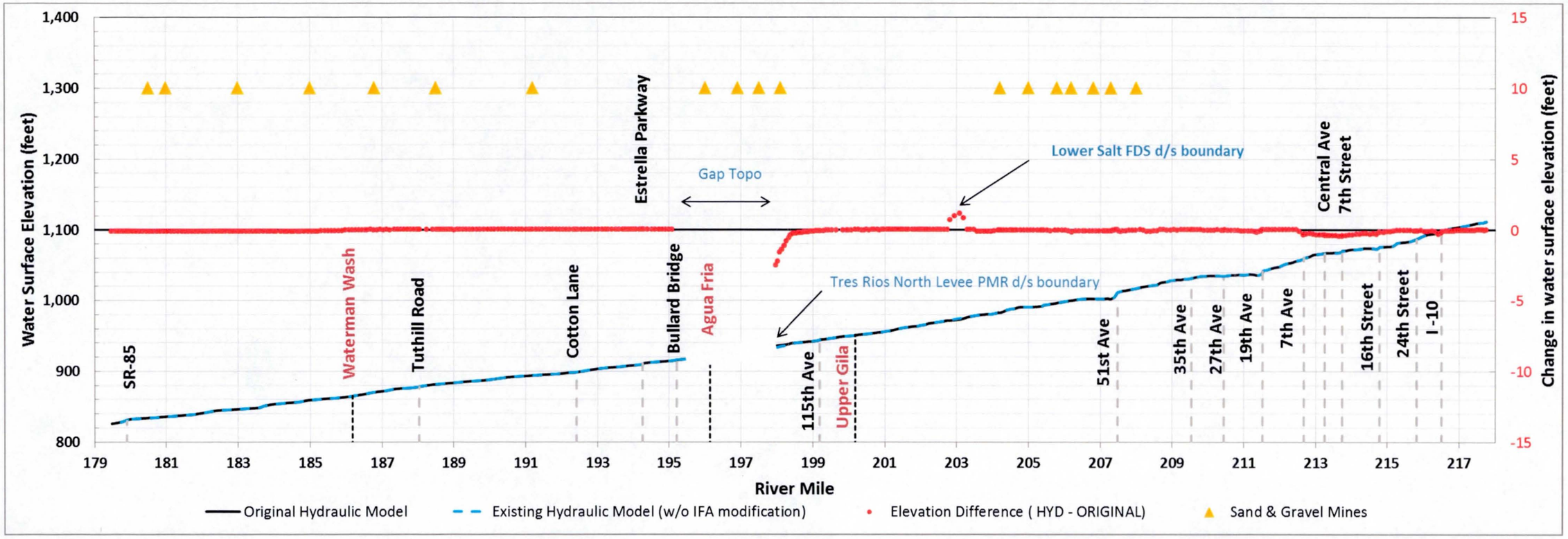

Figure 5-4. Comparison of 1% annual chance flood water surface elevation profiles between Salt/Gila existing conditions hydraulic model before IFA/blocked obstruction adjustments at the sand and gravel mines and the original hydraulic models from various past studies

6 Erosion, Sediment Transport, and Geomorphic Analysis

The main goal of this project is to develop a sediment transport model for the combined Salt/Gila River system from I-10 downstream to SR-85. Discussions in previous sections of this report focused on the development of the base hydraulic model that was created (using both HEC-RAS and HEC-6T) by stitching together four different previously developed models:

1. Lower Salt River FDS hydraulic model (WEST Consultants, Inc., 2015);
2. Tres Rios North Levee PMR hydraulic model (WEST Consultants, Inc., 2012);
3. Tres Rios North Levee PMR intermediate hydraulic model (WEST Consultants, Inc., 2012); and
4. Lower Gila River FDS hydraulic model (Stantec, 2014).

6.1 Previous Sediment Transport Modeling Studies

A range of sediment transport measurements and input information are available from prior and ongoing studies of the Salt/Gila River system. These reports include:

1. Rio Salado Low Flow Channel Design (WEST Consultants, Inc., 2000);
2. Rio Salado Oeste sediment transport study (WEST Consultants, Inc., 2002b);
3. Tres Rios North Levee Preliminary Engineering Design, or PED (WEST Consultants, Inc., 2002a);
4. El Rio Watercourse Master Plan (Stantec, 2006);
5. Gila River Sediment Program (Stantec, 2009);
6. Agua Fria River Sediment Trend Analysis (Kimley-Horn and Associates, 2001); and
7. Waterman Wash Sediment Transport Analysis (URS, 2011).

The Data Collection Report in Appendix A provides details on these previous studies. A short summary of each of these reports follows.

6.1.1 Rio Salado Low Flow Channel Design (RM 210.64 – RM 217.95)

This report was completed by WEST for the LACOE (WEST Consultants, Inc., 2000). It presents hydraulic, sediment transport and scour analysis for the design of the low flow channel in the approximately 5-mile study reach of the Salt River in Phoenix between the I-10 Bridge and the 19th Avenue grade control structure. A total of 33 bed sediment samples were collected by the LACOE upstream of the I-10 Bridge, at I-10 and just downstream of 19th Avenue. The locations of the samples are shown in Figure 6-1. Sieve analyses were conducted for sediment sizes less than 3 inches. For larger sizes, visual percent-mass estimates and photographs of the samples were taken. To determine the gradation of the active bed layer, samples between 0 and 6 feet deep were used. The sediment size in the bed was between 204.8 mm and 0.00725 mm. An HEC-6T model was developed and run for 30 days at the 20% annual chance peak discharge (20,200 cfs) with equilibrium load to determine the gradation of bed layer used in the sediment transport model.

The bed sediment composition was determined to be 20% sand, 60% gravel and 20% cobbles. Since the main suspended sediment material transported in the river was sand, the combination Toffaleti-Meyer-Peter and Müller (TMPM) sediment transport function was used for sediment modeling in HEC-6T. Laursen-Copeland transport function, which results in higher (gravel) transport, was also used to estimate maximum long-term scour. For the inflowing sediment load at the upstream reach of the model, the equilibrium sediment load volumes and gradations were calculated for a wide range of discharges.

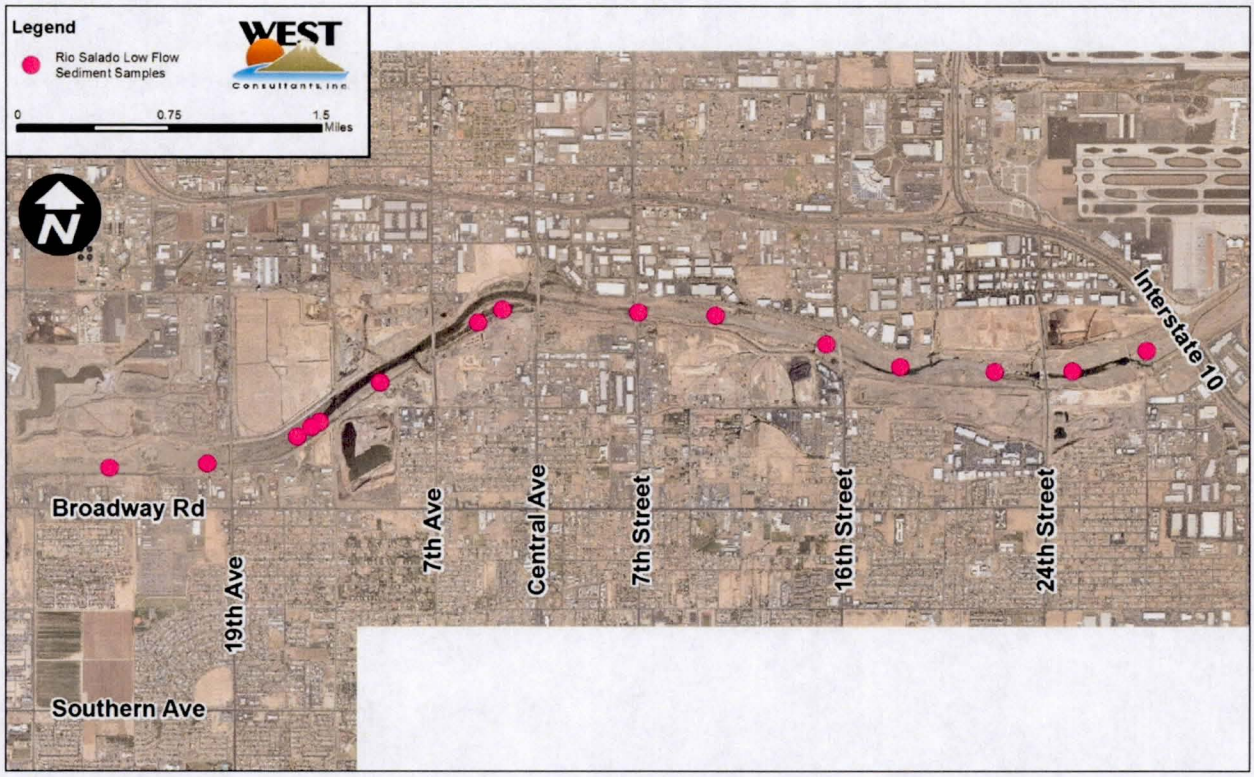

Figure 6-1. Sediment sample locations for the Rio Salado Low Flow Channel Design (WEST Consultants, Inc., 2000)

6.1.2 Rio Salado Oeste Sediment Transport Study (RM 202.09 – RM 211.21)

This study was conducted by WEST on behalf of the LACOE to develop hydraulic and sedimentation analysis of approximately 9.5 miles reach of Salt River between 19th Avenue and 91st Avenue in Phoenix (WEST Consultants, Inc., 2002b). The steady-state hydraulic model was developed in HEC-RAS to delineate flood inundation boundaries and to provide initial geometry for sediment transport analysis. The HEC-6T software was used for numerical sediment transport analysis. The USACE SAMAID program was used to determine the most suitable sediment transport function for the HEC-6T simulation. Yang's sediment transport function was selected for the final model.

Samples of bed materials were collected from 19 locations, 0.5 miles apart (see Figure 6-2). Samples were taken from 0 to 2 feet deep below the bed. In addition to laboratory sieve analysis of bed material

samples, an in-situ particle count consisting of 100 particles spaced at 1-foot intervals was performed. Inflowing sediment load volume and gradation at the upstream boundary of the model was based on an equilibrium analysis using the HEC-6T software. In the HEC-6T sediment transport model, the bed sediment reservoir depth was set to 20 feet and erosion was allowed only within the channel bank stations.

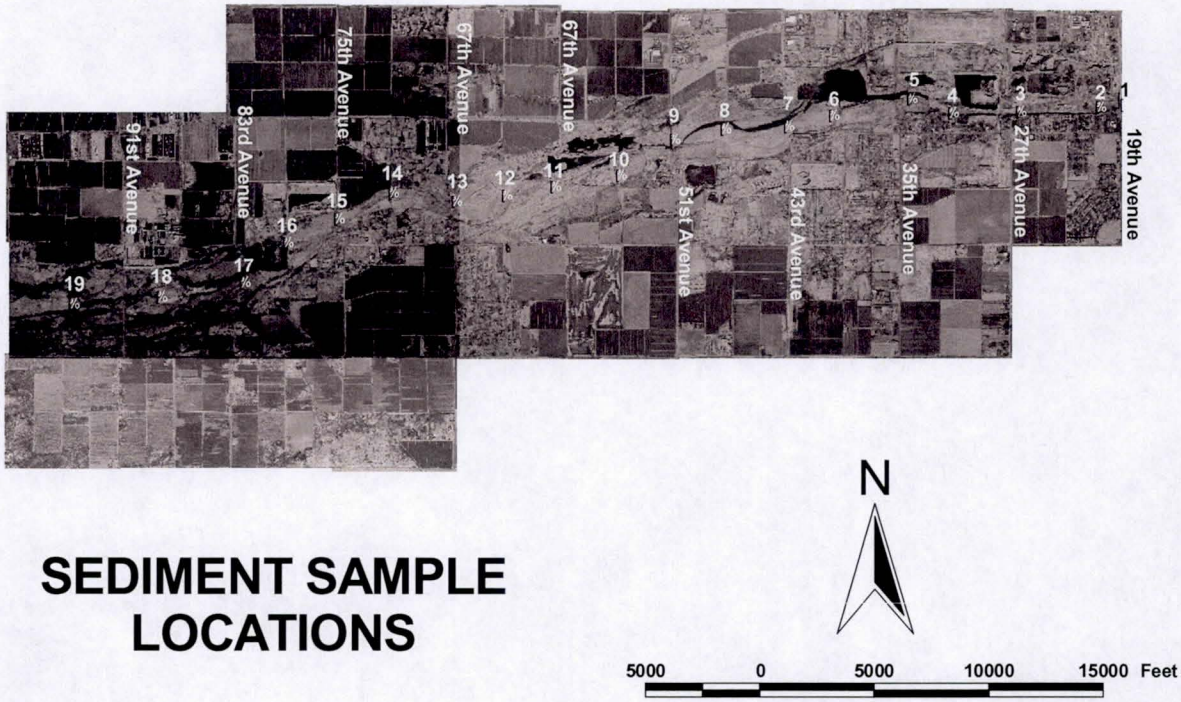

Figure 6-2. Sediment sample locations for Rio Salado Oeste (WEST Consultants, Inc., 2002b)

6.1.3 Tres Rios North Levee PED (RM 195.16 – RM 203.48)

This report was completed for the LACOE and summarized the Preliminary Engineering Design (PED) hydraulic study for the Tres Rios North Levee (WEST Consultants, Inc., 2002a). The project reach was located in the Salt/Gila River system in the Phoenix metropolitan area. The study reach was approximately 8.3 mile long, between 91st Avenue and the Agua Fria River confluence. The purpose of the study was to provide results of the hydraulic, sediment transport, and scour analysis for the design of the Tres Rios North Levee on the north bank of the river.

As a part of the study, the LACOE and WEST personnel collected 22 surface samples in Salt and Gila Rivers (see Figure 6-5). Sediment found at the confluence was used for modeling the Upper Gila River. HEC-RAS was used for hydraulic modeling, and a numerical sediment transport model using HEC-6T was developed using the TMPM sediment transport function. The inflow sediment load volume and gradations were derived from the outflowing sediment rating curve from Rios Salado Oeste model (WEST Consultants, Inc., 2002b).

6.1.4 El Rio Watercourse Master Plan (RM 178.61 – 199.07)

The El Rio Watercourse Master Plan was prepared by Stantec for the District (Stantec, 2006). The purpose of the sediment transport portion of the study was to document existing fluvial characteristics of the Lower Gila River, the desired form of the river, and its future functions. The limits of the study were from the Lower Gila River's confluence with the Agua Fria River downstream to SR-85. An HEC-6T sediment transport model was developed to assess sedimentation and scour processes and to evaluate various structural and nonstructural flood management alternatives. Twelve bed sediment samples were collected as the part of the project. The gradation of bed samples is shown in Figure 6-3 and the sampling locations are shown in Figure 6-5.

In the sediment model, Salt River was modeled as the main stem and Upper Gila as a local inflow. Yang's Stream Power function was used for sediment transport analysis in HEC-6T. The inflow sediment rating curves were based on the analysis and interpretation of USGS data collected near Gillespie Dam. Salt River sediment inflow included: clay, 4 silt sizes, 5 sand sizes and 1 gravel size, with 10% of the total inflowing sediment load coarser than 0.062 mm. Upper Gila sediment inflow included: clay, 4 silt sizes and 5 sand sizes, with 20% of the total inflowing sediment load coarser than 0.062 mm.

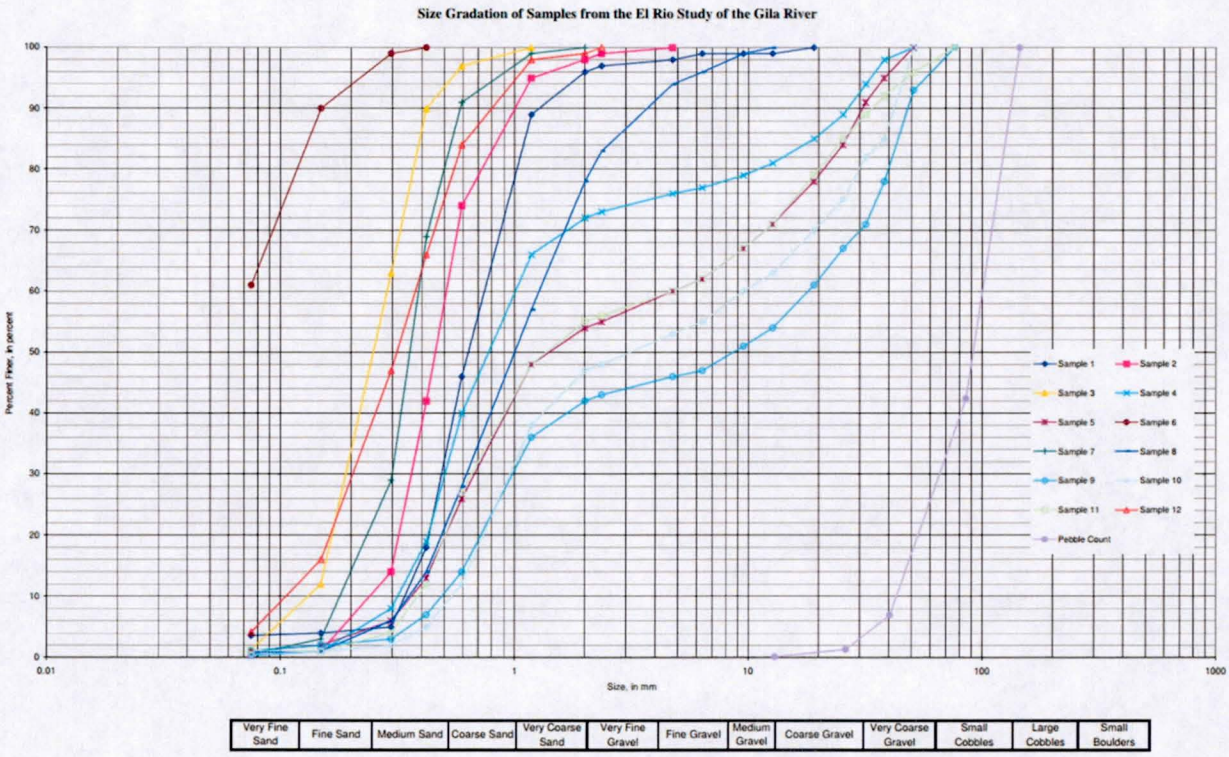

Figure 6-3. Summary of gradations for the sediment samples collected on the Lower Gila River (Stantec, 2006)

6.1.5 Gila River Sediment Program (115th Ave – SR85)

As a part of Gila River Sediment Program, Stantec prepared a report (Stantec, 2009) characterizing bed material size gradation of the Gila River between 115th Avenue and SR85 for the District. Many old and new field data were collected for this purpose. The sample locations taken for this study are shown in Figure 6-5. A statistical analysis procedure was developed to classify bed material samples. Sieving analysis of the samples was performed to develop size gradations.

Source of Samples (1)	No. of Samples (2)
1. For this District project by Stantec:	
Used by Julien and Mielke to develop MRPP	29
Used by Julien and Mielke to test MRPP	18
Used by Stantec to classify samples	12
	59
2. For the El Rio WMP by Stantec (Stantec, 2005)	12
3. For Burlingame by Construction Inspection & Testing Co.	8
4. For the Gila River at Airport Road crossing by Terracon	13
5. For the Cotton Lane Bridge CLOMR by River Research & Design (R2D, 2008)	4
6. For Cotton Lane Bridge by Richer-Atkinson-McBee & Associates for Michael Baker Jr., Inc. (RAM, 2005)	7
7. For Tres Rios North Levee by WEST Consultants, Inc. (WEST, 2004)	7
	110

Figure 6-4. Source of bed material samples for Gila River Sediment Program (Stantec, 2009)

Out of 47 bed material samples of Gila collected during the study, 29 of them were used to develop the statistical tool to classify the bed material. The remaining 18 samples and the samples from other studies (items numbers 2 to 7 in Figure 6-4) were used to test the statistical tool. The important findings from this study are summarized below:

- Soil in the overbank was mainly composed of very fine sand, silt, and clay. Classified as Type A in this study, it represented the wash load that entered the river from the watershed during the runoff.
- Bed material in the study area of Gila River was represented by two sediment types: Type B and Type C. Type B was mainly composed of fined to coarse sand while Type C was composed of very coarse sand, gravel and some small cobbles.
- Type C bed material was more dominant than Type B throughout the study reach.
- In nearly 75 percent of the sampling location, the material was of uniform grain size throughout the depth.
- The surface of the bed was mostly covered by cobbles and gravel. The gravel deposit, however, was not representative of the bed material of the river. The gravel deposits were the result of scour of finer bed material from the bed.

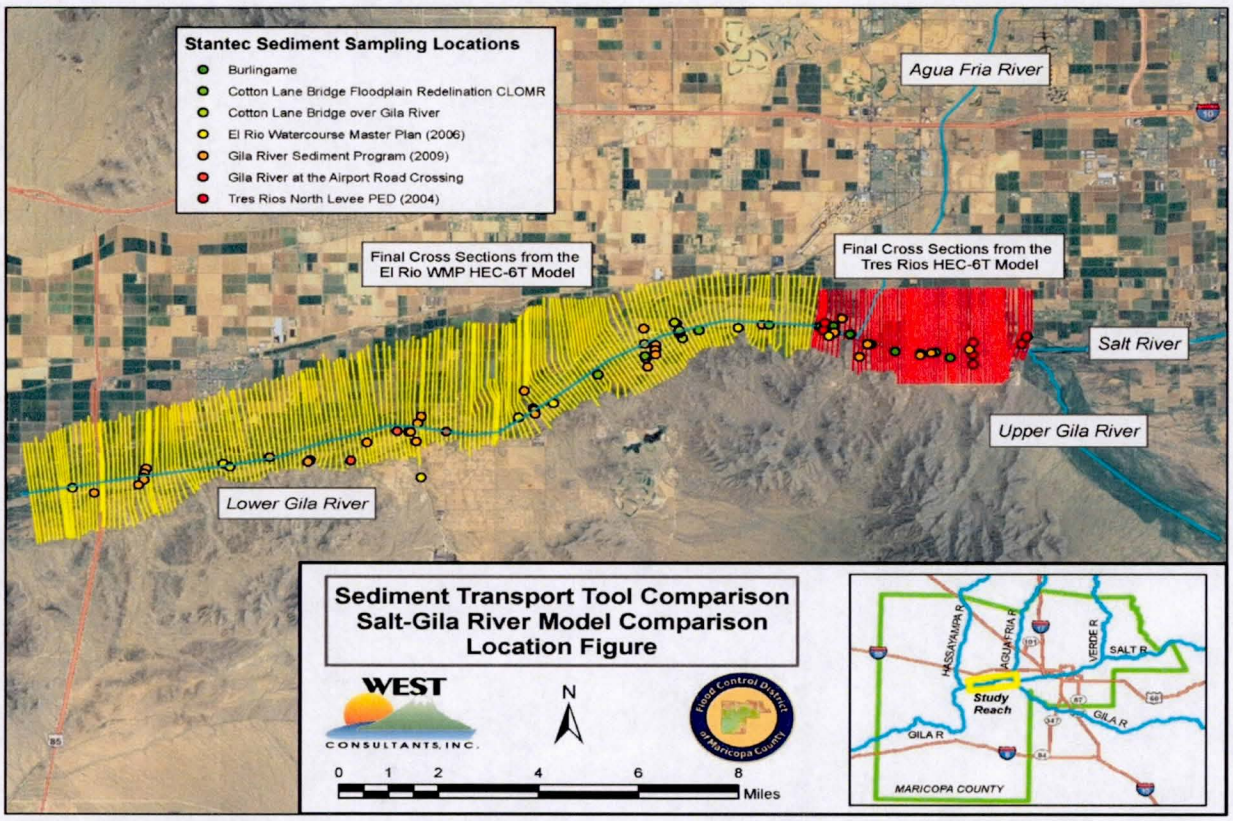

Figure 6-5. Sediment sample locations for Tres Rios North Levee PED (WEST Consultants, Inc., 2002a), the El Rio Watercourse Master Plan (Stantec, 2006), and the Gila River Sediment Program (Stantec, 2009)

6.1.6 Agua Fria River Sediment Trend Analysis

As part of the Agua Fria Watercourse Master Plan, KHA prepared a sediment trend analysis of the Agua Fria River for the District (Kimley-Horn and Associates, 2001). The purpose of the sediment trend analysis was to predict and evaluate the long-term and flood response of the streambed profile of the Agua Fria River based on existing, proposed, and alternative development conditions of the river. The study reach extended from the downstream confluence of the Agua Fria River with the Gila River to the upstream diversion outlet downstream of the New Waddell Dam. The total length of the reach was approximately 33.8 miles.

KHA used the HEC-6 program for sediment modeling. The models included an existing river condition model, a model representing the full sand and gravel mining condition in the reach, a full encroachment model, and a grade control structure model. Four sediment transport functions were selected for the analysis: Yang's stream power, Toffaleti-Schoklitsch (TS), Meyer-Peter and Müller (MPM), and Toffaleti-MPM (TMPM). Bed sediment gradations for the model were developed from 42 samples collected by KHA. The samples were collected every half-mile from the Gila River confluence to north of SR-74.

6.1.7 Waterman Wash Sediment Transport Analysis

The technical memorandum with subject "RVAMP – Waterman Wash Sediment Transport Analysis" was prepared by URS for the District (URS, 2011). The memorandum contains the fluvial analysis for both a single storm event and a long-term flood event of Waterman Wash located in Rainbow Valley. The Waterman Wash study reach starts at the confluence with the Lower Gila River and extends approximately 16.4 miles upstream. For channel hydraulic and sediment transport modeling, HEC-RAS version 4.1 was used. Historical aerial images and empirical methods were used to develop the channel geometry for the model. The frequency hydrograph for upstream study reach and tributaries were obtained from the Rainbow Valley ADMP Hydrology Report (URS, 2010).

Sediment samples were collected from channel bed and banks of the study area. The sediment predominately consisted of gravels and coarse sands. The median grain size was in the range 0.15 to 12.7 mm. Sieve analyses were done to calculate the sediment gradations. Based on the channel characteristics, the Meyer-Peter Müller (MPM) transport function was used for the sediment transport model. Due to the lack of gaged flow and sediment data, equilibrium sediment transport rating curves were developed to estimate the sediment inflow from the upstream reach and the tributaries. These curves were based on grain size distribution of supply reaches, an estimated range of peak flows, hydraulic characteristics of the supply reaches, and the MPM transport function.

6.2 Sediment Transport Modeling Data

Additional input data are needed for a sediment transport beyond the data needed for a hydraulic model. These data include:

1. Definition of the hydrology for the sediment transport model;
2. Definition of the bed material sediment gradations;
3. Definition of the moveable bed boundary limits;
4. Definition of the inflowing sediment load from main stem channel and tributaries; and
5. Selection of the sediment transport function.

6.2.1 Sediment Transport Model Hydrology

The hydrology for the sediment transport models was based on historic flood records as well as the 1% annual chance flood hydrograph. Inflow hydrographs were specified at the upstream limit of the study (near the I-10 Bridge), at the confluence of the Salt and Gila Rivers, at the confluence of the Gila and Agua Fria Rivers, and at the confluence of the Gila River and Waterman Wash. The historic flood records used for this study are discussed in Section 4.2. The 1% annual chance flood hydrographs used in this study are discussed in Section 4.3.

6.2.2 Bed Material Sediment Gradations

As mentioned previously, the sediment gradations used in this study were taken from previous reports. From I-10 Bridge to 19th Avenue, the sediment samples from the Rio Salado Low Flow Channel study were used (WEST Consultants, Inc., 2000). In this study, a total of 33 bed sediment samples were collected by the LACOE and the locations are shown in Figure 6-1. The sediment samples were taken as deep as 16 feet below the bed. Sieve analysis was conducted for sediment size less than 3 inches. For larger sizes, visual percent-mass estimates and photographs of the samples were taken. To determine the gradation of the active bed layer, samples between 0 and 6 feet deep were used. The sediment size in the bed was between 0.00725 mm and 204.8 mm.

From 19th Avenue to 91st Avenue, the sediment gradations from the Rio Salado Oeste project were used (WEST Consultants, Inc., 2002b). Samples of bed materials were collected from 19 locations (see Figure 6-2), 0.5 miles apart. Samples were taken from 0 to 2 feet deep below the bed. In addition to laboratory sieve analysis of bed material samples, an in-situ particle count consisting of 100 particles spaced at 1 foot intervals was performed.

From 91st Avenue to the confluence with the Agua Fria River, sediment gradations were taken from the Tres Rios North Levee PED study (WEST Consultants, Inc., 2002a). As a part of the study, the LACOE and WEST personnel collected 22 surface samples in Salt and Gila Rivers. The locations of the sediment samples for Tres Rios North Levee PED study are shown in Figure 6-5.

From Salt/Gila River confluence with Agua Fria River to SR-85, the sediment gradations were taken from the El Rio Watercourse Master Plan (Stantec, 2006). Twelve sediment samples were taken from the study reach to develop the gradations. The locations of the sediment samples for El Rio Watercourse Master Plan and the Gila River Sediment Program are shown in Figure 6-5.

The bed gradation data reflected in the Salt/Gila River sediment transport model are shown in Figure 6-6, Figure 6-7 and Figure 6-8.

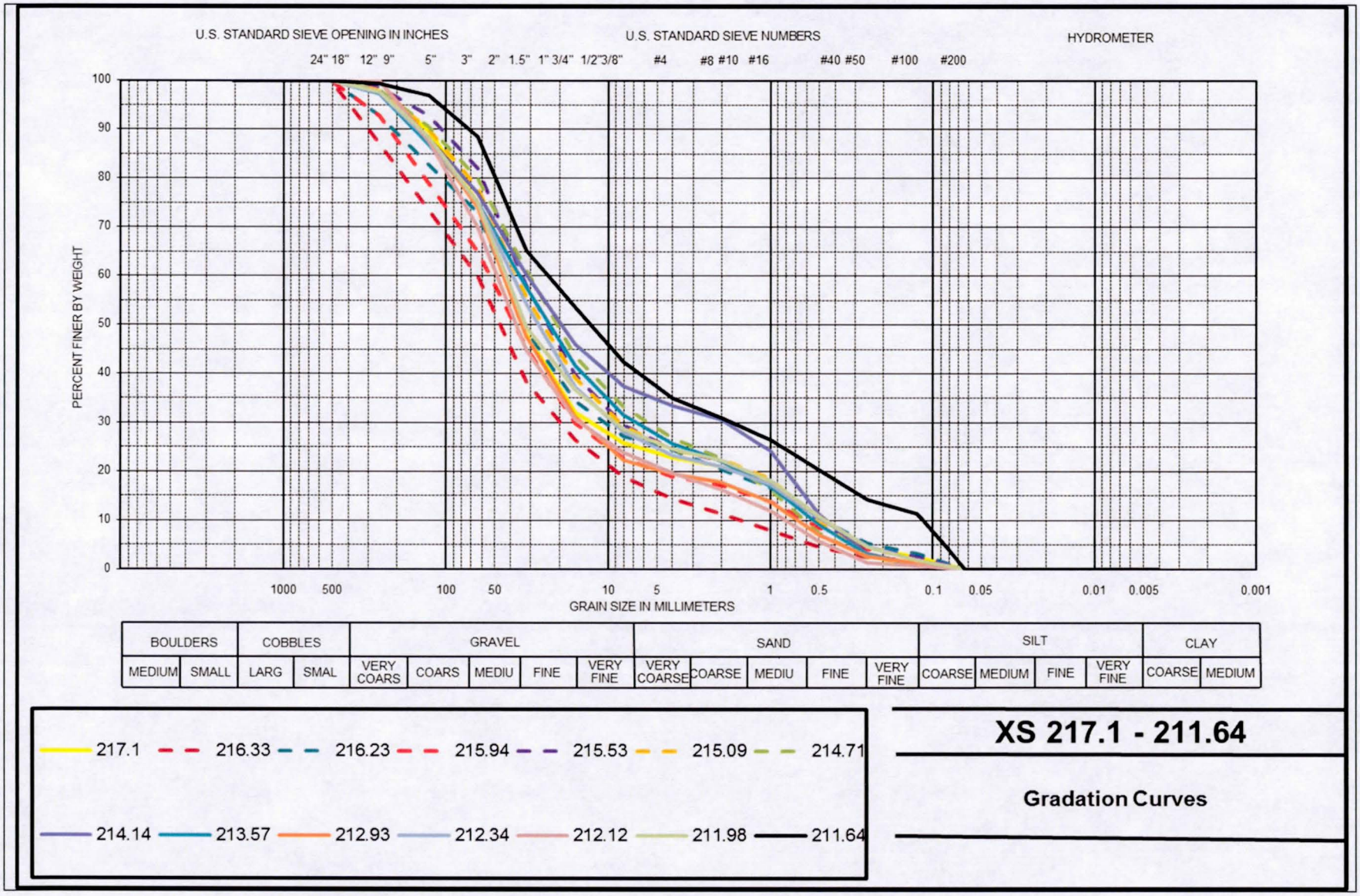

Figure 6-6. Bed gradation data for cross-sections between RM 211.64 and RM 217.1

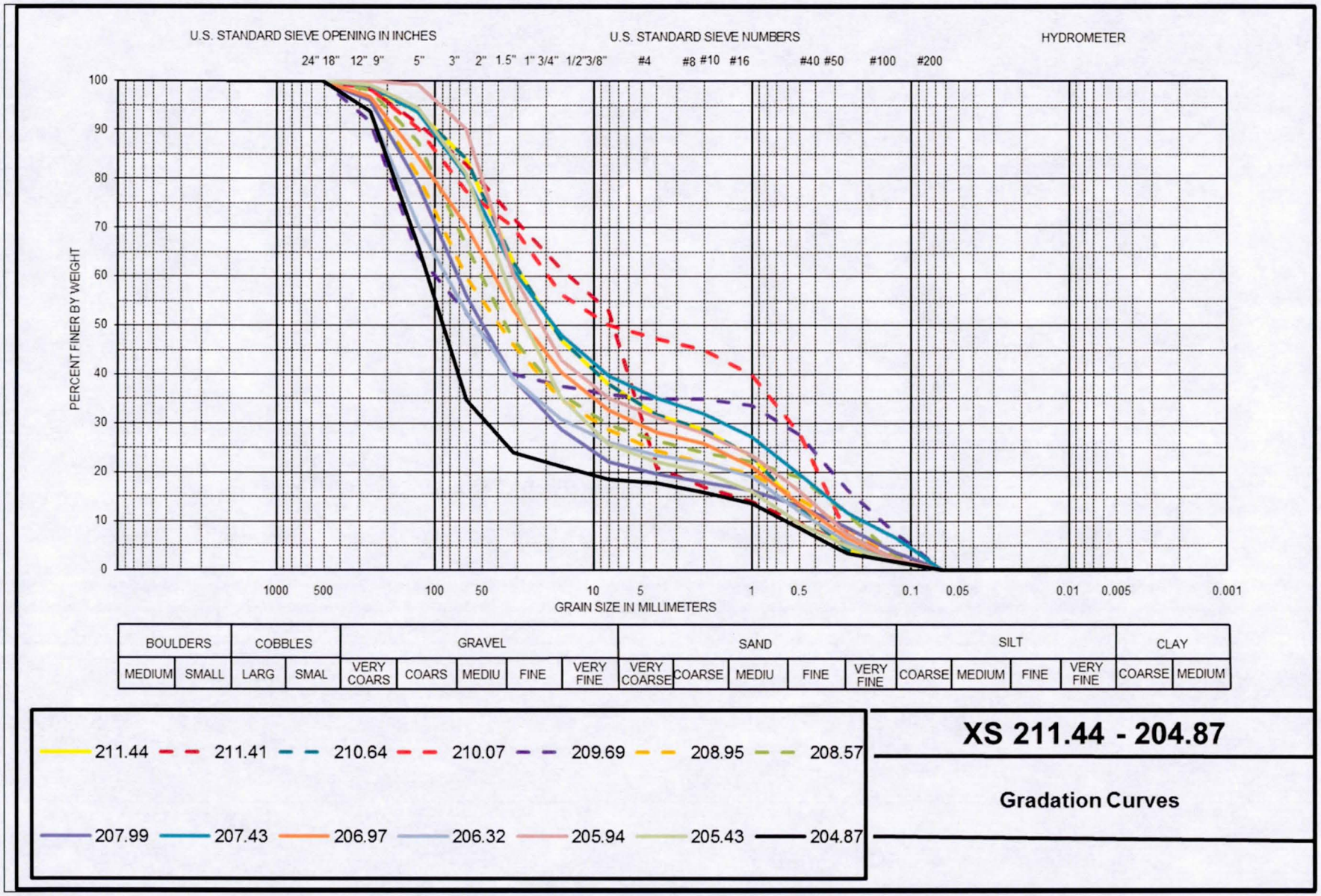

Figure 6-7. Bed gradation data for cross-sections between RM 204.87 and RM 211.44

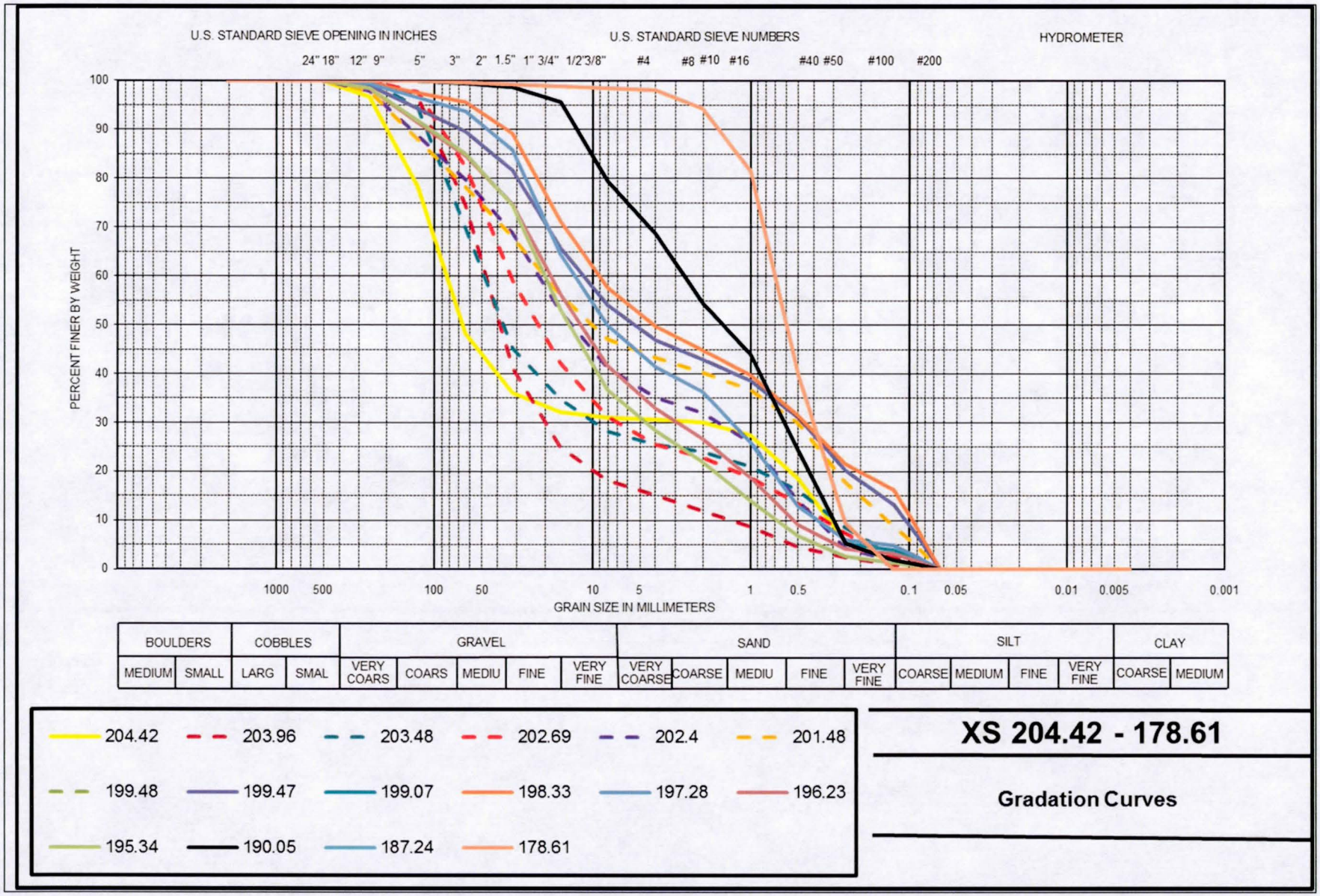

Figure 6-8. Bed gradation data for cross-sections between RM 178.61 and RM 204.42

6.2.3 Moveable Bed Boundary Limits

The end points of erosional/depositional limit were initially assumed to be 300 feet outside of the left and right bank stations. In the final sediment transport model, the limits were within the main channel (i.e., the moveable bed limits were set at the cross-sections bank stations). For the cross-sections with sand and gravel pits without berm protection, the erosional/depositional limits were expanded to include the pits.

Apart from cross-sections containing the grade control structures, the maximum erosional bed depth of 20 feet was assumed.

6.2.4 Inflow Sediment Loads

Locations of sediment inflows in the Salt/Gila River study reach are shown in Figure 6-9. At the upstream end of the model (i.e., the I-10 Bridge) the sediment boundary condition is based on inflow sediment rating curve develop for the Rio Salado Low Flow Channel study (WEST Consultants, Inc., 2000) and listed in Table 6-1. In the Rio Salado Low Flow Channel study, the Toffaleti, Meyer-Peter Müller (TMPM) transport function was used to calculate equilibrium bed material load for a range of discharges up to 166,000 cfs. The equilibrium sediment load calculations were performed in HEC-6T model between the cross-sections 217.38 and 217.95, just upstream of the I-10 Bridge, using an average slope of 0.0022 ft/ft. The sediment load in Rio Salado Low Flow Channel study was defined with 13 classes of sediment sizes representing the bed material. The smallest size was Very Fine Sand (VFS) and the largest one was Small Boulders (SB). The equilibrium load calculated by HEC-6T also provided the fraction of each sediment classes.

There are three tributaries in the study reach: Upper Gila, Agua Fria and Waterman Wash (labeled as 2, 3, and 4, respectively, in Figure 6-9). In the current study, these washes were not modelled explicitly. Instead their sediment contribution was accounted for by using sediment inflow rating curves at their respective confluences. These inflow rating curves were either developed or obtained from results of past sediment transport studies on these tributaries.

The sediment inflow rating curve for the Upper Gila River was obtained from the Sediment Transport Tool study report (WEST Consultants, Inc., 2011). In this study, the sediment outflow of the Upper Gila River at the confluence with Salt/Gila River system was estimated using the HEC-6T sediment model from the Tres Rios North Levee PED (WEST Consultants, Inc., 2002a). The range of the rating table was expanded by adding few points for low and high flows by extrapolation. The sediment inflow rating curve for the Upper Gila River is shown in Table 6-2.

The sediment inflow rating curve for the Agua Fria River was developed using the downstream sediment outflow condition from the Agua Fria River sediment transport model (Kimley-Horn and Associates, 2001). From the model results, best fit curves were calculated for total sediment load and sediment load for individual grain sizes. Based on these curves, the sediment load-discharge relationships for the Agua Fria River were developed. This process was previously completed in the Sediment Transport Tool study (WEST Consultants, Inc., 2011). The rating table from WEST (2011) was extrapolated for low and high flows. The sediment inflow rating curve for the Agua Fria River is provided in Table 6-3.

A similar approach was used to develop the sediment inflow rating curve for Waterman Wash. From the HEC-RAS sediment transport model results for Waterman Wash (URS, 2011), best fit curves were calculated for total sediment load and sediment load for individual grain sizes. Based on these curves, the sediment load-discharge relationships for Waterman Wash were developed. The sediment inflow rating curve from the Waterman Wash is shown in Table 6-4.

Figure 6-9. Locations of sediment inflow (marked by an arrow and number) in the study reach: (1) I-10 Bridge, (2) Upper Gila, (3) Agua Fria and (4) Waterman Wash

Table 6-1. Upstream sediment inflow boundary condition (WEST, 2000)

Q (cfs)	100	500	1,000	6,000	12,200	20,200	53,000	87,000	166,000
Q_s (tons/day)	10	284	646	5,458	16,140	30,679	90,000	153,700	321,120

Table 6-2. Sediment inflow rating curve for the Upper Gila River (WEST, 2011)

Q (cfs)	100*	9,000	13,000	18,000	21,000	32,000	38,000	46,000	100,000*
Q_s (tons/day)	1	6,514	7,282	11,953	14,123	24,263	24,683	34,988	92,292

* extrapolated values

Table 6-3. Sediment inflow rating curve for the Agua Fria River (Kimley-Horn, 2001)

Q (cfs)	100*	1,000*	5,800	9,000	20,000	30,000	44,000	54,000	70,000*
Q_s (tons/day)	134	3184	40,055	76175	137,211	262,483	561,655	981,454	1,095,520

* extrapolated values

Table 6-4. Sediment inflow rating curve for the Waterman Wash

Q (cfs)	10	1,000	2,000	4,000	5,000	7,000	9,000	11,000	13,000
Q_s (tons/day)	7	1,012	2,122	4,451	5,650	8,094	10,587	13,119	15,683

6.2.5 Selection of the Sediment Transport Function

The Rio Salado Low Flow study reach was used for calibration of sediment parameters including the sediment transport function. During the calibration process, HEC-6T sediment model (WEST Consultants, Inc., 2000) was run for the period 2000 to 2013 using several sediment transport functions available in HEC-6T. Results showed that the sediment transport functions did not have significant effects on the resulting topography of the river. As a result, TMPM and Yang sediment transport functions were considered in the calibration of the HEC-RAS sediment transport model since they have been considered suitable for the Salt/Gila River system by past reports. The overall spatial pattern of bed elevation from both HEC-6T and HEC-RAS calibration runs showed Yang's sediment transport function was slightly better than TMPM function. Hence, Yang's transport function was selected for sediment transport analysis of Salt/Gila River system. The details of the calibration process are discussed in Section 6.5.

6.3 Development of the Existing Conditions HEC-RAS Sediment Transport Model

The geometric data of the existing conditions combined Salt/Gila River HEC-RAS base hydraulic model was used in the HEC-RAS sediment transport model. Initially, the number of cross-sections was thinned by removing nearly half of the cross-sections that are present in the hydraulic model to improve numeric stabilities of the sediment transport model. This change also has the benefit of allowing for a larger computational time step, which reduces the overall run time. In this case, run time is quite important because even with these changes, run times are approximately 30 hours. However, after discussions with the District, it was decided to have the existing conditions sediment transport model be based on all the cross-sections present in the hydraulics model in an effort to better capture the sediment transport in the pits.

The end points of erosional/depositional limit were defined to be within the main channel. For the cross-sections with sand and gravel pits without berm protection, the erosional/depositional limits were expanded to include the pits. Apart from cross-sections containing the grade control structures, the maximum erosional bed depth of 20 feet was assumed. In certain cross-sections where the IFAs were removed from the sand and gravel pits as a part of hydraulic model development and where the pit was not located in the main channel, the invert elevation of the pit was so low that no flow occurred in the main channel. This resulted in termination of the sediment transport model run since the sediment transport calculations are based on the main channel flow. Thus, in these situations, IFAs were added in the pit at the elevation of the bank station to have the low flows contained within the main channel and to eliminate the model error from the deep offline pits.

6.4 Development of the Proposed Conditions HEC-RAS Sediment Transport Model

The geometric data of the proposed conditions combined Salt/Gila River HEC-RAS hydraulic model was used to develop the HEC-RAS sediment transport model. As with the existing conditions sediment transport model, the proposed conditions sediment transport model utilized all the cross-sections from the hydraulic model. For the proposed conditions model, it was also assumed that all the permitted

sand and gravel pits were built out according to their permitted mining plan. The summary of the cross-section modifications for the proposed condition model is shown in Table 5-1.

Other modifications were similar to the exiting condition sediment model geometry. The bank stations were used to limit the erosion/deposition within the main channel for all cross-sections except the cross-sections with sand and gravel pits where the limits were expanded to include the pits. Apart from cross-sections containing the grade control structures, the maximum erosional bed depth of 20 feet was assumed. For cross-sections with offline pits deeper than the main channel invert, IFA's were added in the pit at the elevation of the nearest bank station in order to prevent the model from crashing.

6.5 Calibration of the Existing Conditions HEC-RAS Sediment Transport Model

Since calibration of the entire model reach is not possible for various reasons, calibration was performed on an individual reach of the overall study area. After discussions with the District, the Rio Salado Low Flow study reach (approximately I-10 to 24th Avenue) was chosen for the calibration process. The initial geometry (2000 condition) and sediment models of the study were taken from the Rio Salado Low Flow study (WEST Consultants, Inc., 2000). The final geometry (2013 condition) was obtained from the recent Lower Salt FDS (WEST Consultants, Inc., 2015). Calibration was completed for both the HEC-RAS and HEC-6T models. The calibration period was from 2000 to 2013. Note that the vertical datum used in the calibration process was NGVD29 and not NAVD88.

6.5.1 The Calibration Reach

The calibration reach was chosen to be the study reach for the Rio Salado Low Flow Channel Design study (WEST Consultants, Inc., 2000). The Rio Salado Low Flow Channel Design reach was found to be the most suitable reach for the calibration because of the comparatively fewer man-made changes in this reach. The upstream boundary of the calibration reach is RM 217.95 and the downstream boundary is at RM 210.64. Because of the observed mining activity near the downstream boundary, only the reach upstream of RM 211.49 was considered for result comparisons during the calibration. A grade control structure exists near RM 211.49, which is close to the 24th Avenue Bridge. Downstream of this bridge, there appears that sand and gravel mining activities have occurred as evident in the thalweg profile plot in Figure 6-10.

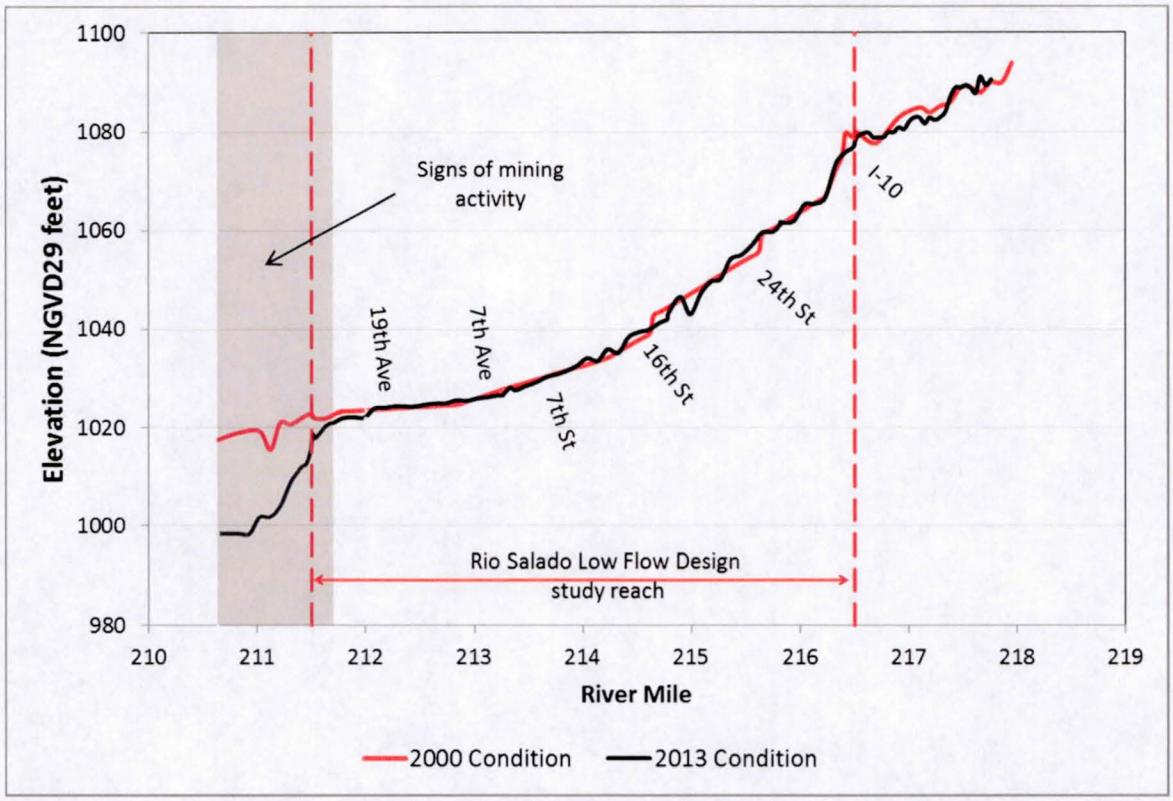

Figure 6-10. Thalweg profile for the initial and final geometry of the calibration reach

6.5.2 Geometric Data for the Calibration Reach

Based on the available topographic data and hydrological records of the study reach, the calibration period was set between 2000 and 2013. The Rio Salado Low Flow Channel Design project used existing condition topography from the year 2000 and applied low flow design cuts to develop the cross-section geometry for the hydraulic and sediment models (WEST Consultants, Inc., 2000). This geometry was considered as the initial condition for the calibration model assuming that the area outside of the low flow channel is representative of the conditions after the channel was constructed in 2000.

The latest geometric data of the study reach was obtained from the Lower Salt FDS (WEST Consultants, Inc., 2015), which is based on the 2013 topographic dataset. This geometric data was used as the final condition for the calibration reach of the models. The final condition geometry used NAVD88 vertical datum. It was much easier and reliable to convert final geometry to NGVD29 in HEC-RAS than to convert the initial geometry (available as HEC-6T cross-sections) to NAVD88. Therefore, NGVD29 datum was used for the calibration runs.

6.5.3 Calibration Runs

Calibration runs were performed using both the HEC-RAS and HEC-6T sediment models of the Rio Salado reach. The Rio Salado Low Flow Design study (WEST Consultants, Inc., 2000) used an HEC-RAS model for the hydraulic analysis and an HEC-6T model for the sediment transport analysis. The calibration of the HEC-6T model for this study utilized the same HEC-6T sediment model as Rio Salado Low Flow Design. To

perform the calibration with HEC-RAS, the HEC-RAS hydraulic model for Rio Salado was converted into an HEC-RAS sediment model by incorporating sediment data such as bed gradation, erosion/deposition limit, and grade control structures, etc. All of these data were readily available in the HEC-6T sediment model of the Rio Salado reach (i.e., the calibration reach). However, there were certain differences between the HEC-RAS hydraulic model for the Rio Salado reach and the HEC-6T model that posed difficulty while developing the HEC-RAS calibration sediment model.

6.5.3.1 Discrepancies between Rio Salado HEC-RAS hydraulic model and HEC-6T sediment model

There were several discrepancies between Rio Salado HEC-RAS hydraulic model and HEC-6T sediment model. First, there were small differences in the reach lengths between the two models (i.e., the Rio Salado HEC-RAS hydraulic model and the Rio Salado HEC-6T sediment model).

Second, the model extents were different between the two models. The Rio Salado HEC-RAS hydraulic model (RM 207.99 to RM 217.95) extended beyond the current calibration study reach (RM 210.64 to RM 217.95). The Rio Salado hydraulic model was extended further downstream in order to reduce the boundary condition effect (WEST Consultants, Inc., 2000). A stage rating curve at RM 210.64 was developed using the hydraulic model and this curve was used as the boundary condition in the HEC-6T sediment model (WEST Consultants, Inc., 2000).

Third, the Rio Salado Low Flow Design HEC-RAS model had approximately twice as many cross-sections as the HEC-6T model. For the HEC-RAS sediment calibration model, the additional cross-sections were deleted so that both models (i.e., Rio Salado Low Flow Design HEC-RAS model and HEC-6T sediment model) had same cross-sections in all locations except near the bridges.

6.5.3.2 Discrepancies between Rio Salado models and the Lower Salt River FDS model

There were also discrepancies between the initial (i.e., Rio Salado models or 2000 condition) and the final geometries (i.e., Lower Salt FDS or the 2013 condition) that caused problems in developing the HEC-RAS sediment calibration model. The discrepancies between the two geometries included bridge information, cross-sectional reach length, and lateral extent of the cross-sections. These discrepancies were resolved using the latest available information from the 2013 geometry.

6.5.4 Hydrology and Inflowing Sediment Load for the Calibration Runs

As already mentioned above, the calibration was performed using both HEC-RAS and HEC-6T sediment model of the Rio Salado reach for the period between 2000 and 2013. The upstream boundary discharge time series of the calibration model was based on the observed daily discharges at the Priest Drive gage (District gage 4523). No flow periods were excluded while days with less than 100 cfs were assigned 100 cfs. It should be noted that flow of 100 cfs or less is very small to have major influence on the sediment transport results. The flow time series used as input to the calibration model is shown in Figure 6-11. The inflowing sediment load rating curve was same as the Rio Salado Low Flow Channel Design study (WEST Consultants, Inc., 2000) and is shown in Figure 6-12.

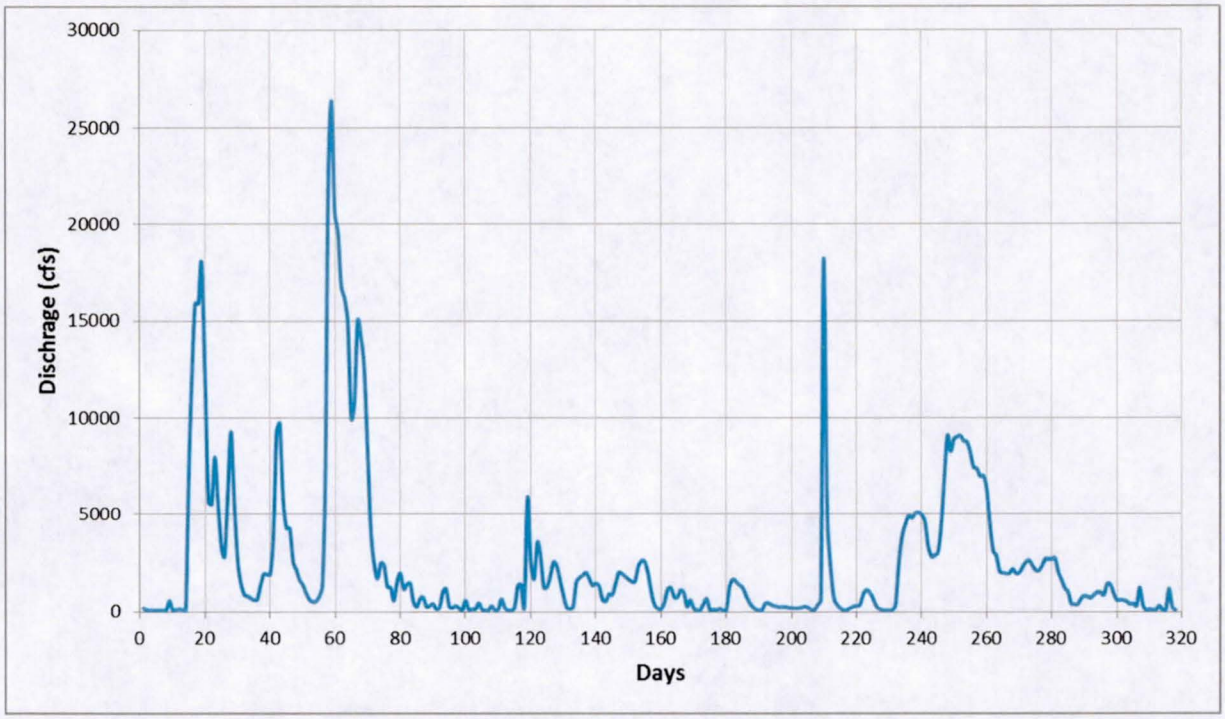

Figure 6-11. Upstream boundary (RM 217.95) discharge time series developed using observed data at the Priest Drive gage

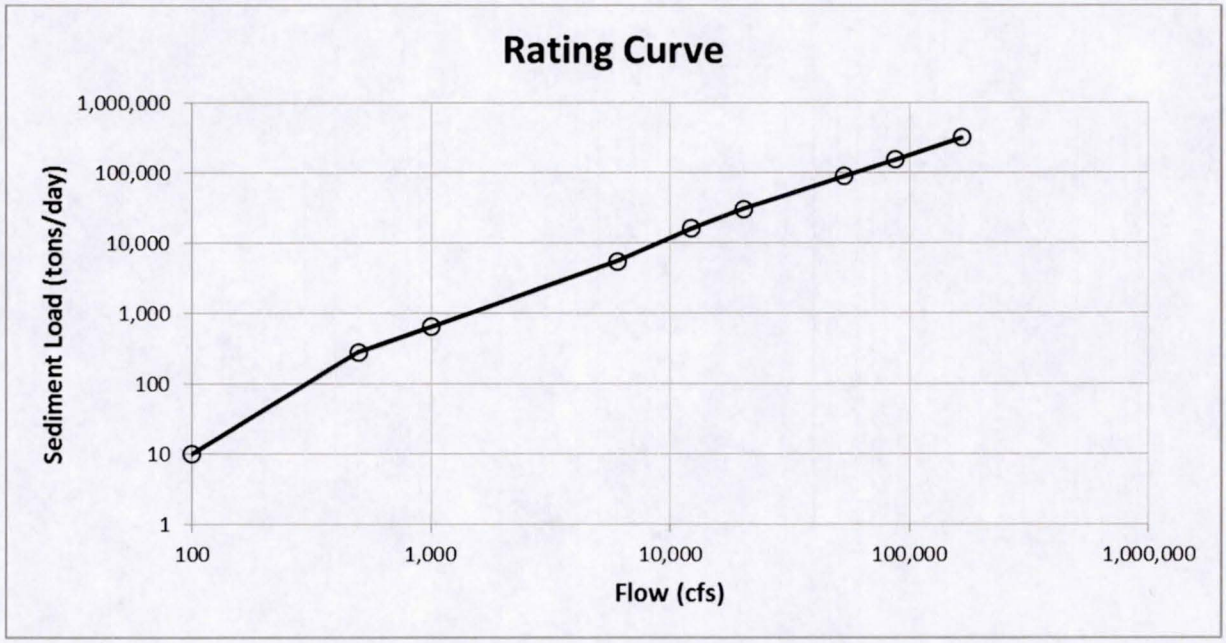

Figure 6-12. Inflow sediment rating curve at the upstream boundary for the calibration model

6.5.5 Calibration Process

During the calibration, a number of parameters were varied to examine their effect on the model results in terms of average bed and thalweg elevations. The following parameters were considered for the calibration process:

1. Sediment transport functions;
2. Inflow sediment rating curves;
3. Manning's *n*-value;
4. Movable bed limits; and
5. Model parameters (such as time step, hydraulic weighting factors, SPI factor, etc.)

From the comparison of the initial and final geometries, the movable bed limits in the calibration model were found to be acceptable and were not changed as part of the calibration efforts. Assuming suitable model parameters were used during the Rio Salado study, they were ignored as well. As the District had recommended not altering Manning's value in the models, the calibration results using varying Manning's value were shown for informational purpose only. Thus, the conclusions from calibration process were based on varying transport functions and inflow sediment loading conditions.

The resulting topography during the calibration run was compared with the 2013 topography. In order to compare the simulated results with the 2013 topography, both the average bed elevations and the thalweg elevations were computed at each cross-section. The overall fit between the final model results and the 2013 topography was based on the root mean square error (RMS) value of the whole reach and visual observation of the cross-sections. The RMS error values were rounded to the tenth decimal place. The common cross-sections between the initial and final condition models between RM 211.5 and I-10 Bridge were utilized to calculate the RMS error. The cross-sections between the grade control structures at RM 216.23 and RM 216.40 were also ignored because those cross-sections showed abnormally high scour depths that could not be contained by changing any model parameters.

The average bed elevation calculated by HEC-6T was found to be not representative of the elevation observed in the cross-section plot. Manually, the average bed elevation was estimated by subtracting hydraulic depth from the water surface elevation. Since the total hydraulic depth is not available in HEC-6T, the results from HEC-6T model were used to build a steady flow HEC-RAS model (note that this model was just used to generate results that were not available in HEC-6T) to estimate the average bed elevations.

6.5.6 Calibration Results for HEC-6T Model

6.5.6.1 Variation in Sediment Transport Model Function

Several sediment transports functions were tested during the calibration process. The transport functions used for the HEC-6T runs are listed in Table 6-5. The average elevation profiles produced by the different transport functions did not change much, and they did not deviate significantly from the 2013 average bed elevation profile. The RMS error of the HEC-6T runs using different transport functions was in the range 2.1 to 2.3 feet. Figure 6-13 shows the average bed elevation profile plot for Toffaleti, Meyer-Peter Müller (TMPM) and Yang's stream power (Yang) functions. The locations with

larger deviation in average bed elevation were mostly bridges, and such these deviations could be ignored for calibration purposes.

Similarly, Figure 6-14 shows the thalweg profiles for HEC-6T calibration runs using TMPM and Yang's functions. The calculated RMS errors for the different transport functions were in the range of 1.4 to 2.1 feet. For all the transport functions, the thalweg RMS errors were slightly smaller than the corresponding RMS error for average bed elevation.

From the results of this analysis, it can be concluded that the sediment model is not very sensitive to the used sediment transport functions. Thus, the TMPM and Yang transport functions were selected for further calibration evaluation since they are suitable for medium sand and gravel rivers and have been used in previous sediment studies in the Salt/Gila River system [(WEST Consultants, Inc., 2000) and (WEST Consultants, Inc., 2002b)].

Table 6-5. Sediment transport functions used in the HEC-6T calibration runs

1.	Toffaleti, Meyer-Peter Müller	7.	Colby (1964)
2.	Yang's stream power (1973)	8.	Toffaleti-Schoklitsch
3.	Toffaleti (1969)	9.	Meyer-Peter Müller (1948)
4.	Duboy's	10.	Schoklitsch
5.	Einstein	11.	Madden's Modification of Laursen (1985)
6.	Ackers-White (1973)		

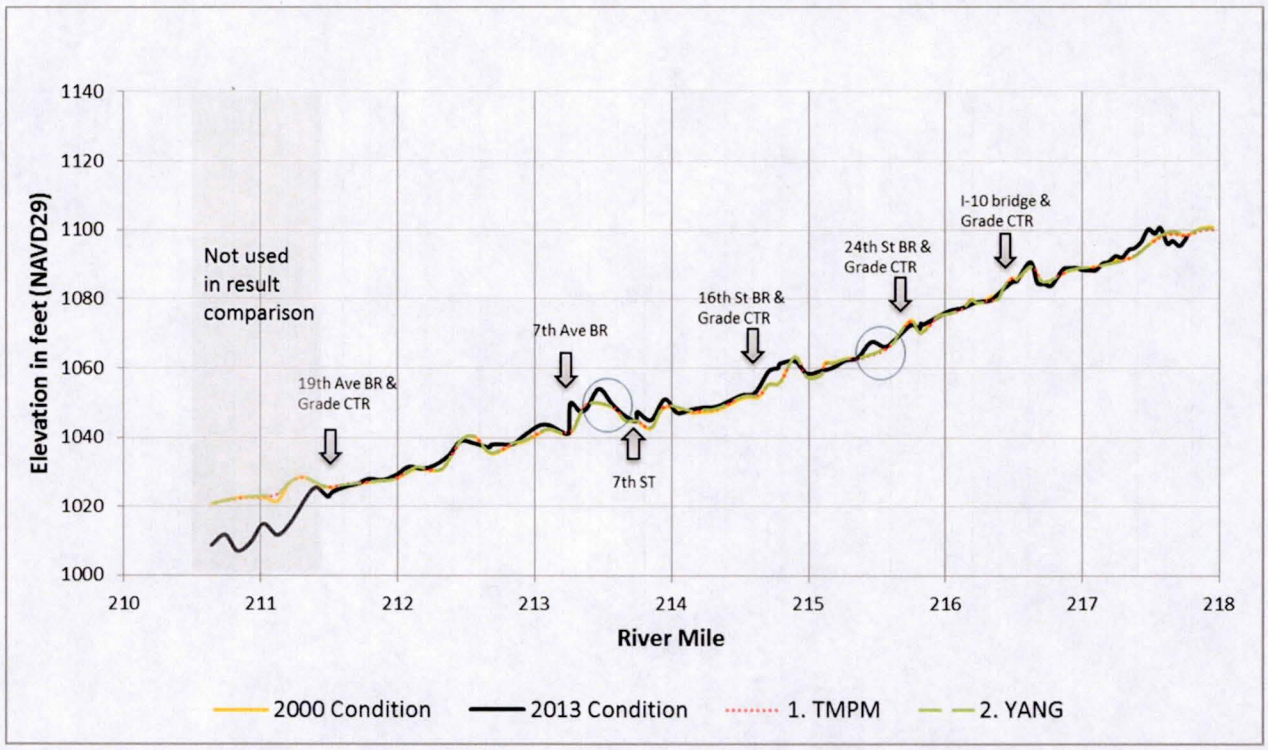

Figure 6-13. Average bed elevation profile of HEC-6T runs using TMPM and Yang sediment transport function

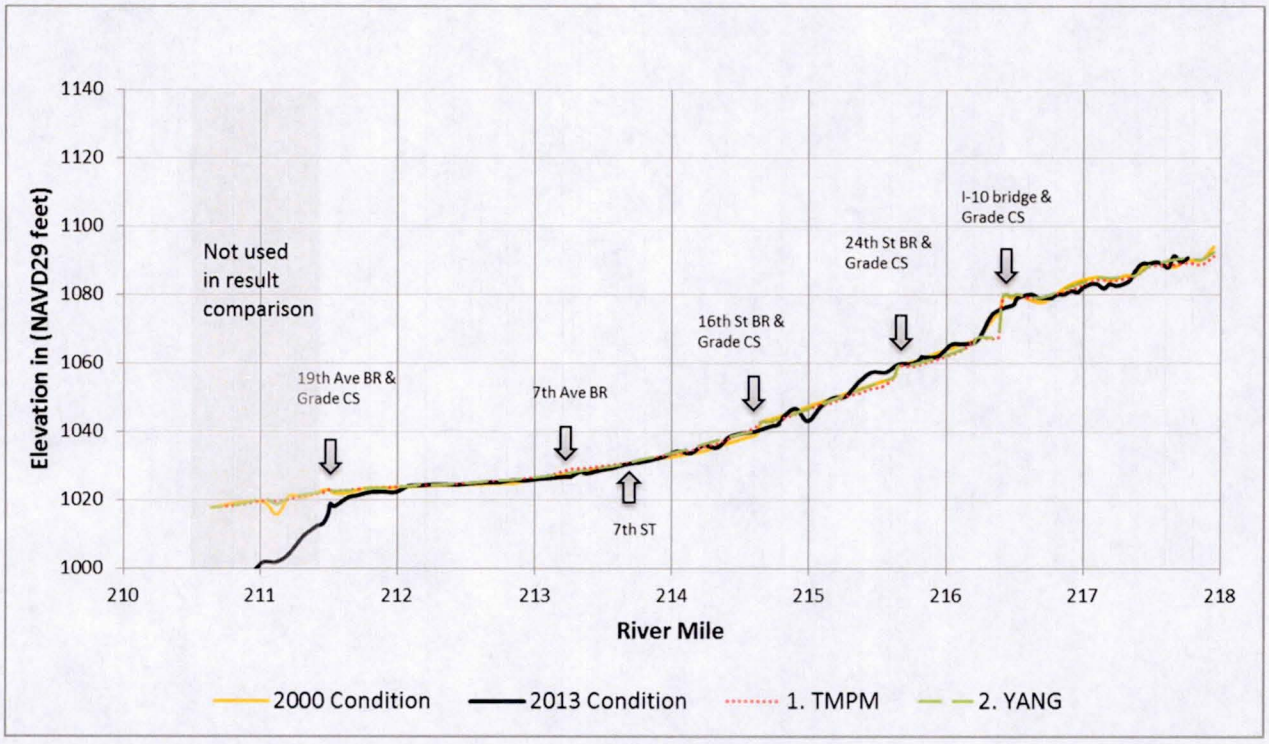

Figure 6-14. Thalweg profile plot for 2000 and 2013 geometries, and for HEC-6T runs using TMPM and Yang functions

6.5.6.2 Variation in Manning's Roughness

The Manning's roughness values were increased by 10 and 20 percent for the calibration models using TMPM and Yang transport functions. The RMS errors of the runs are shown in Table 6-6.

As can be seen in Table 6-6, the model is relatively insensitive to variations in Manning's roughness values as well as sediment transport function. The sum of the two elevation errors was the least for the base model using Yang sediment transport.

Table 6-6. Root mean square error (feet) for HEC-6T calibration runs with varying Manning's roughness values

SN	Manning's roughness value		RMSE in average bed elevation (ft)	RMSE in thalweg elevation (ft)
1	TMPM			
		Base	2.2	1.6
		+10%	2.3	1.6
		+20%	2.3	1.5
2	Yang			
		Base	2.2	1.5
		+10%	2.3	1.5
		+20%	2.3	1.4

6.5.6.3 Variation in Sediment Loading

Two sediment loading scenarios were used for the calibration model using TMPM and Yang transport functions. In the two scenarios the sediment loading at the upstream boundary was increased and decreased by 20%, respectively. The results are shown in Table 6-7.

For both transport functions, the model is relatively insensitive to the upstream sediment loading (as it is for the Manning's roughness values). In comparison, the base model using Yang appeared to be the best model as it gave the least error in thalweg, second smallest average bed elevation error, and the smallest sum of the two errors.

Table 6-7. Root mean square error (feet) for calibration runs using different upstream sediment loading condition

SN	Sediment Loading		RMSE for average bed elevation (ft)	RMSE for thalweg elevation (ft)
1	TMPM			
		Base	2.2	1.6
		+20% Load	2.3	1.7
		-20% Load	2.3	1.6
2	Yang			
		Base	2.2	1.5
		+20% Load	2.3	1.5
		-20% Load	2.3	1.5

6.5.7 Calibration Results for HEC-RAS Sediment Transport Model

HEC-RAS calibration model was based on the HEC-RAS hydraulic model of Rio Salado Low Flow Design study (WEST Consultants, Inc., 2000). Sediment data such as bed gradation, erosion/deposition limit, and grade control structures, etc., were obtained from the HEC-6T model of the same study.

One advantage of HEC-RAS over HEC-6T is that it can incorporate hydraulic structures like bridges and culverts. HEC-RAS v. 4.1, however, has very few sediment transport functions that limit its ability to use best transport function during the calibration process. Unlike HEC-6T model, HEC-RAS v. 4.1 currently does not have an option to allow deposition outside of the erosion limits within predefined limits.

Due to the limitations of HEC-RAS v. 4.1 regarding sediment modeling, fewer calibrations runs were performed using HEC-RAS. As for the use of sediment transport functions, both the Yang and TMPM sediment transport functions would ideally be chosen. These methods were selected based on the conclusion from the HEC-6T calibration runs in the previous section. HEC-RAS v. 4.1 was used for Yang sediment transport function. Since the current version did not have TMPM transport function, HEC-RAS v. 5.0 beta was used for calibration runs using TMPM sediment transport function. For the two transport functions, inflowing sediment load and the Manning's roughness values were varied during the calibration runs using HEC-RAS in the same manner as they were when using HEC-6T. The results from these runs are shown in Table 6-8.

The HEC-RAS base model using the TMPM function gave smaller RMS errors than the Yang function. Changing sediment load and Manning's *n*-value resulted in larger elevation errors in both TMPM and Yang runs. However, with the HEC-6T simulation results, the model runs using HEC-RAS are not very sensitive to the changes in sediment transport function, Manning's *n*-value, or sediment inflow load.

Compared to HEC-6T runs, HEC-RAS models had larger RMSEs associated with the thalweg elevations. There was no significant difference between the two model results in terms of average bed elevation.

Table 6-8. Root mean square errors (feet) for HEC-RAS calibration runs

SN	Method		RMSE for average bed elevation (ft)	RMSE for thalweg elevation (ft)
1	TMPM			
		Base	2.2	1.7
		+20% Load	2.3	1.9
		-20% Load	2.3	1.9
		+10% *n*-value	2.3	2.0
		+20% *n*-value	2.3	2.0
2	YANG			
		Base	2.3	1.8
		+20% Load	2.3	2.1
		-20% Load	2.5	2.0
		+10% *n*-value	2.6	1.9
		+20% *n*-value	2.6	1.8

6.5.8 Spatial Pattern for the Calibration Runs

The thalweg elevation was used to examine the erosion and deposition pattern along the calibration reach based on the actual topographic data. In Figure 6-15, the difference in "observed" thalweg elevation between 2013 and 2000 conditions are plotted along the study reach. This plot shows the change in thalweg elevation from an erosional and depositional perspective. At a location with positive difference, deposition of the same amount is required during the calibration runs. Similarly, for a negative difference, erosion is necessary in the calibration runs.

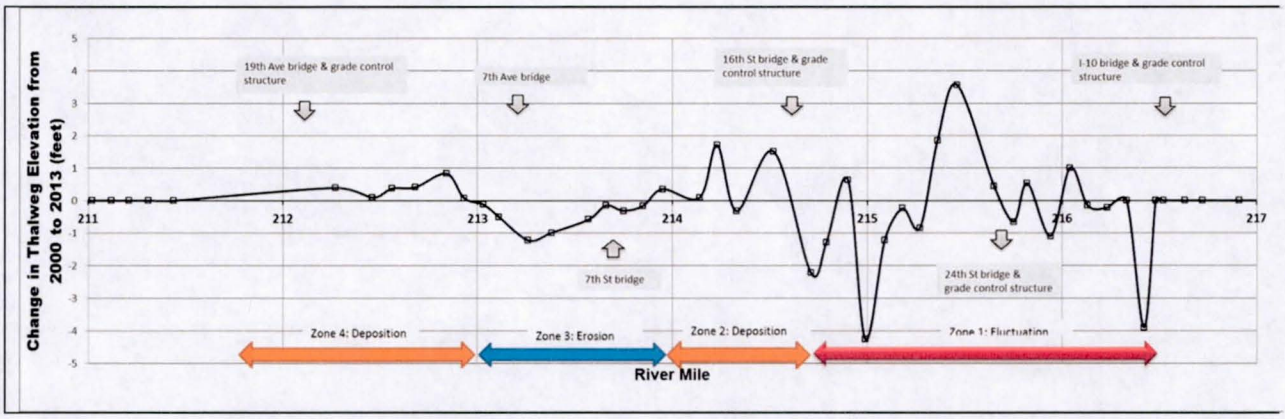

Figure 6-15. Observed thalweg elevation difference between 2013 and 2000 conditions along the calibration reach

In Figure 6-15, four zones were identified according to erosion-deposition patterns based on the topography changes between 2000 and 2013. Zone 1 (I-10 bridge to 16th Street bridge) had a sequence of alternating erosion and deposition processes. Respectively downstream of I-10 and 24th Street

bridges, nearly four feet erosion and deposition was observed. Zone 2 and Zone 4 mostly had deposition while Zone 3 located between those two had erosion.

Spatial erosion-deposition magnitude pattern for base calibration runs are shown in Figure 6-16. The y-axis gives the elevation difference between the results of calibration runs and the 2000 condition geometry. In Zone 1, not one method appears to follow the observed pattern consisting of alternate erosion and deposition as shown in Figure 6-15. In this zone, the HEC-6T calibration simulations predominantly had erosional characteristics while the HEC-RAS calibration simulations had both erosional and depositional characteristics.

In the reach downstream of 16th Street bridge (Zone 2, 3 and 4), deposition was predominant in all the calibration runs. Comparison of the deposition depths at RM 212.8 and RM 214.2 showed HEC-6T model using Yang function was closest to the observed deposition magnitudes. Furthermore, in Zone 3, the Yang transport function appeared to perform better than the TMPM function. In Zone 3, erosion was expected but the TMPM function caused deposition. Yang transport function, on the other hand, had very little deposition or erosion in this zone. The results for other calibration parameters are not shown in the figure, but it was found that the parameters affected only the magnitude of erosion and deposition while retaining the same pattern as the base model.

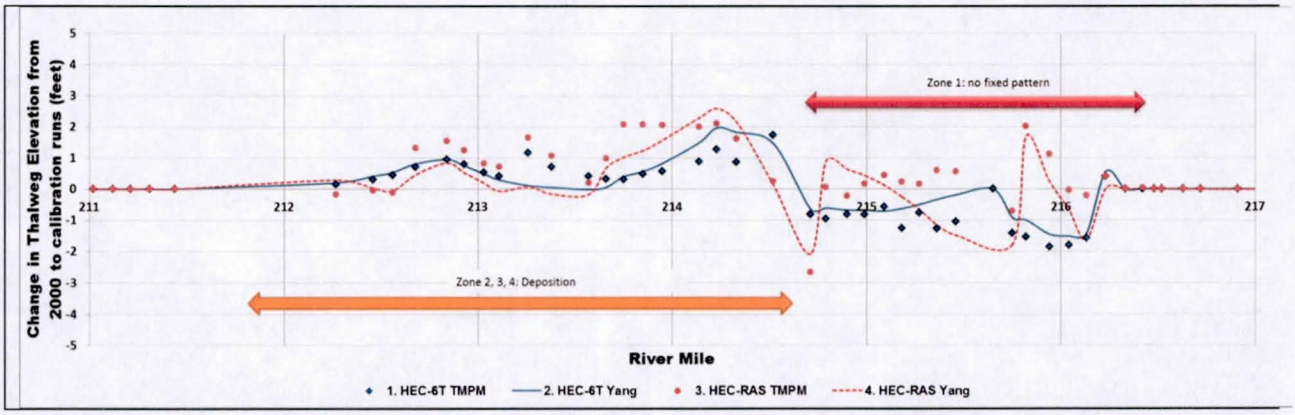

Figure 6-16. Erosional-depositional pattern for HEC-6T/HEC-RAS runs using TMPM and Yang transport functions

6.5.9 Conclusions from Calibration Runs

- For the ongoing Salt/Gila Sediment Transport Study, the Rio Salado Low Flow study reach was chosen for the calibration of HEC-RAS and HEC-6T sediment models. The initial geometry and sediment data were taken from the Rio Salado Low Flow study (WEST Consultants, Inc., 2000) while the final geometry was obtained from Lower Salt FDS (WEST Consultants, Inc., 2015). The calibrations models were run for the period of 2000 to 2013 using flow value measured at Priest Drive gage and equilibrium sediment inflow calculated at the upstream boundary. The simulated topography was compared with the latest 2013 topography using average bed elevation and thalweg elevation.

- Three calibrations parameters were focused mainly in this study – sediment transport function, Manning's *n*-value, and the inflow sediment load. Results from HEC-6T simulations using eleven different sediment transport functions showed the sediment transport functions did not have significant effects on the resulting topography of the river. As a result, TMPM and Yang sediment transport functions were selected for calibration of inflow sediment load as these are considered suitable for Salt/Gila River system that transports medium sand and gravel.
- During the Manning's *n*-value calibration runs, increasing the Manning's *n*-value had a tendency to increase the overall RMS error. However, there was not a significant sensitivity to the calibration runs based on variations in the Manning's *n*-value.
- During the inflow sediment load calibration runs, deviation of the sediment load from the base condition was accompanied by increased elevation errors. In the case of the HEC-6T calibration runs, the base model of the Yang transport function gave the least elevation errors while in the case of HEC-RAS runs, the base model of TMPM performed the best. In terms of root mean square error of the two elevations, the advantage of Yang over TMPM and of TMPM over Yang in HEC-6T and HEC-RAS calibration runs, respectively, were marginal. However, there was not a significant sensitivity to the calibration runs based on variations in the input sediment load.
- The observed erosional/depositional patterns along the thalweg provided additional information regarding the performance of various models. Downstream of 16th Street Bridge, the HEC-6T model using Yang sediment transport function provided better estimates for observed deposition pattern and magnitude. Upstream of 16th Street Bridge, however, no simulations were able to replicate the observed erosion/deposition pattern.
- Sediment transport in rivers is a complex process. Sediment transport in the Salt/Gila River system is also complicated by absence of inflow sediment data and mining activity along the river. Comparatively RSME values in simulated channel bed elevations were observed at locations with bridge and grade control structures.
- The objective of the current study was to perform limited calibration in order to select the most suitable sediment transport function and sediment loading condition that can be used for sediment transport study of the Salt/Gila reach between I-10 Bridge and SR-85. Based on our results, HEC-6T and HEC-RAS models using Yang sediment transport function and the initial inflow sediment loading along with the base Manning's *n*-value provided a better match with the observed condition during the calibration period and as such are recommended for sediment transport calculations on the Salt/Gila reach between I-10 Bridge and SR-85.

6.6 Creation of the HEC-6T Sediment Transport Models (Existing and Proposed Conditions)

Once the existing and proposed conditions sediment transport models were created in HEC-RAS, both were converted into HEC-6T (version 5.13.22_08T) using the conversion tool created by Mobile Bed Hydraulics called RAS2H6T (MBH Software, 2006). While this software is effective at converting HEC-RAS geometry files into HEC-6T format for the general cross-section ground points, there were still

several items that had to be converted manually from HEC-RAS into HEC-6T. For example, bridges are not converted from HEC-RAS to HEC-6T when using MBH's conversion tool. Thus, WEST wrote a Visual Basic for Applications (VBA) macro within an Excel spreadsheet to assist with converting the various bridges inside the HEC-RAS model to HEC-6T format. The results from the spreadsheet macro were then used to update the HEC-6T file manually. Other items that needed to be manually examined and entered into HEC-6T included the vertically varied *n*-values in the Tres Rios North Levee reach of the sediment transport models along with the placement of the ineffective flow areas. More details on the conversion process follows.

Initially, RAS2H6T (MBH Software, 2006) was used to convert hydraulic model cross-sections to HEC-6T model cross-sections. This tool takes HEC-RAS geometric file (extension .gxx, where xx is any number) as an input and produces HEC-6T model file (extension .T5). The T5 file obtained from above tool had the following issues:

1. The cross-sections upstream and downstream of bridges in HEC-RAS were required to be merged to form a single effective cross-section in HEC-6T since HEC-6T cannot simulate bridge structures. A VBA tool was developed separately to perform this function. The VBA tool also took pier data to incorporate piers as ground points in the cross-section.
2. The conversion tool did not have the capacity to create equivalent ineffective flow in HEC-6T. Instead, the conversion tool simply added "X3 10" cards, which defined two ineffective flow areas at the left and right bank stations, respectively. The elevation of each effective flow area was equal to the corresponding elevation of the bank station. Moreover, modeling of ineffective flow area in HEC-6T was very limited compared to HEC-RAS. In order to simulate the HEC-RAS ineffective flow areas in HEC-6T as well as possible, the X3 cards were manually adjusted and XL cards were added as necessary.
3. The conversion tool could not convert blocked obstructions in HEC-RAS to ground points in HEC-6T. Therefore, cross-sections with blocked obstructions were manually corrected.
4. The conversion tool was unsuccessful in creating Manning's *n*-value record for cross-sections with flow-Manning's relationship (i.e., the vertically adjusted Manning's *n*-value). For these cross-sections, a steady-state HEC-RAS model was run to calculate the effective Manning's *n*-value for the overbank areas and the main channel for each flow. Then NV records were created with above Manning's *n*-values and flows.
5. Even with the above corrections, the water surface elevation between HEC-RAS base hydraulic model and HEC-6T base hydraulic model did not match in numerous cross-sections, especially in the downstream portion of the model (also see discussion is Section 5.8). To correct this issue, the Manning's *n*-values were altered to bring the error within 1 foot of the computed water surface elevations from the HEC-RAS base hydraulic model. The calibration was done for three flows (i.e., the 1%, 2%, and 10% annual chance flows). In this process the original Manning's *n*-value records were replaced by NV record. The NV record can use up to 5 flows to define the Manning's *n*-values at the left overbank, the main channel, and the right overbank.

In HEC-RAS, the downstream boundary condition was defined as normal flow using a normal slope 0.00147. HEC-6T on the other hand only supports water surface elevation rating curve. Therefore, a

rating curve was developed from the HEC-RAS base hydraulic model and used in HEC-6T as the downstream boundary condition.

6.7 Sediment Transport Modeling Results

The various sediment transport models described in this report were run and the results are presented in this section. It was expected that the sand and gravel mining operations would have a large impact on the sediment transport modeling results. In general, these impacts would be redirection of flow through the pits and away from the former channel alignments; erosion upstream and downstream of the pits; and deposition of sediment in the pits themselves.

The erosion or deposition was assumed to occur uniformly between the stream banks. Although it is not likely that the cross-sectional shape will stay constant over time, the assumptions of one-dimensional sediment transport modeling are best presented as average bed elevation changes. Thus, the results are presented here in terms of changes in the average bed elevation for both the main channel and the entire cross-section. Average bed elevations are not easily obtained from HEC-RAS or HEC-6T, so a VBA macro was written to calculate the average bed elevations from the results.

In addition, another useful parameter is the minimum thalweg elevation of a cross-section during the simulation period. This would represent the most degradation at a given cross-section that would be expected to occur. Note that the minimum channel thalweg elevation plots do not show areas of aggradation; they only show the maximum degradation that could occur. The minimum channel thalweg elevation was also calculated for 1% annual chance flood hydrograph simulation runs. For the historic runs, the thalweg elevations at the end of the simulation are presented instead.

As a representation of the amount of sediment that passes each cross-section, the cumulative mass outflow (in tons) was calculated for each cross-section.

To check the overall results of the model runs, general trends from the previous sediment transport model runs were compared to the sedimentation results from this study. However, a direct comparison is not possible at this time as the previous sediment transport models were using a different starting geometry, had different pit dimensions, used a different sediment transport function, used different hydrology, had different model extents, and bridges may not have been explicitly modeled in the older studies, etc. However, it would still be useful to make this comparison to determine if the new results were somewhat similar to the results from previous studies.

6.7.1 Existing Condition Model with Historic Flow Series

6.7.1.1 HEC-RAS Model

The first sediment transport model run was the existing conditions HEC-RAS model for the Salt/Gila River system using the historic inflow series. Figure 6-17 shows the initial and final invert elevations along with the change in the bed elevations for the cross-section. The average invert change throughout the study reach is -1.4 feet. In the reach between the I-10 Bridge and the confluence with

the Upper Gila, there are areas of scour and deposition. Most of these large areas of deposition or scour can be attributed to the sand and gravel mining pits or the local topography. For example, the large spike of deposition near 27th Avenue is occurring in a sand and gravel pit owned by the Portland Cement Company. This pit is approximately 40 feet deep and is located in the main channel of the Lower Salt River. Because of the size of this sand and gravel pit and the low velocities that would be experienced in the pit, sediment deposition would be expected in this area. For the historic flow runs, there is approximately 34 feet of deposition in the 40 foot deep pit.

The historic flow simulation shows approximately 20 feet of degradation downstream of 51st Avenue. The topography in this area indicates that there is a significant drop in the channel bottom (approximately 25 feet) through this bridge at the start of the simulation. This large drop in the channel bottom would have a tendency to increase the velocity and hence the scour in the area.

The results show a similar pattern for the average bed elevation for the cross-section (see Figure 6-18) and for the main channel (see Figure 6-19) as for the invert elevations (see Figure 6-17). Obviously, the results using the average bed calculations show damped peaks in aggradation and degradation when compared to looking at the invert elevation. However, the pattern is still similar with aggradation occurring near 27th Avenue and degradation occurring in most of the reach downstream of 51st Avenue. The average change in average bed elevation for the entire cross-section is 0.02 feet. The average change in average bed elevation for the main channel alone is -1.2 feet.

The total cumulative mass outflow for the Salt/Gila River system is shown in Figure 6-20. This figure indicates that the cumulative inflow into the system is somewhat constant until the large sand and gravel pits at 35th Avenue and 51St Avenue. At these locations, sediment drops out into the mining pits, significantly reducing the cumulative mass inflow. After that point, sediment inflows from the Upper Gila River, the Agua Fria River, Waterman Wash, and the erosion in the cross-sections themselves increases the cumulative mass inflow consistently to the downstream end of the reach.

6.7.1.2 HEC-6T Model

The initial and final invert along with the invert change for the existing Salt/Gila River system under historic conditions for HEC-6T can be seen in Figure 6-21. The average invert change throughout the study reach is 0.2 feet. The results are similar to the results generated from HEC-RAS (see Figure 6-17). In general, both the HEC-RAS model and the HEC-6T model predict aggradation or degradation in the same locations for the historic conditions. Generally, the HEC-RAS model predicts lower aggradation peaks and greater degradation troughs compared to the HEC-6T model. Averaged across the entire reach, the HEC-RAS model predicts an invert elevation that is about 1.5 feet lower than the HEC-6T model.

The results show a similar pattern for the average bed elevation for the cross-section (see Figure 6-22) and for the main channel (see Figure 6-23) as for the invert elevations (see Figure 6-21). The results using the average bed calculations show damped peaks in aggradation and degradation when compared to looking at the invert elevation. However, the pattern is still similar with aggradation occurring

upstream of 51st Avenue and degradation occurring in most of the reach downstream of 51st Avenue. The HEC-6T results show higher levels of aggradation than does the HEC-RAS results for the same scenario. The average change in average bed elevation for the entire cross-section is 0.3 feet. The average change in average bed elevation for the main channel alone is 0.1 feet.

The total cumulative mass outflow for the Salt/Gila River system using HEC-6T is shown in Figure 6-24. The pattern of the total cumulative mass outflow along the river system is similar for both HEC-RAS and HEC-6T (compare Figure 6-20 to Figure 6-24). However, the cumulative mass outflow for HEC-RAS at SR-85 (21,795,410 tons) is higher than for HEC-6T (15,262,349 tons). This reduction is cumulative mass outflow agrees with the invert change results. Since the HEC-6T model has, on average, 1.5 feet less degradation that would mean there would be less sediment mobilized and delivered to the SR-85 Bridge.

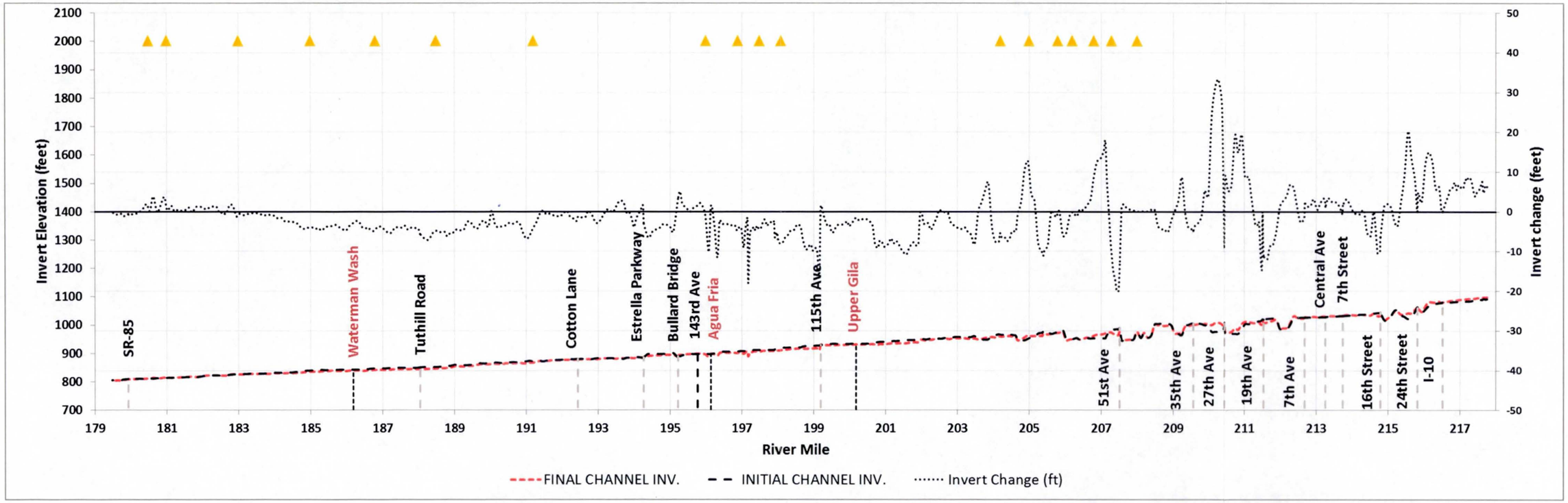

Figure 6-17. Invert profile change at the end of the simulation for the existing conditions HEC-RAS model with historic flow series

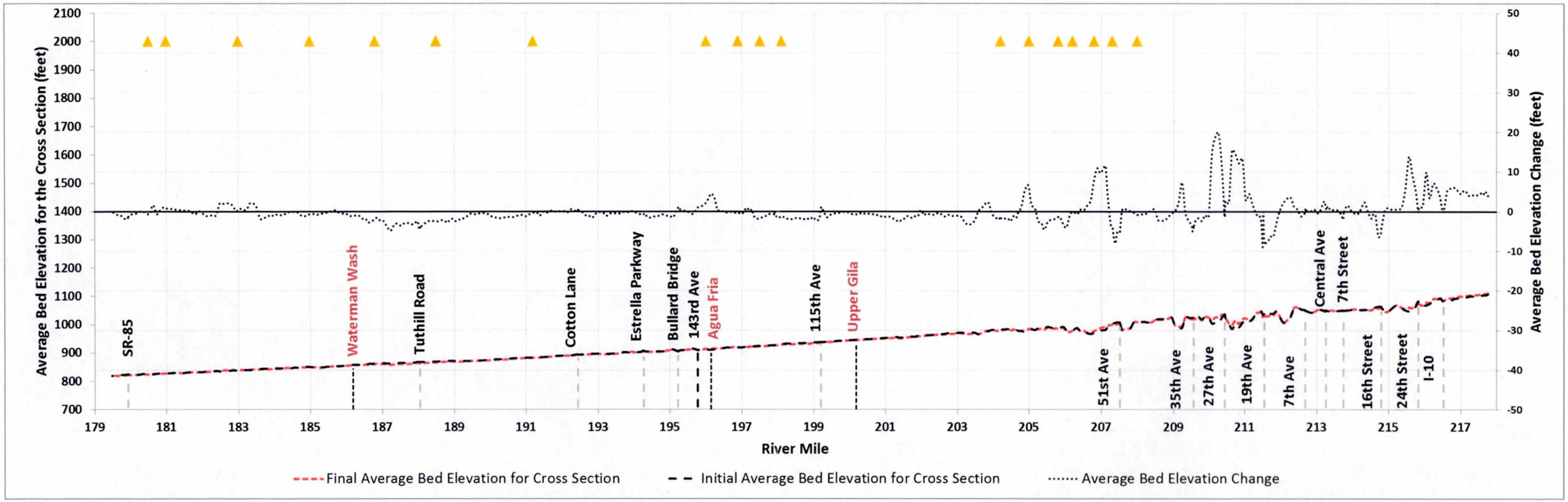

Figure 6-18. Change in average bed for the cross-section for the existing conditions HEC-RAS model with historic flow series

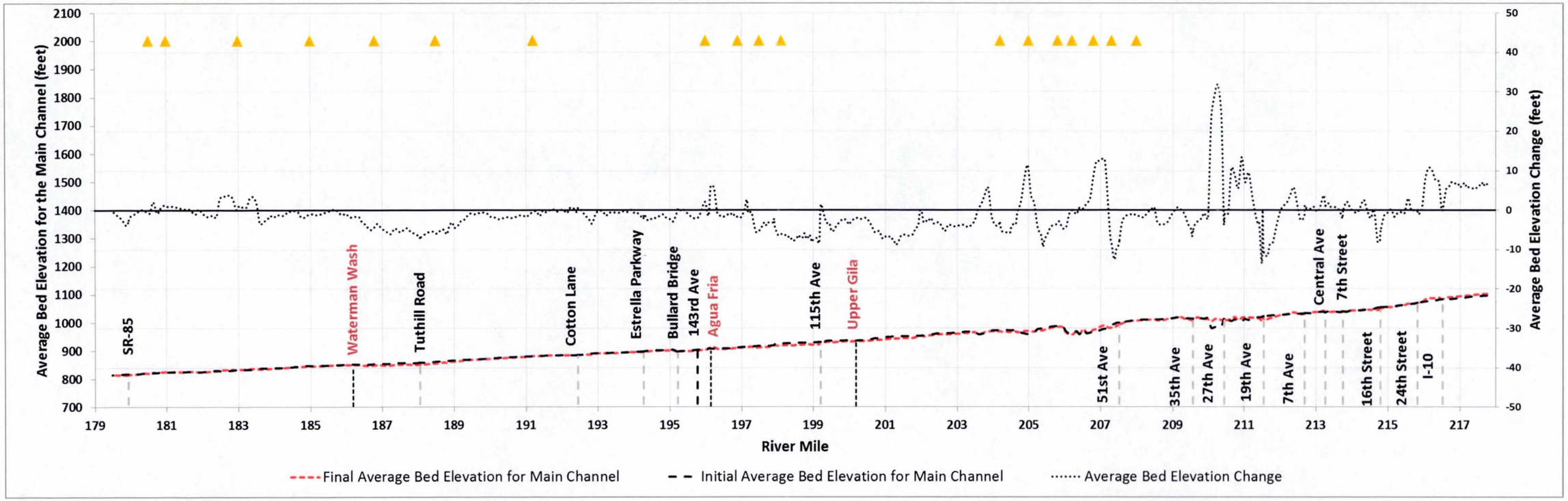

Figure 6-19. Change in average bed for the main channel for the existing conditions HEC-RAS model with historic flow series

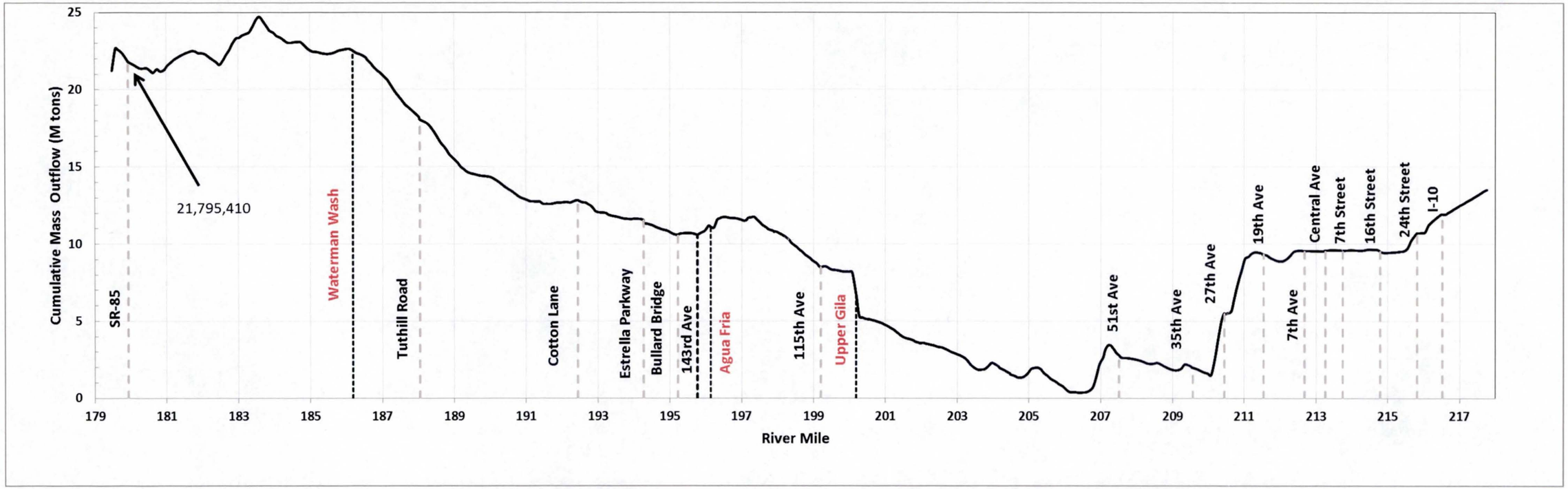

Figure 6-20. Cumulative total sediment outflow for existing conditions HEC-RAS model with historic flow series

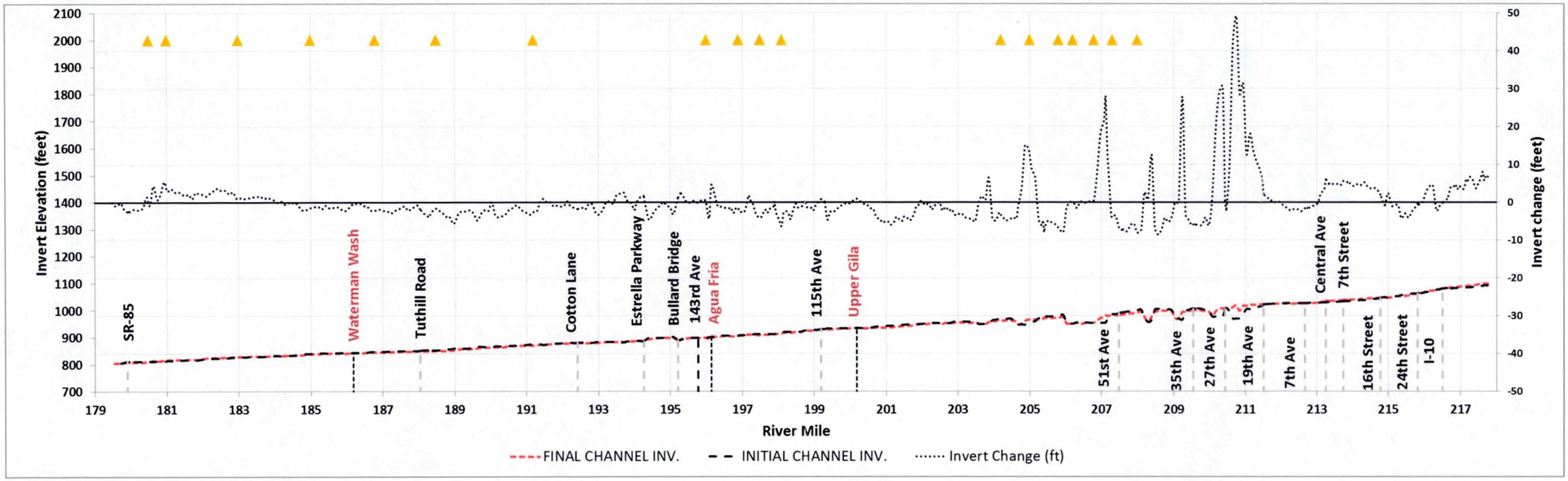

Figure 6-21. Invert profile change at the end of the simulation for the existing conditions HEC-6T model with historic flow series

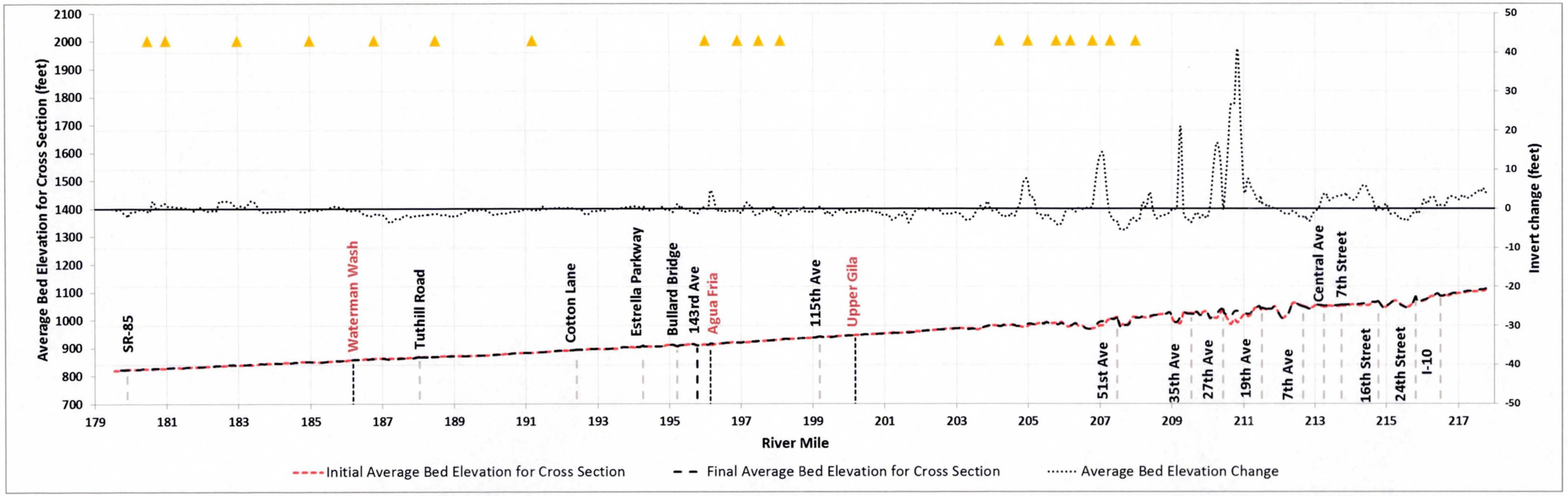

Figure 6-22. Change in average bed elevation for the cross-section for the existing conditions HEC-6T model with historic flow series

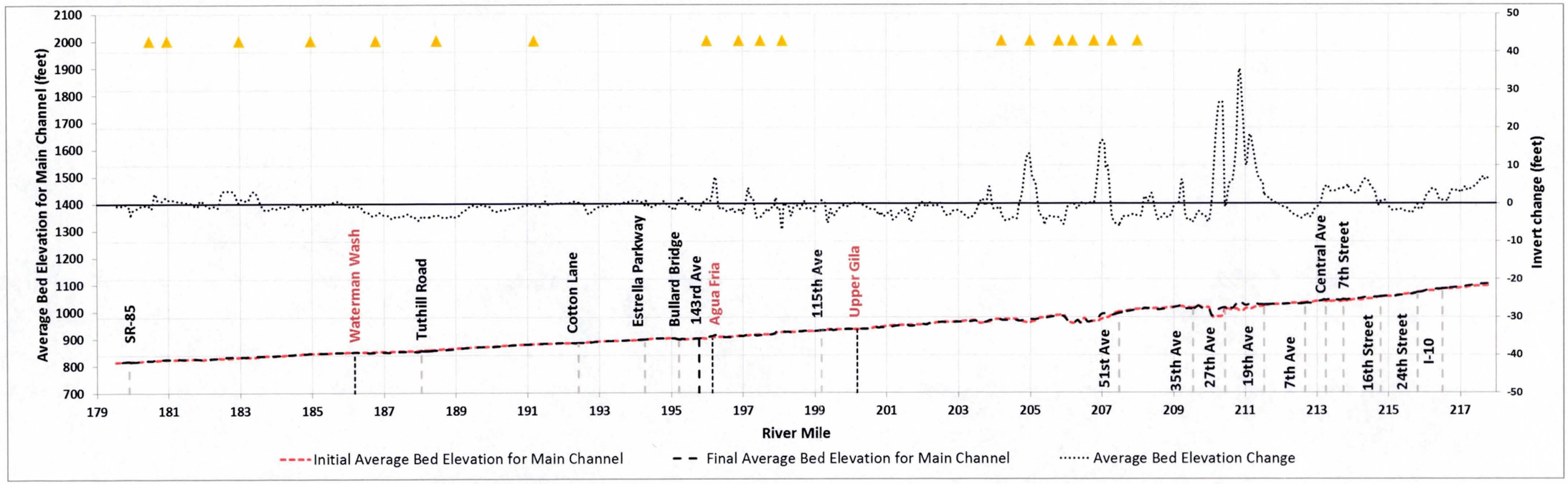

Figure 6-23. Change in average bed elevation for the main channel for the existing conditions HEC-6T model with historic flow series

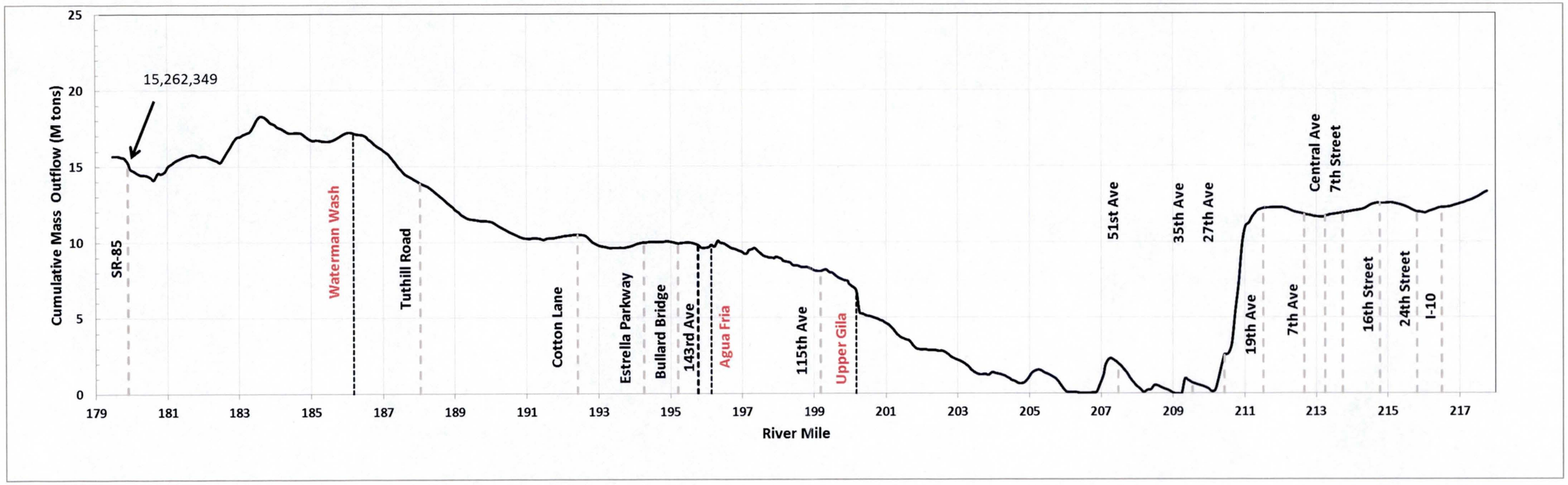

Figure 6-24. Cumulative total sediment outflow for existing conditions HEC-6T model with historic flow series

6.7.2 Proposed Condition Model with Historic Flow Series

6.7.2.1 HEC-RAS Model

The HEC-RAS sediment transport model was also run for the proposed conditions model for the Salt/Gila River system using the historic inflow series for the Salt River, the Upper Gila River, the Agua Fria River, and Waterman Wash. Figure 6-25 shows the initial and final invert elevations along with the change in the invert elevations. While the results shown in this figure generally agrees with the HEC-RAS existing conditions historic model, the built-out sand and gravel mines in the proposed conditions causes significantly more deposition at various locations along the river, as would be expected. In general, there is degradation downstream of about 51st Avenue. The average invert change throughout the entire reach is -0.1 feet, about 1.5 feet higher than the average invert change for the existing conditions (-1.4 feet). This increase in the average invert change is again due to the deposition in the new sand and gravel mines.

The results show a similar pattern for the average bed elevation for the cross-section (see Figure 6-26) and for the main channel (see Figure 6-27) as for the invert elevations (see Figure 6-25). Obviously, the results using the average bed calculations show damped peaks in aggradation and degradation when compared to looking at the invert elevation. However, the pattern is still similar with aggradation occurring in the proposed pits and degradation occurring in most of the reach downstream of 51st Avenue. The average change in average bed elevation for the entire cross-section is 0.2 feet. The average change in average bed elevation for the main channel alone is -1.5 feet.

The total cumulative mass inflow for the Salt/Gila River system under proposed conditions is shown in Figure 6-28. This figure is similar to the cumulative mass inflow plot for existing conditions except at the location of proposed sand and gravel mines, sediment drops out of the system and causes a drop in the cumulative mass outflow (e.g., near RM 197 and 181). A smaller amount of sediment is delivered to the SR-85 Bridge (compared to the existing conditions) because additional sediment is deposited in the proposed sand and gravel pits.

6.7.2.2 HEC-6T Model

The initial and final invert along with the invert change for the Salt/Gila River system under proposed conditions and historic flow for HEC-6T can be seen in Figure 6-29. The average invert change throughout the study reach is 2.1 feet. These results are similar to the results generated from HEC-RAS (see Figure 6-25). In general, both the HEC-RAS model and the HEC-6T model predict aggradation or degradation in the same locations for the historic conditions. Generally, the HEC-RAS model predicts lower aggradation peaks and greater degradation troughs compared to the HEC-6T model. Averaged across the entire reach, the HEC-RAS model predicts an invert elevation that is a little more than 2 feet lower than the HEC-6T model for the proposed conditions. As with the HEC-RAS model, the increase in the average invert elevation from the existing to proposed conditions is a result of the sediment depositing in the gravel pits.

The results show a similar pattern for the average bed elevation for the cross-section (see Figure 6-30) and for the main channel (see Figure 6-31) as for the invert elevations (see Figure 6-29). The results using the average bed calculations show damped peaks in aggradation and degradation when compared to looking at the invert elevation. However, the pattern is still similar with aggradation occurring upstream of 51st Avenue and degradation occurring in most of the reach downstream of 51st Avenue. The HEC-6T results show higher levels of aggradation than does the HEC-RAS results for the same scenario. The average change in average bed elevation for the entire cross-section is 0.5 feet. The average change in average bed elevation for the main channel alone is 0.0 feet.

The total cumulative mass outflow for the Salt/Gila River system using HEC-6T is shown in Figure 6-32. The pattern of the total cumulative mass outflow along the river system is similar for both HEC-RAS and HEC-6T (compare Figure 6-28 to Figure 6-32). However, the cumulative mass outflow for HEC-RAS at SR-85 (16,184,170 tons) is significantly higher than for HEC-6T (5,002,768 tons). This reduction is cumulative mass outflow agrees with the invert change results. Since the HEC-6T model has, on average, more than 2 feet less degradation that would mean there would be less sediment mobilized and delivered to the SR-85 Bridge.

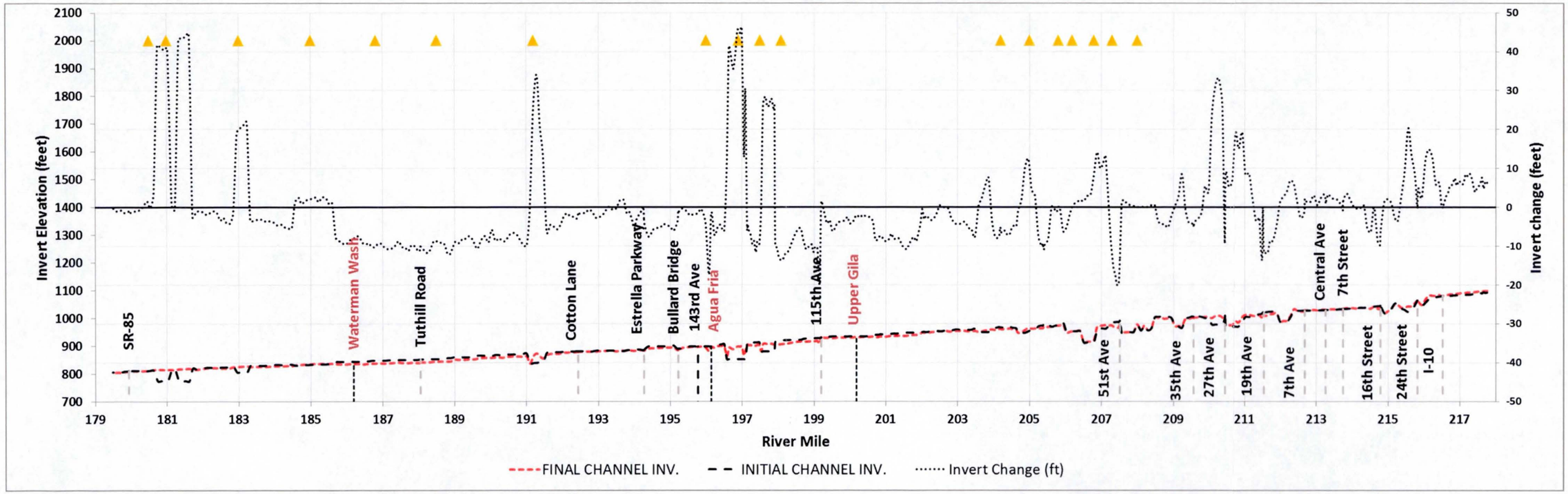

Figure 6-25. Invert profile change at the end of the simulation for the proposed conditions HEC-RAS model with historic flow series

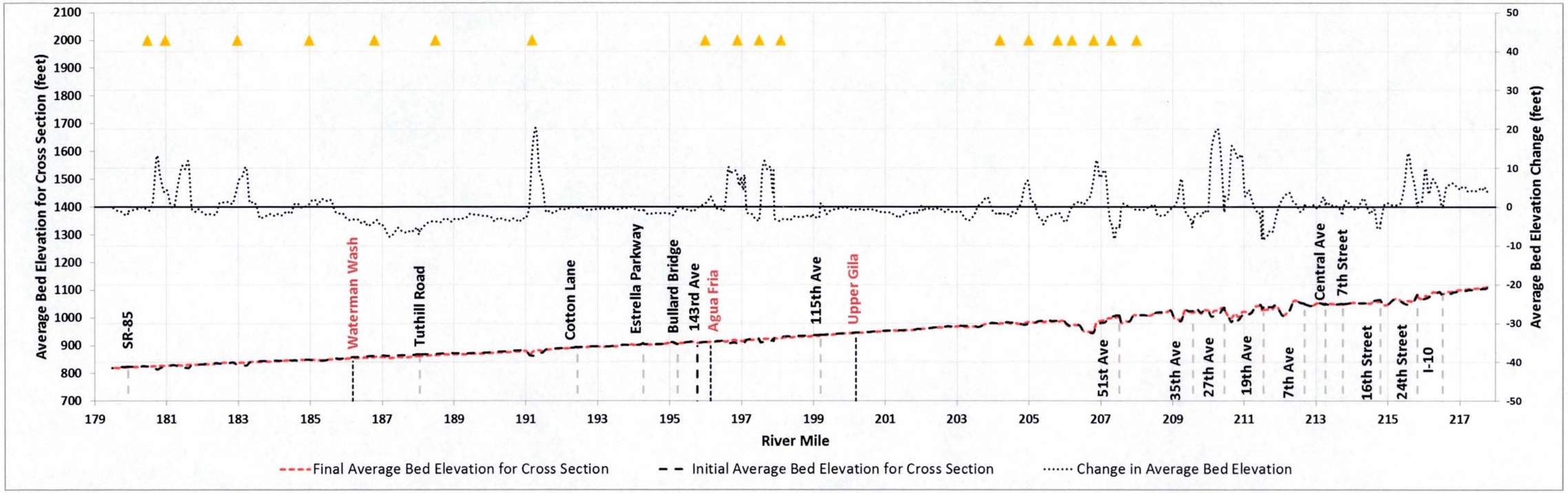

Figure 6-26. Change in average bed elevation for the cross-section for the proposed conditions HEC-RAS model with historic flow series

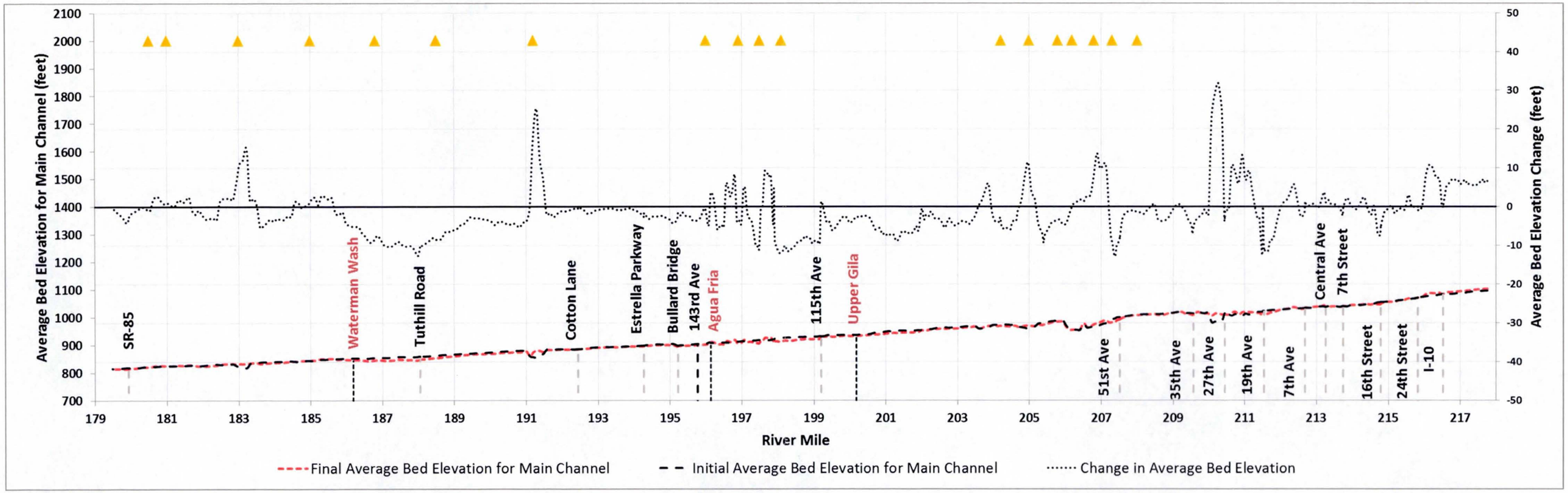

Figure 6-27. Change in average bed elevation for the main channel for the proposed conditions HEC-RAS model with historic flow series

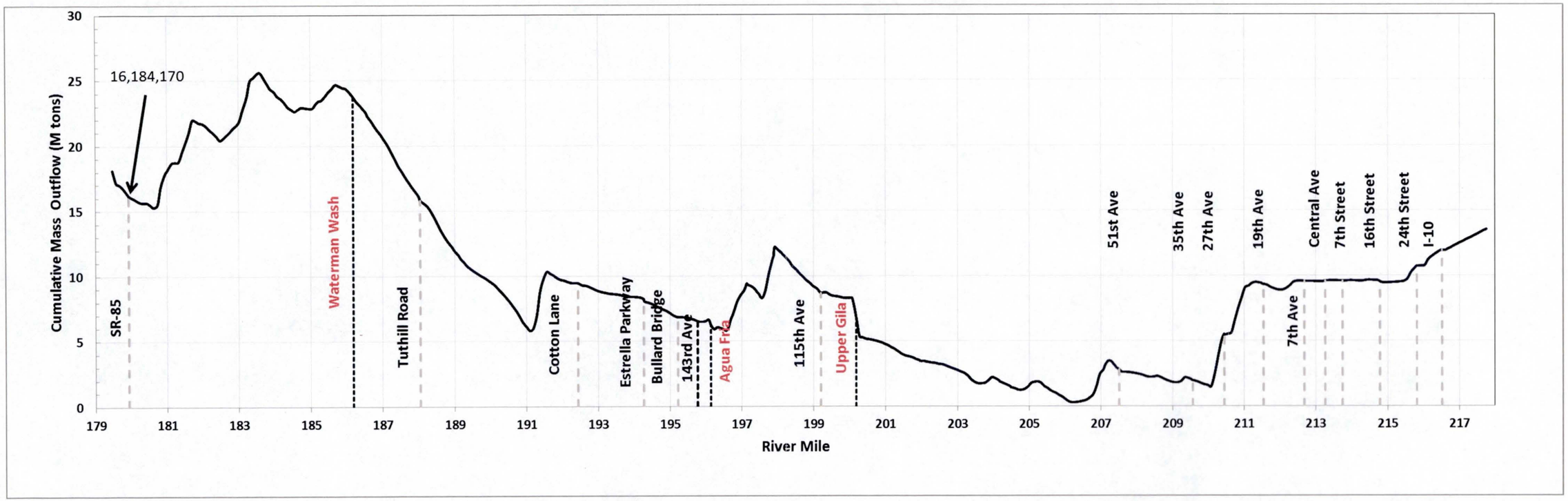

Figure 6-28. Cumulative total sediment outflow for proposed conditions HEC-RAS model with historic flow series

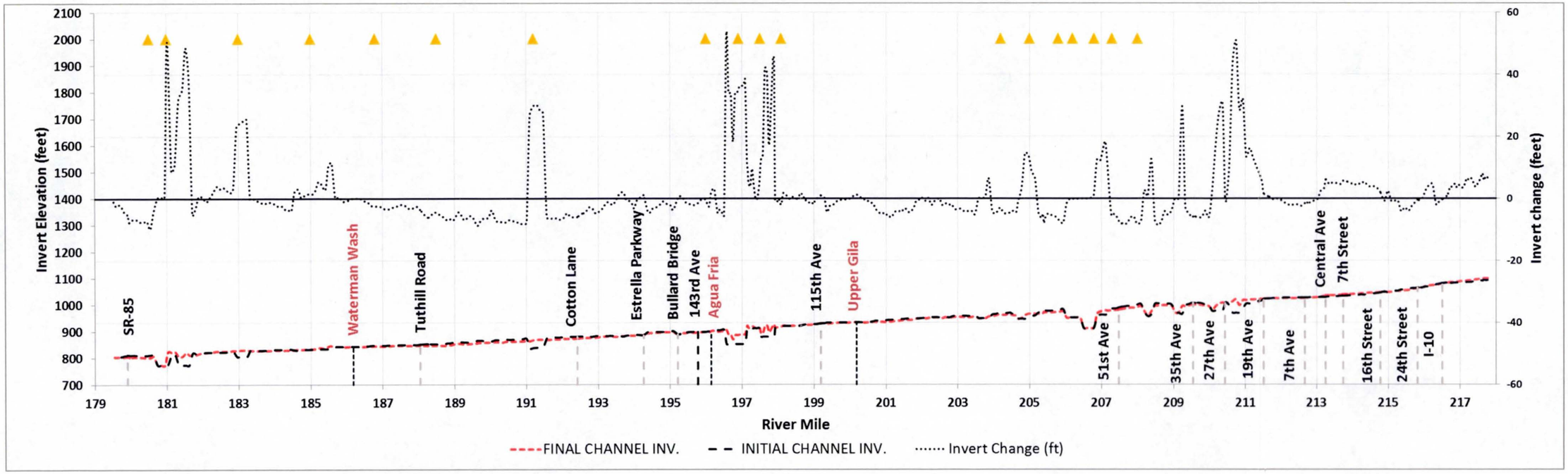

Figure 6-29. Invert profile change at the end of the simulation for the proposed conditions HEC-6T model with historic flow series

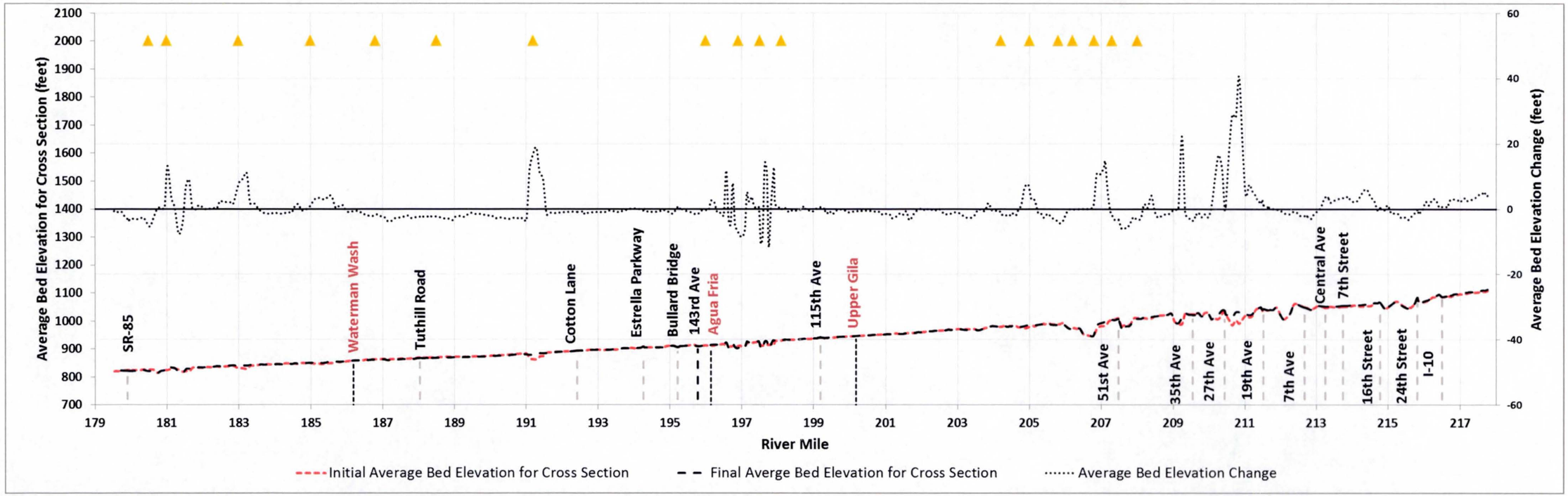

Figure 6-30. Change in average bed elevation for cross-section for the proposed conditions HEC-6T model with historic flow series

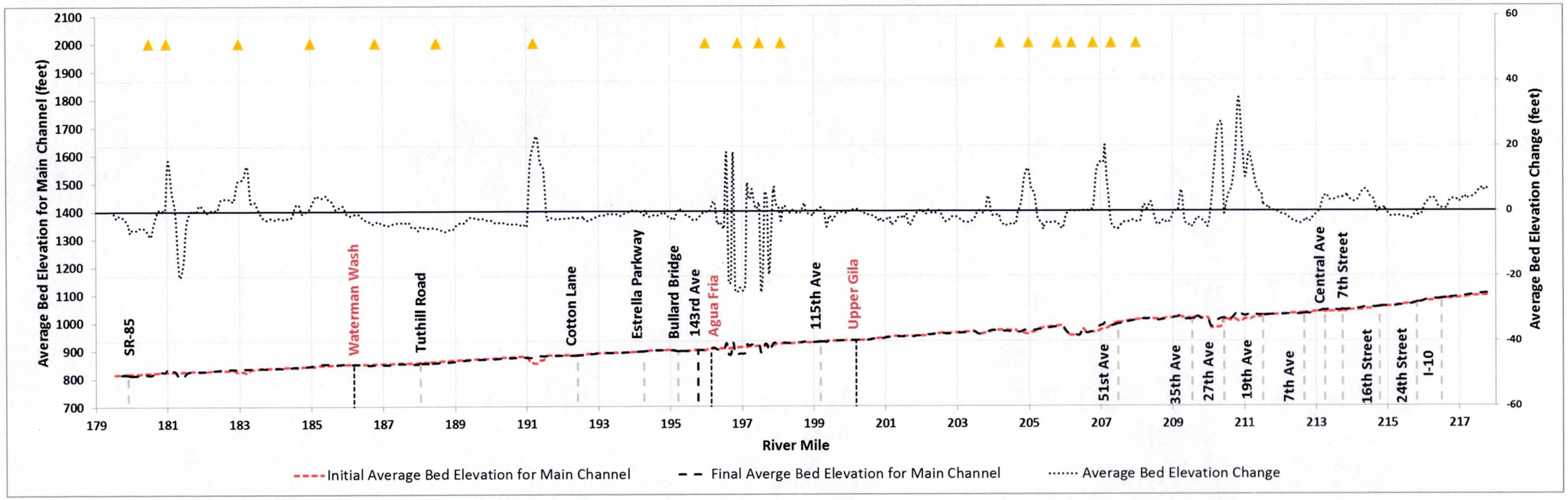

Figure 6-31. Change in average bed elevation for main channel for the proposed conditions HEC-6T model with historic flow series

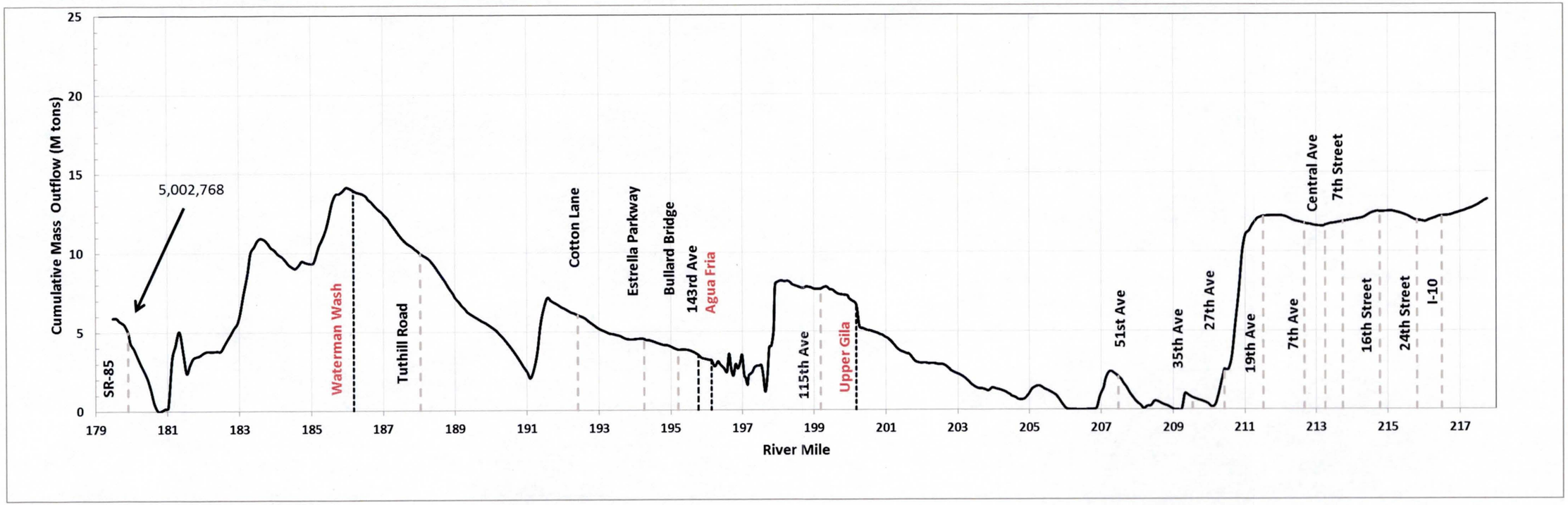

Figure 6-32. Cumulative total sediment outflow for proposed conditions HEC-6T model with historic flow series

6.7.3 Existing Condition Model for the 1% Annual Chance Flood Hydrograph

6.7.3.1 HEC-RAS Model

The sediment transport model was also run for the existing conditions model for the Salt/Gila River reach using the 1% annual chance flood hydrograph inflow series. Figure 6-33 shows the initial and minimum invert elevations along with the river. This figure shows that the minimum channel invert is about 10 feet below the initial invert near 19th Avenue and about 18 feet below the initial invert near 51st Avenue. These are areas were degradation was observed for the existing conditions HEC-RAS model with the historic inflow series. The amount of degradation is less in the 1% annual chance flood conditions than the historic conditions because the flows are much less in the 1% annual chance flood scenario. The average invert change through the entire study reach is -1.1 feet (i.e., the difference between the initial invert and the minimum invert).

The change in the average bed elevation (between the initial simulation time step and the final simulation time step) for both the entire cross-section and the main channel are shown in Figure 6-34 and Figure 6-35, respectively. The average bed elevation change for the entire cross-section was -0.2 feet while the average bed elevation change for the main channel only was -0.6 feet. In addition, the average bed elevation changes show aggradation occurring in between 19th Avenue and 27th Avenue as well as downstream of 51st Avenue. Both of these areas indicate that sediment is depositing in the large sand and gravel mining operations in those areas.

The total cumulative mass inflow for the Salt/Gila River system under existing conditions with the 1% annual chances flood hydrograph is shown in Figure 6-36. This figure is similar to the cumulative mass inflow plot for existing conditions historic flows. However, a smaller amount of sediment is delivered to the SR-85 Bridge because the flows are smaller for this scenario.

6.7.3.2 HEC-6T Model

The initial and minimum invert along with the invert change for the Salt/Gila River system under existing conditions for HEC-6T can be seen in Figure 6-37. The average invert change throughout the study reach is -0.9 feet (i.e., the difference between the initial invert and the minimum invert). These results are similar to the results generated from HEC-RAS (see Figure 6-33). In general, both the HEC-RAS model and the HEC-6T model predict degradation in the same locations for the historic conditions. Generally, the HEC-RAS model predicts greater degradation troughs compared to the HEC-6T model. Averaged across the entire reach, the HEC-RAS model predicts an invert elevation that is about 0.2 foot lower than the HEC-6T model for the existing conditions.

The change in the average bed elevation (between the initial simulation time step and the final simulation time step) for both the entire cross-section and the main channel are shown in Figure 6-38 and Figure 6-39, respectively. The average bed elevation change for the entire cross-section was 0.0 feet while the average bed elevation change for the main channel was -0.1 feet. In general, the HEC-6T plots show more aggradation in the mining pits upstream of 51st Avenue. Downstream of 51st Avenue, both HEC-RAS and HEC-6T show degradation.

The total cumulative mass outflow for the Salt/Gila River system using HEC-6T is shown in Figure 6-40. The pattern of the total cumulative mass outflow along the river system is similar for both HEC-RAS and HEC-6T (compare Figure 6-36 to Figure 6-40). In addition, the cumulative mass outflow for HEC-RAS at SR-85 (3,636,192 tons) is approximately the same as it is for HEC-6T (3,216,918 tons). Still, since the HEC-6T model is predicting less degradation overall compared to the HEC-RAS model, there should be less sediment delivered to SR-85 for the HEC-6T model when compared to the HEC-RAS model.

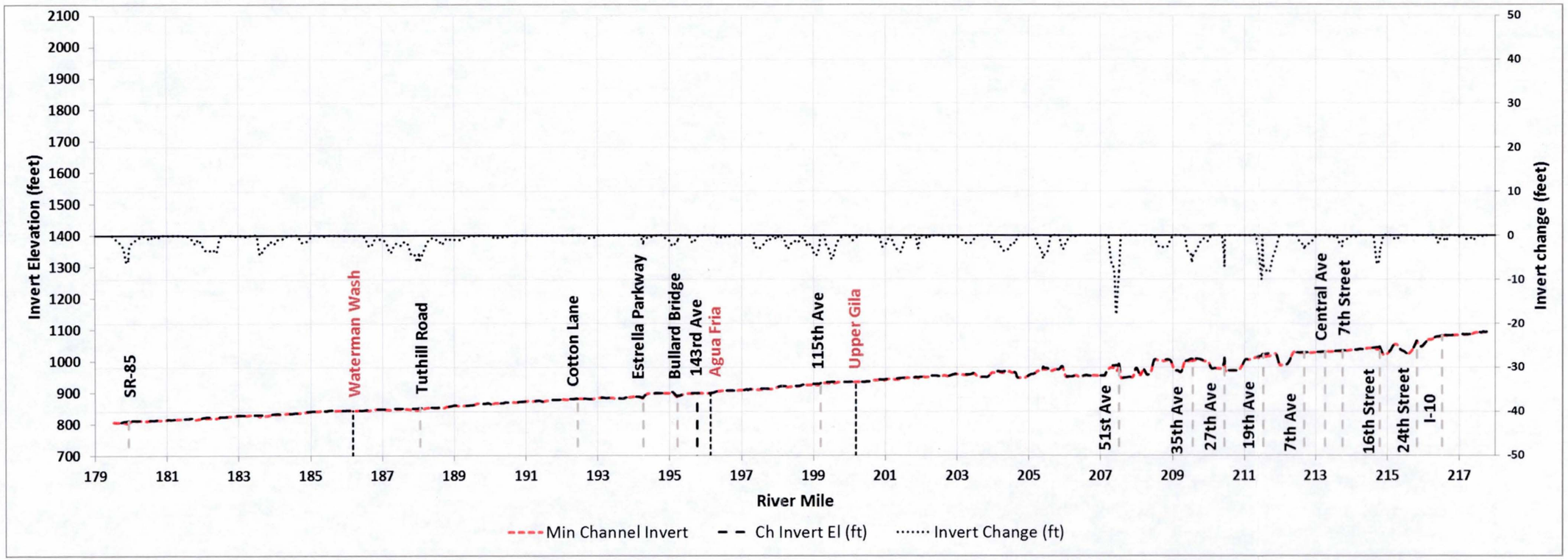

Figure 6-33. Maximum invert profile change for existing conditions HEC-RAS model with 1% annual chance flow series

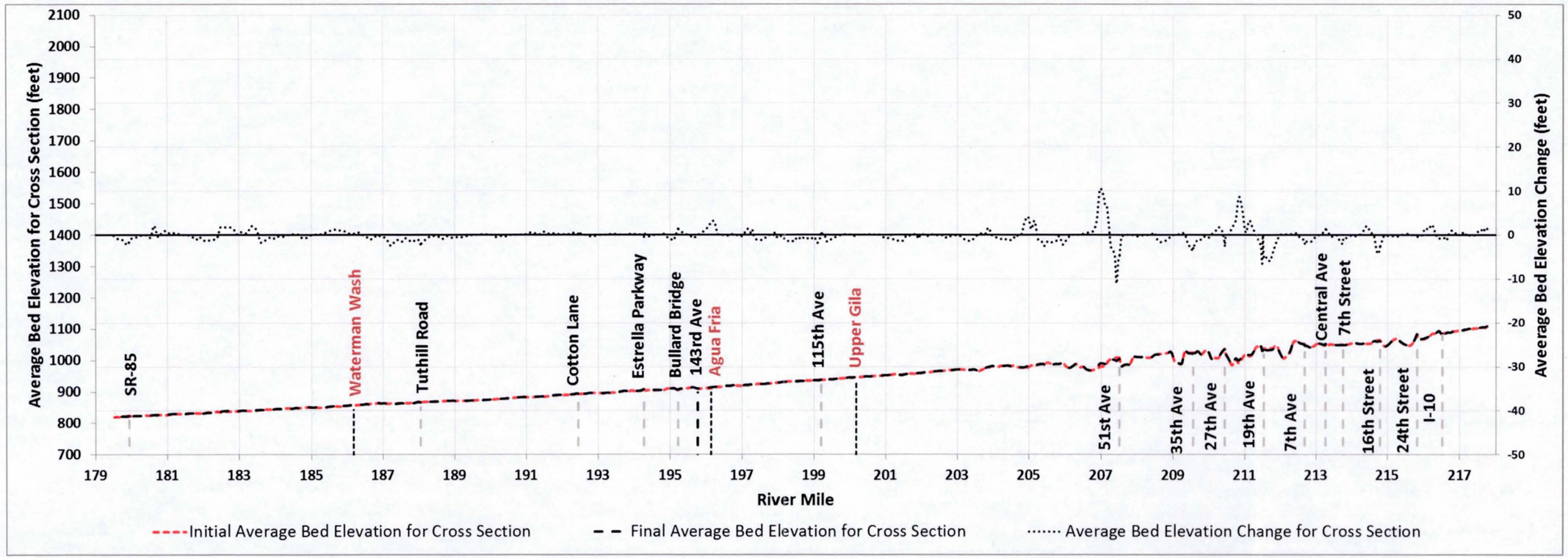

Figure 6-34. Change in the average bed elevation for the entire cross-section for existing conditions HEC-RAS model with 1% annual chance flow series

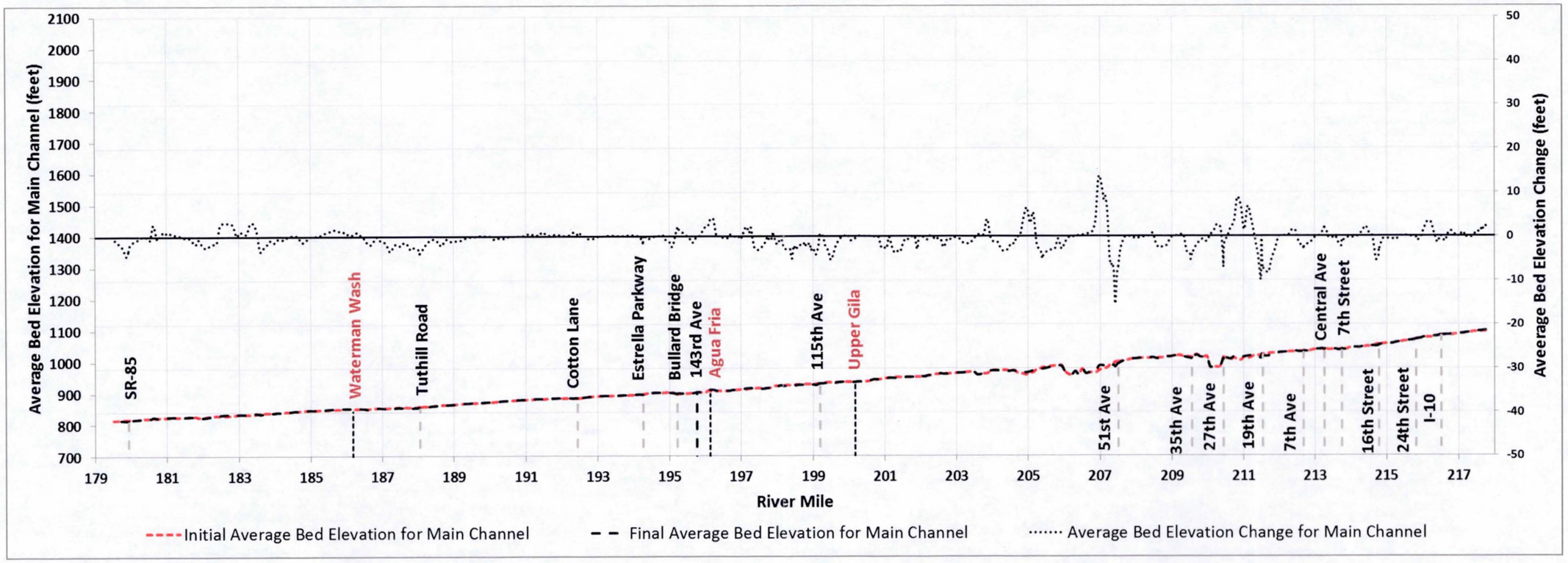

Figure 6-35. Change in the average bed elevation for the main channel for existing conditions HEC-RAS model with 1% annual chance flow series

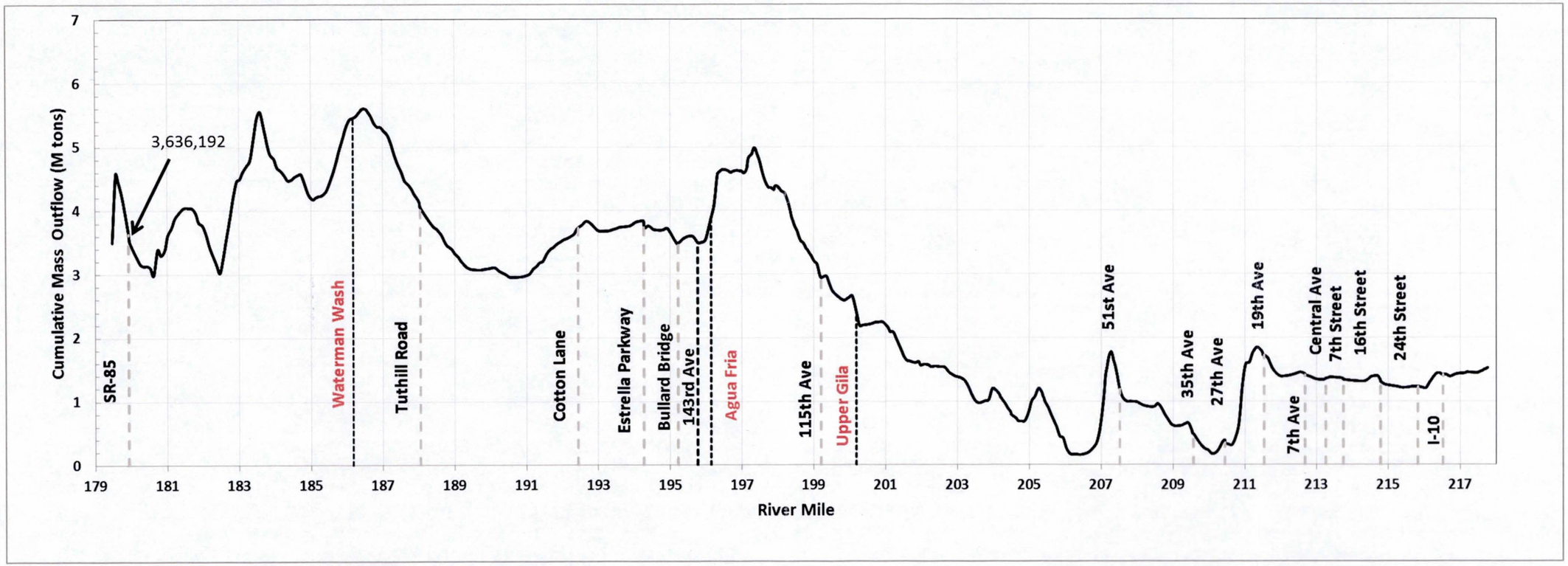

Figure 6-36. Cumulative total sediment outflow for existing conditions HEC-RAS model with 1% annual chance flood hydrograph

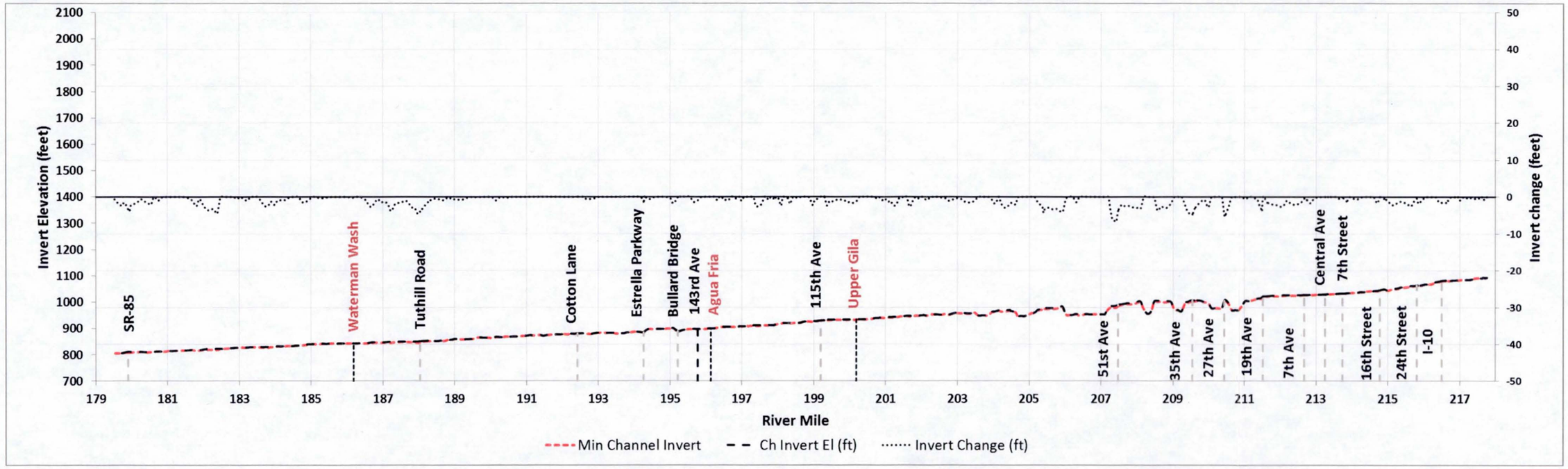

Figure 6-37. Maximum invert profile change for existing conditions HEC-6T model with 1% annual chance flow series

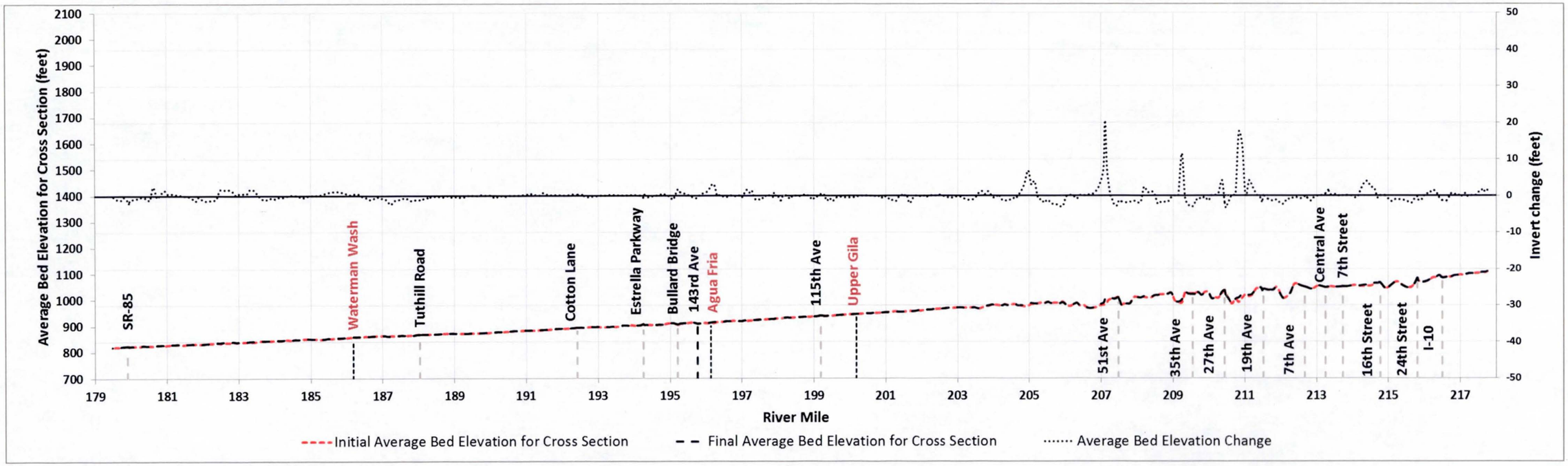

Figure 6-38. Change in the average bed elevation for the entire cross-section for existing conditions HEC-6T model with 1% annual chance flow series

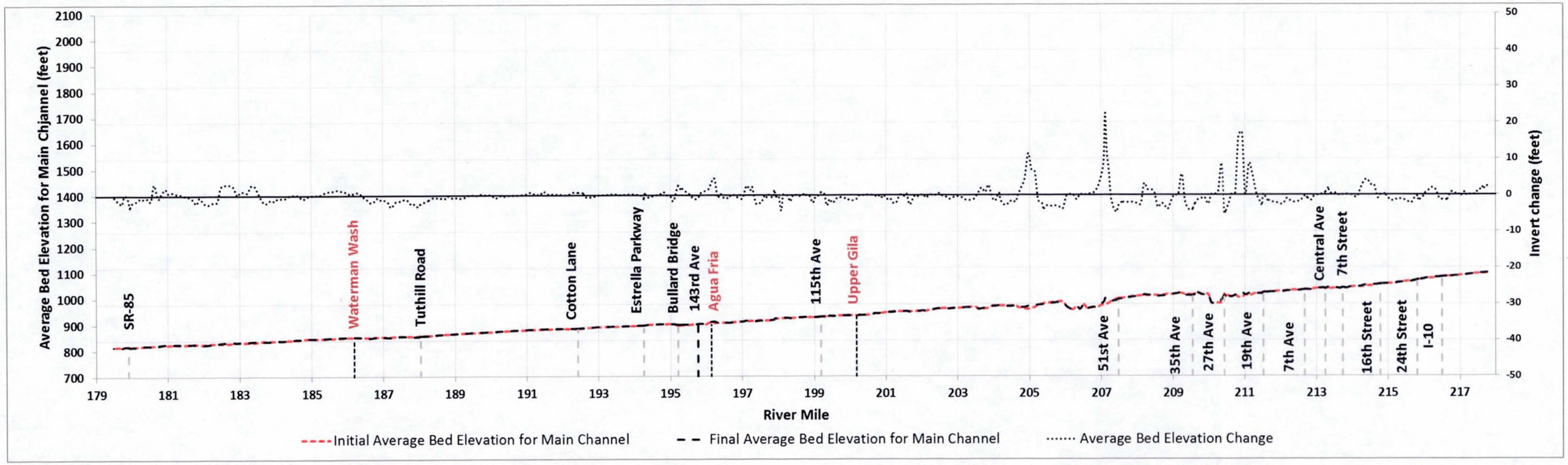

Figure 6-39. Change in the average bed elevation for the main channel for existing conditions HEC-6T model with 1% annual chance flow series

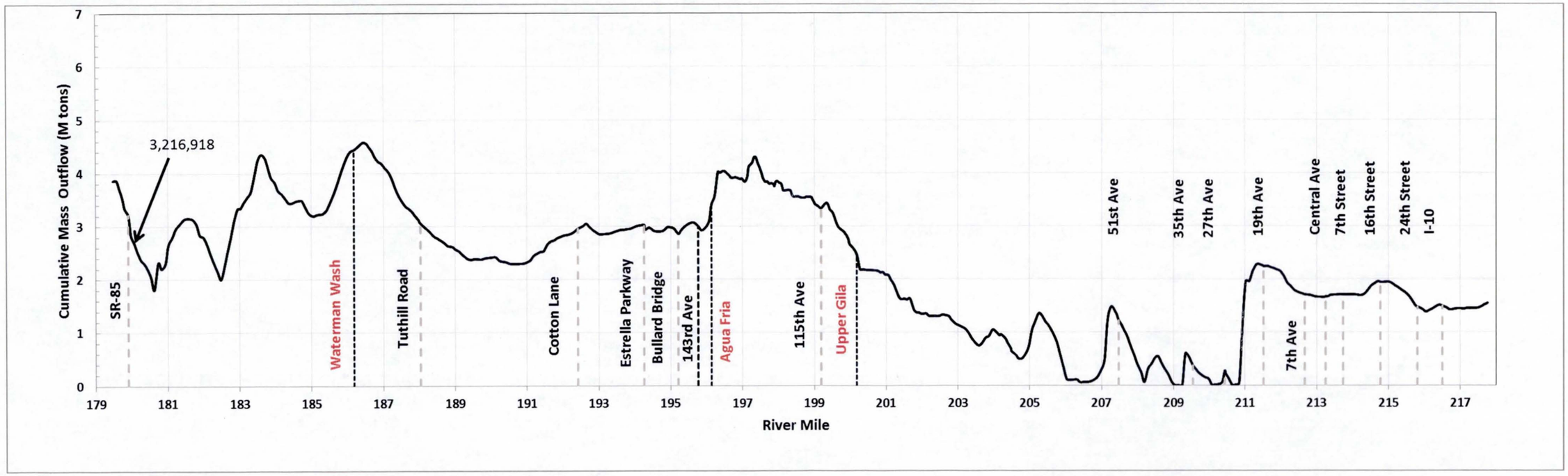

Figure 6-40. Cumulative total sediment outflow for existing conditions HEC-6T model with 1% annual chance flood hydrograph

6.7.4 Proposed Conditions Model for the 1% Annual Chance Flood Hydrograph

6.7.4.1 HEC-RAS Model

The HEC-RAS sediment transport model was also run for the proposed conditions model for the Salt/Gila River system reach using the 1% annual chance flood hydrograph inflow series. Figure 6-41 shows the initial and minimum invert elevations along with the river. This figure shows that the minimum channel invert is about 10 feet below the initial invert near 19th Avenue and about 18 feet below the initial invert near 51st Avenue. These are areas were degradation was observed for the proposed conditions HEC-RAS model with the historic inflow series. The amount of degradation is less in the 1% annual chance flood conditions than the historic conditions because the flows are much less in the 1% annual chance flood scenario. The average invert change through the entire study reach is -1.5 feet (i.e., the difference between the initial invert and the minimum invert).

The change in the average bed elevation (between the initial simulation time step and the final simulation time step) for both the entire cross-section and the main channel are shown in Figure 6-42 and Figure 6-43, respectively. The average bed elevation change for the entire cross-section was -0.1 feet while the average bed elevation change for the main channel only was -0.7 feet. As with the existing conditions model, the average bed elevation changes show aggradation occurring in between 19th Avenue and 27th Avenue as well as downstream of 51st Avenue. Both of these areas indicate that sediment is depositing in the large sand and gravel mining operations in those areas. In addition, the proposed conditions model shows areas of aggradation in proposed pits upstream of the Agua Fria River, downstream of Cotton Lane, and in between Waterman Wash and SR-85.

The total cumulative mass inflow for the Salt/Gila River system under proposed conditions with the 1% annual chances flood hydrograph is shown in Figure 6-44. This figure is similar to the cumulative mass inflow plot for proposed conditions historic flows. However, a smaller amount of sediment is delivered to the SR-85 Bridge because the flows are smaller for this scenario.

6.7.4.2 HEC-6T Model

The initial and minimum invert along with the invert change for the Salt/Gila River system under proposed conditions for HEC-6T can be seen in Figure 6-45. The average invert change throughout the study reach is -1.2 feet (i.e., the difference between the initial invert and the minimum invert). These results are similar to the results generated from HEC-RAS (see Figure 6-44). In general, both the HEC-RAS model and the HEC-6T model predict degradation in the same locations for the historic conditions. Generally, the HEC-RAS model predicts greater degradation troughs compared to the HEC-6T model. Averaged across the entire reach, the HEC-RAS model predicts an invert elevation that is about 0.3 foot lower than the HEC-6T model for the existing conditions.

The change in the average bed elevation (between the initial simulation time step and the final simulation time step) for both the entire cross-section and the main channel are shown in Figure 6-46 and Figure 6-47, respectively. The average bed elevation change for the entire cross-section was 0.1 feet while the average bed elevation change for the main channel was -0.2 feet. In general, the HEC-6T

plots show more aggradation in the mining pits upstream of 51st Avenue. Downstream of 51st Avenue, both HEC-RAS and HEC-6T show degradation with the occasional spike of aggradation in a proposed pit.

The total cumulative mass outflow for the Salt/Gila River system using HEC-6T is shown in Figure 6-48. The pattern of the total cumulative mass outflow along the river system is similar for both HEC-RAS and HEC-6T (compare Figure 6-44 to Figure 6-48). In addition, the cumulative mass outflow for HEC-RAS at SR-85 (2,779,939 tons) is approximately the same as it is for HEC-6T (2,617,400 tons). Still, since the HEC-6T model is predicting less degradation overall compared to the HEC-RAS model, there should be less sediment delivered to SR-85 for the HEC-6T model when compared to the HEC-RAS model.

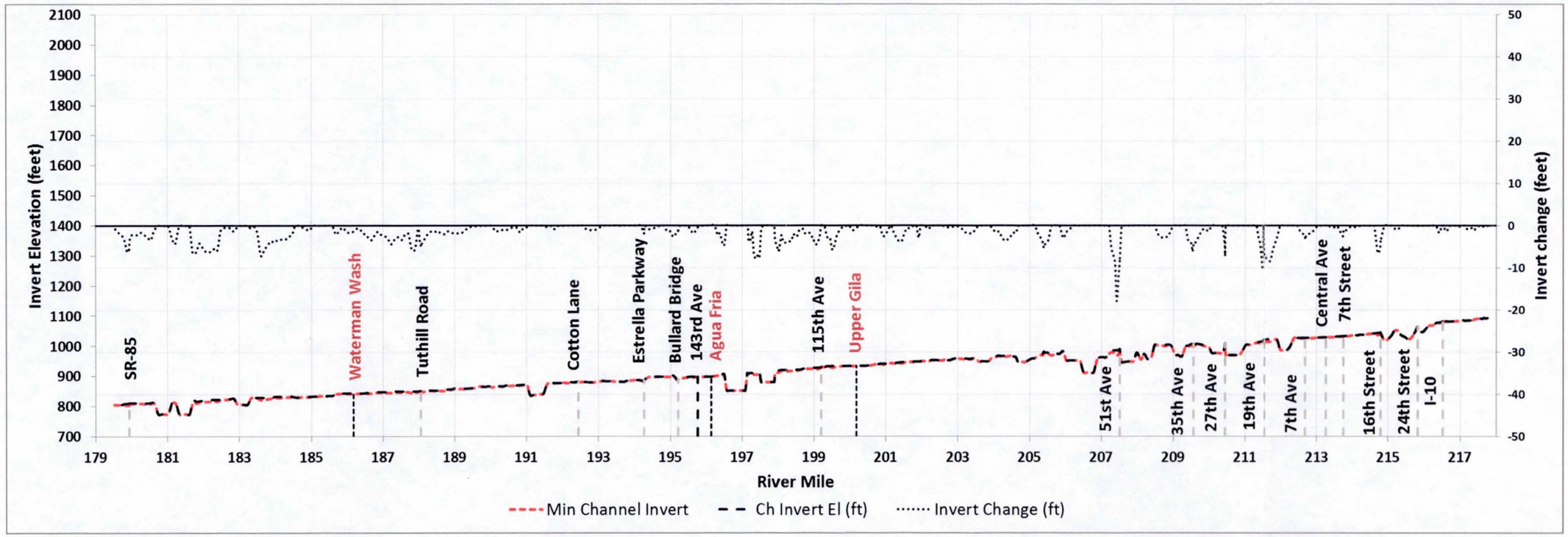

Figure 6-41. Maximum invert profile change for proposed conditions HEC-RAS model with 1% annual chance flow series

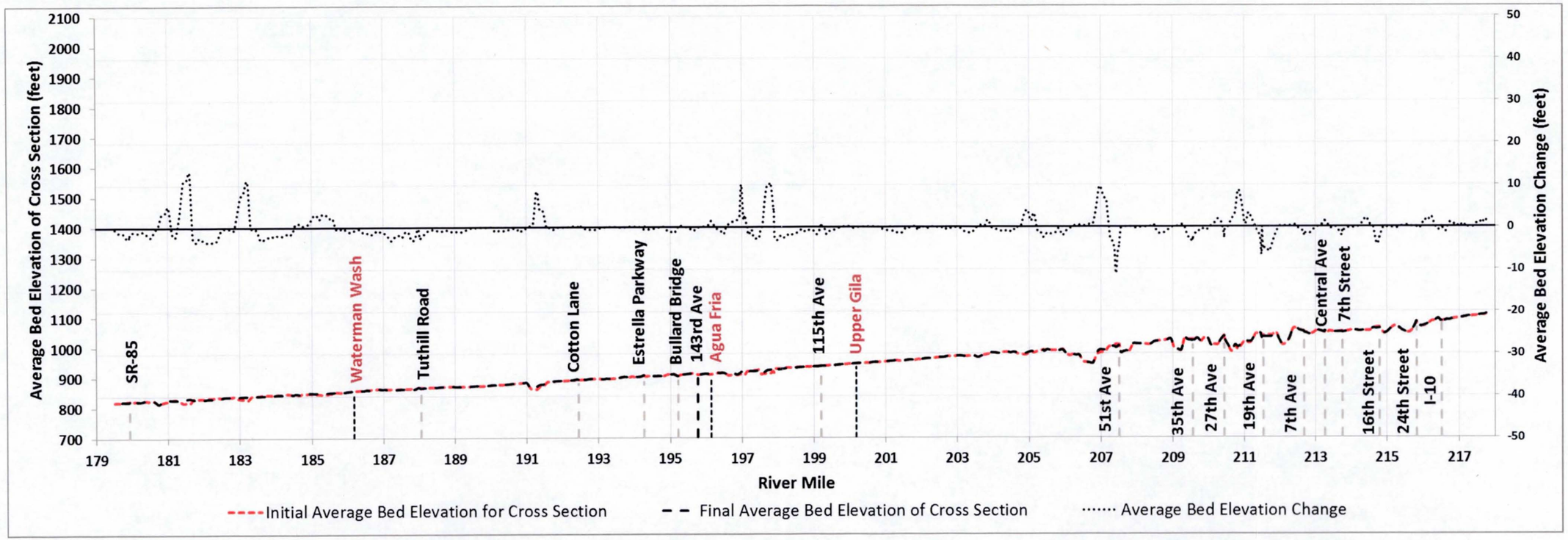

Figure 6-42. Change in average bed elevation of the cross-section for proposed conditions HEC-RAS model with 1% annual chance flow series

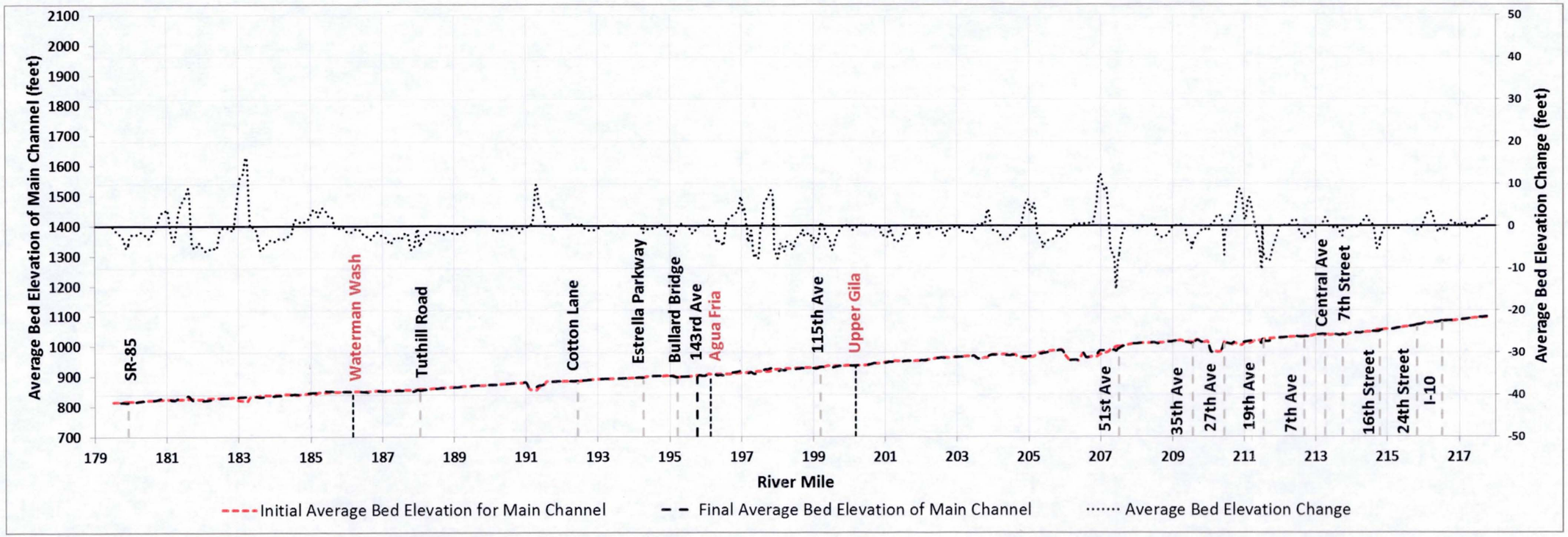

Figure 6-43. Change in average bed elevation of the main channel for proposed conditions HEC-RAS model with 1% annual chance flow series

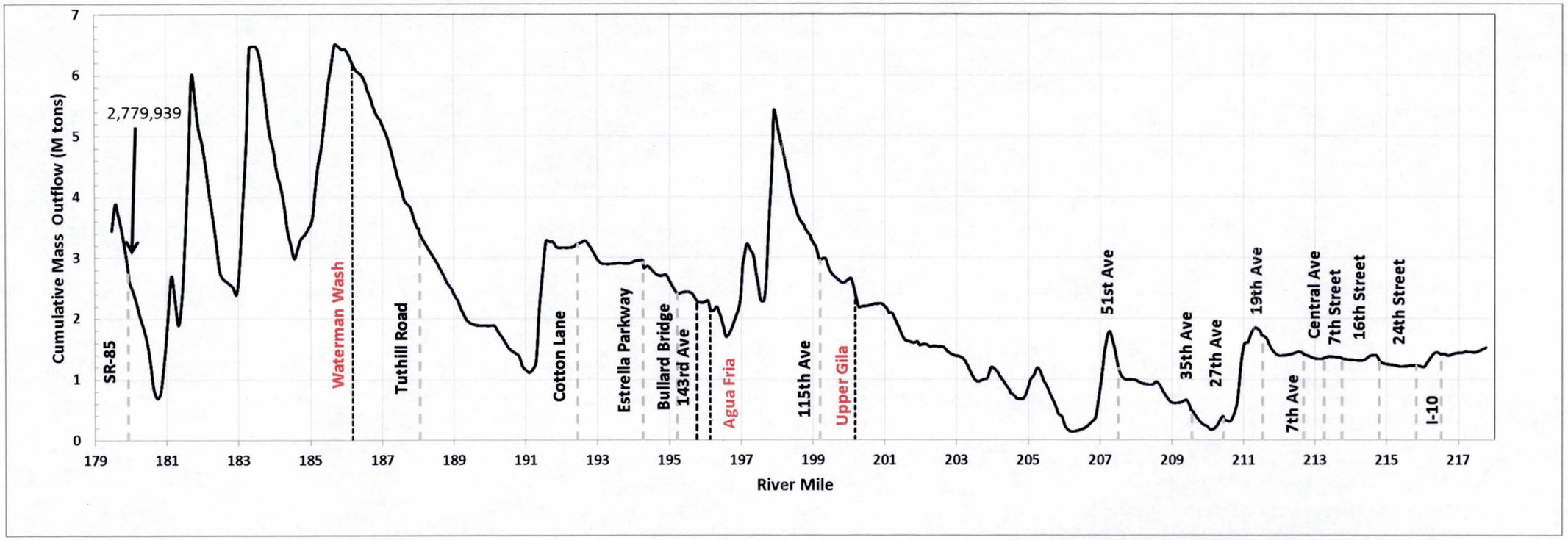

Figure 6-44. Cumulative total sediment outflow for proposed conditions HEC-RAS model with 1% annual chance flood hydrograph

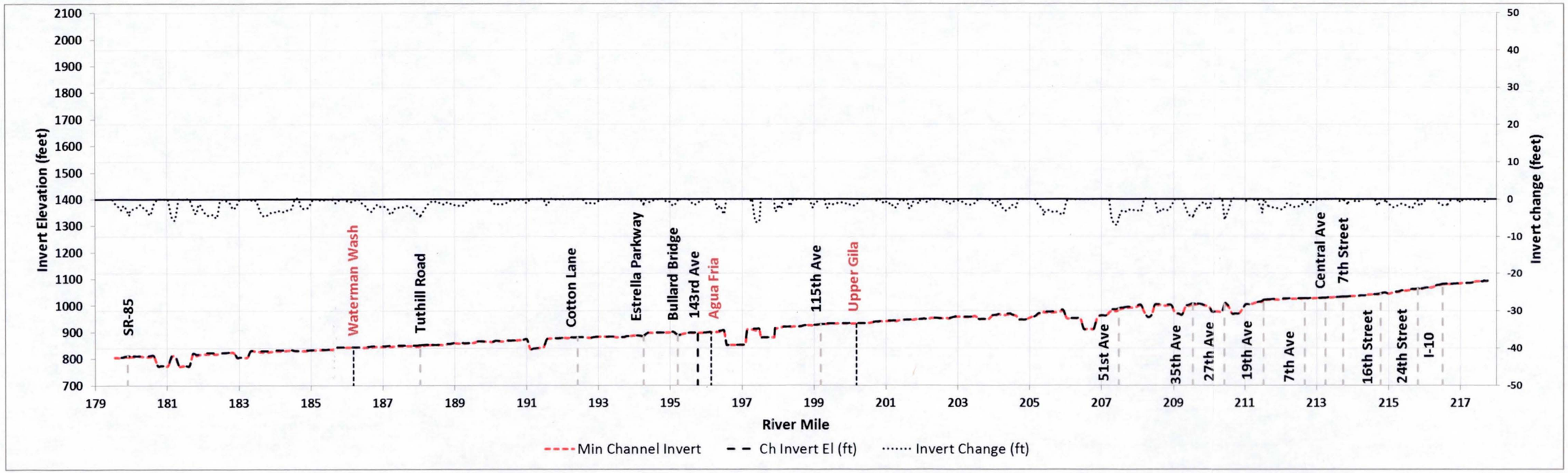

Figure 6-45. Maximum invert profile change for proposed conditions HEC-6T model with 1% annual chance flow series

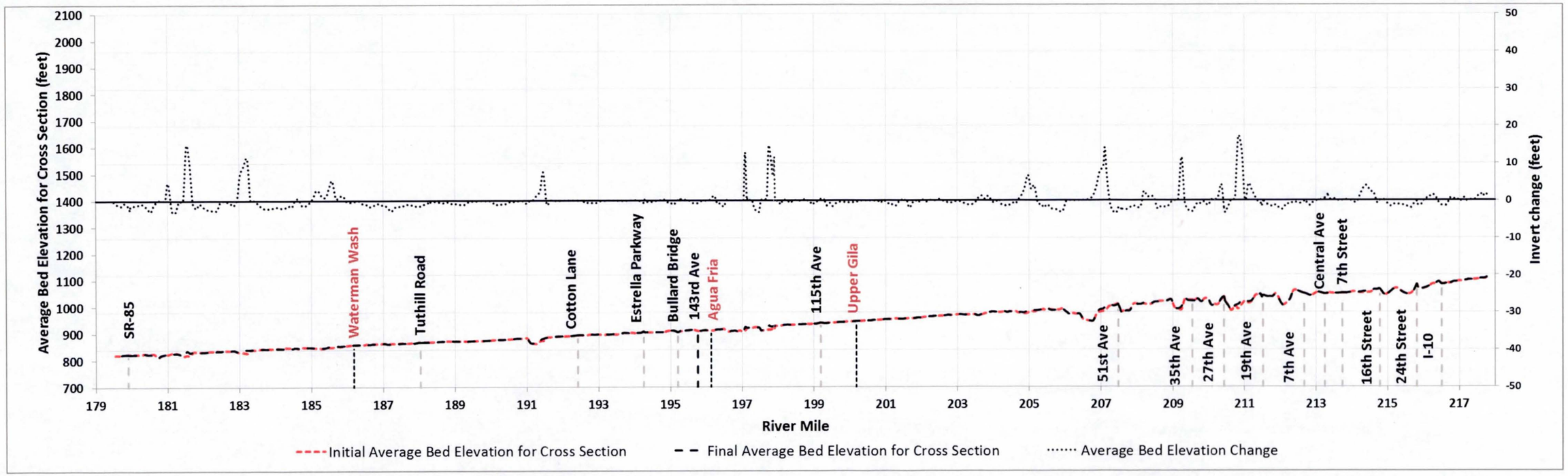

Figure 6-46. Change in average bed elevation for cross-section for proposed conditions HEC-6T model with 1% annual chance flow series

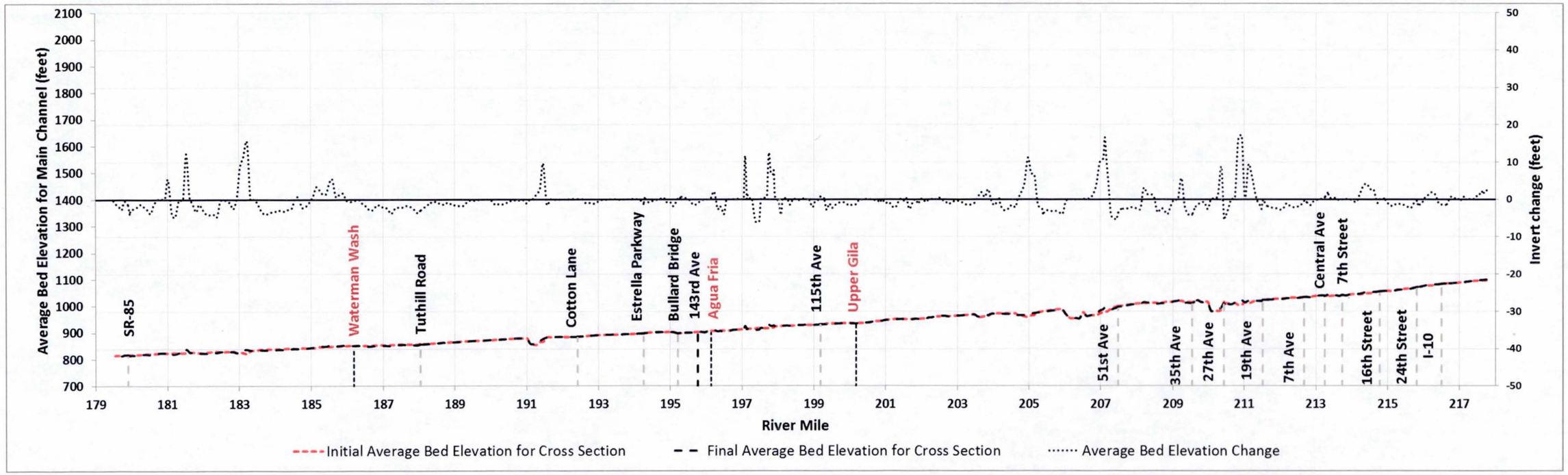

Figure 6-47. Change in average bed elevation for main channel for proposed conditions HEC-6T model with 1% annual chance flow series

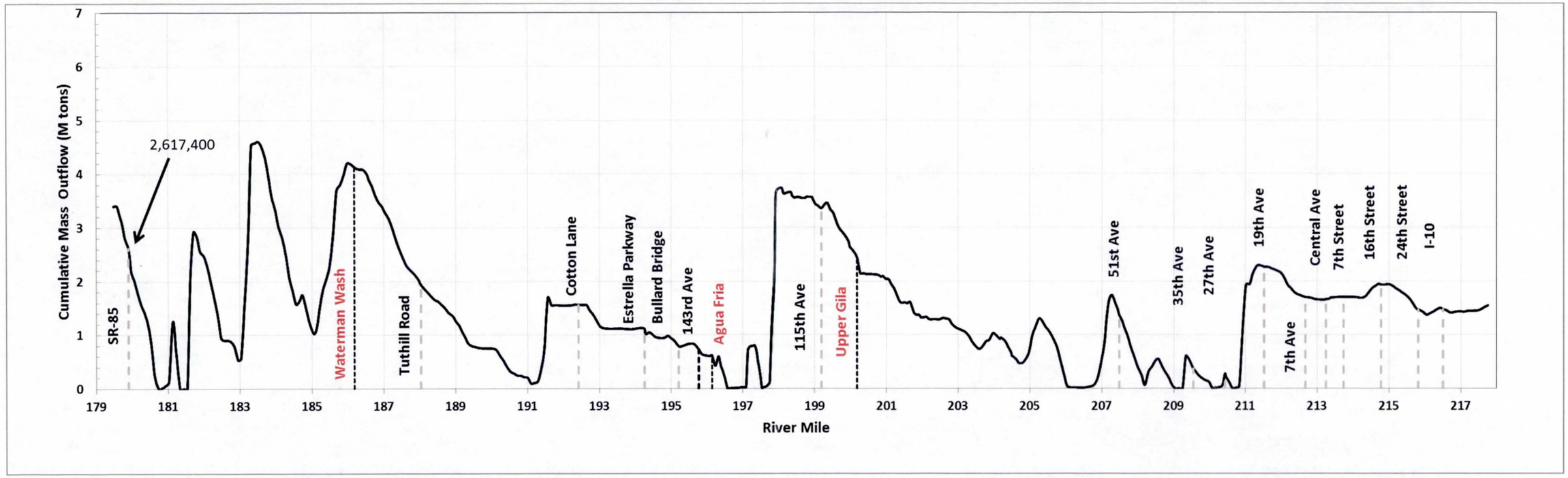

Figure 6-48. Cumulative total sediment outflow for proposed conditions HEC-6T model with 1% annual chance flood hydrograph

6.7.5 Sediment Issues Encountered During the Study

The District utilizes sediment transport models to assist in determining the sediment impacts on existing and proposed sand and gravel mines. One of the criteria that the District looks at is the amount of degradation that occurs at the upstream and downstream end of pits. The sediment transport modeling results indicated that in locations that had multiple pits (i.e., locations where there are two or more pits in the same cross-section) that the simulated degradation at the upstream and downstream ends of the pits was not as much as would be expected. These multiple pit locations typically occur when there is a sand and graveling mining operation in both the overbanks (offline) and main channel (inline) in the same location. Because HEC-RAS and HEC-6T sediment transport model is a one-dimensional model, when there are multiple pits on one cross-section, the degradation occurring at the upstream and downstream end of the pits may not be accurate.

To more effectively model the degradation at the upstream and downstream ends for multiple pits in one cross-section, the following modeling technique is suggested. When there are multiple pits in one cross-section, each pit should be modeled independently with its own discharge hydrograph and geometric data. Each independent model will have only one pit and rest of the pit's geometry data (such as GR cards in HEC-6T) should be removed from the cross-section. For example, an inline pit should only have one inline pit and rest of the inline or offline pits should be removed by deleting its corresponding geometry data. Similarly if an offline pit is being modeled, the rest of the inline and offline pits should be removed from this model by deleting their corresponding geometry data. The corresponding discharge hydrograph should be developed accordingly.

There are two locations along the study reach where multiple pits were encountered. The first set covers permits FA94-072 (inline pit), SG03-004A (offline pits), and SG05-03 (offline pit). These three pits are located just downstream of 51st Avenue and overlap as shown in Figure 6-49. The second location covers SG14-004 (offline), SG15-001 (offline), SG07-003 (offline), and SG04-002 (offline with a small section inline). This group of sand and gravel operations is located downstream of Avondale Boulevard and overlap each other as shown in Figure 6-50. For these two areas, it is recommended that the modeling described above be used when analyzing these pits with sediment transport modeling techniques.

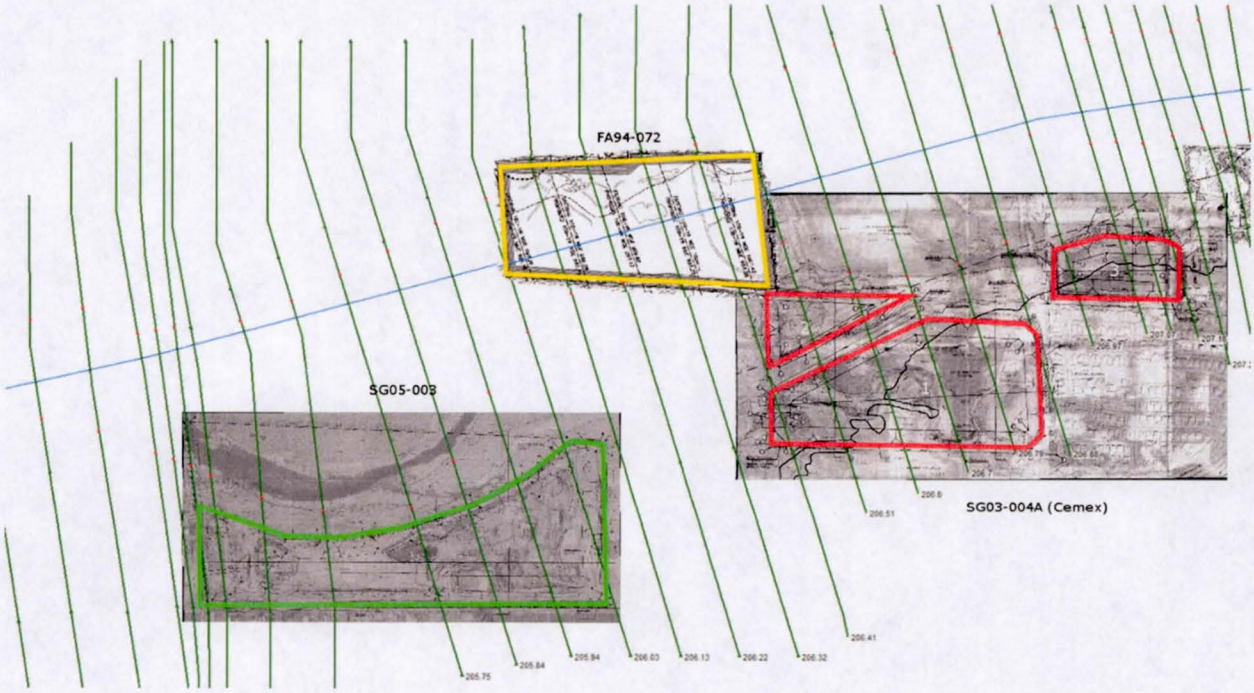

Figure 6-49. Plan view of first set of multiple pits located just downstream of 51st Avenue

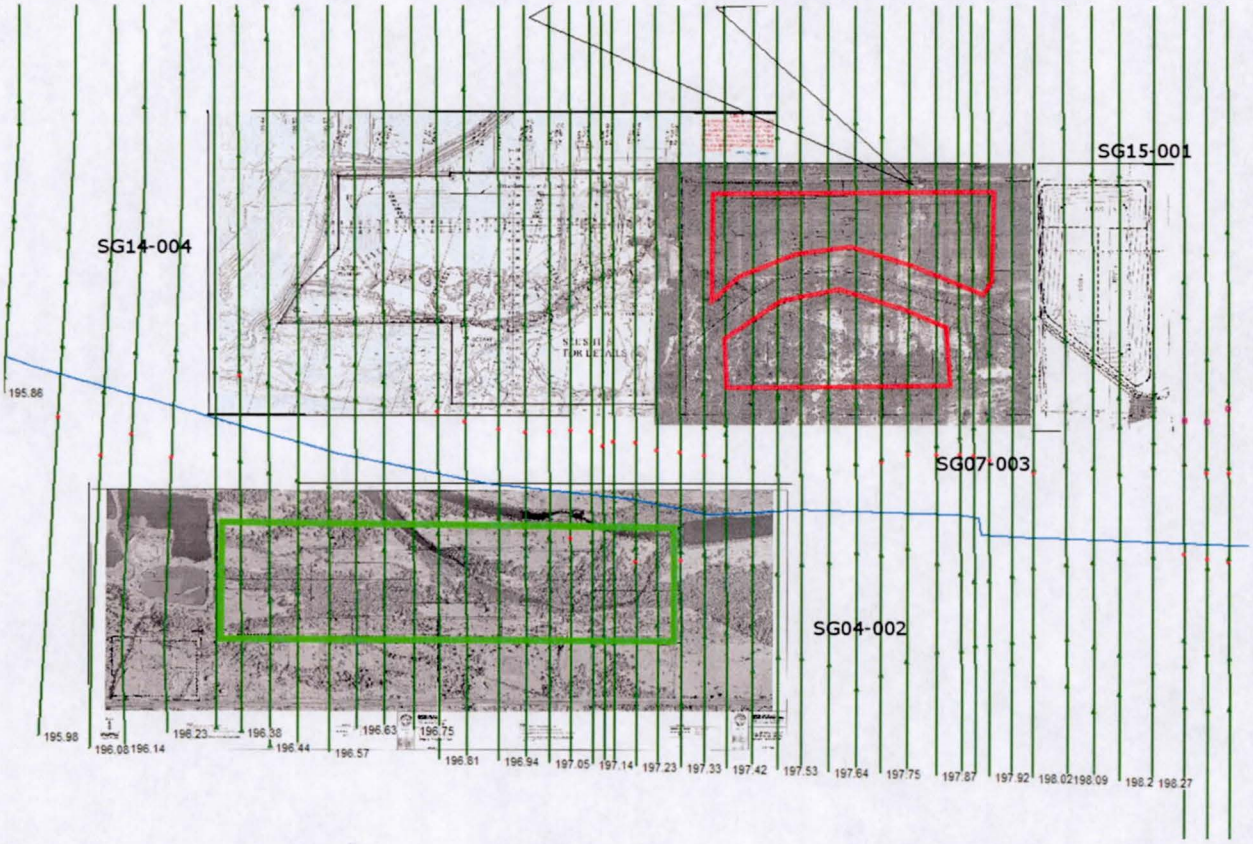

Figure 6-50. Plan view of second set of multiple pits located downstream of Avondale Boulevard

6.7.6 Comparison with Previous Sediment Transport Studies

To check the overall results of the model runs, general trends from the previous sediment transport model runs were compared to the sedimentation results from this study. However, a direct comparison is not possible as the previous sediment transport models were using a different starting geometry, had different pit dimensions, used a different sediment transport function, used different hydrology, had different model extents, and bridges may not have been explicitly modeled in the older studies, etc. However, it is still possible to make some generalized comparisons between this current study and the previous sediment transport studies.

6.7.6.1 El Rio Sediment Transport Study

Thus current study makes use of the same sediment gradations used in the El Rio sediment transport HEC-6T model (Stantec, 2006). However, for the El Rio model was based on older topographic data and, more significantly, the sediment rating curves used in the El Rio model are quite different than the sediment rating curves used in this study. The sediment rating curves used in the El Rio study delivers more sediment to the system than the ones used in this current study. Because of this, comparing the cumulative sediment outflow at a location like the SR-85 Bridge would not be useful as the differences between the two studies is most likely a result of the different sediment inflow rating curves.

General trends of the invert change can be made between the El Rio model and the models developed for this study. Figure 6-51 shows the initial and final average bed elevations for the El Rio existing conditions HEC-6T sediment transport model (Stantec, 2006). In general, this figure shows degradation from approximately RM 198 to RM 192, no change in bed elevation from RM 192 to RM 189, and degradation again from RM 189 to RM 179. A somewhat similar pattern is seen in the HEC-6T existing conditions historic flows model (see Figure 6-22 and Figure 6-23). The main difference is that the HEC-6T model results for this study do not show degradation downstream of approximately RM 184. There are several different factors between the two sediment transport models such as different initial conditions geometry, different historic flow hydrographs, different sediment inflow hydrographs, etc. Despite these differences there are still similar patterns that can be observed.

6.7.6.2 Rio Salado Low Flow Channel Design

The performance of the newly developed sediment transport models compared to the sediment transport model developed for the Rio Salado Low Flow Channel (WEST Consultants, Inc., 2000) was discussed in Section 6.5.

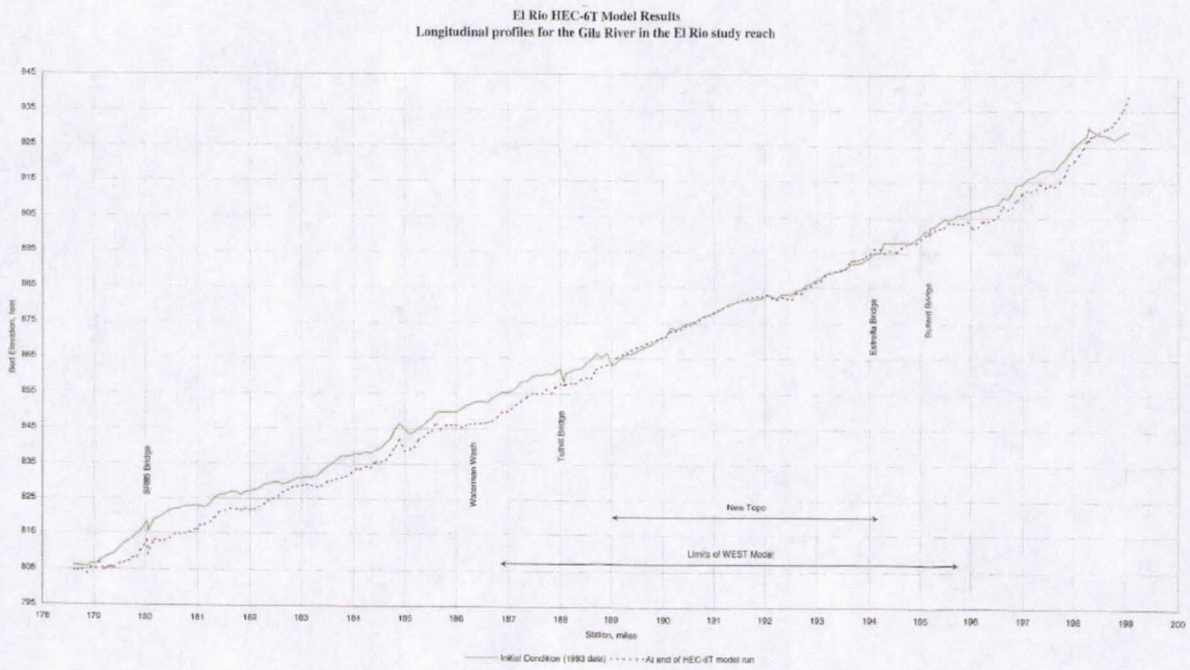

Figure 6-51. Initial and final average bed elevations for the El Rio sediment transport study (Stantec, 2006)

6.7.6.3 Rio Salado Oeste Study

The existing conditions historic runs for both HEC-RAS and HEC-6T were compared with the results generated from the Rio Salado Oeste study (WEST Consultants, Inc., 2002b). The results for HEC-RAS (shown in Figure 6-17, Figure 6-18, and Figure 6-19) agree with the results from the sediment transport study completed for the Rio Salado Oeste reach (i.e., from 19th Avenue to 91st Avenue). A similar trend in also seen in the HEC-6T results (see Figure 6-21). The Rio Salado Oeste report indicated that degradation typically occurred downstream of 35th Avenue while aggradation occurred upstream of the 35th Avenue Bridge due to milder slopes that allowed for backwater conditions and depositing of sediment (WEST Consultants, Inc., 2002b). Also note that the pit upstream of 35th Avenue (near 27th Avenue) was much smaller in 2002 when the Rio Salado Oeste study was completed. Comparison between the results for the Rio Salado Oeste study (WEST Consultants, Inc., 2002b) and this current study are shown in Figure 6-52. For the most part, the average bed elevations agree fairly well between the two studies. There are a few places (e.g., near RM 210 and 206.5) where the current study results have much lower average bed elevations than the Rio Salado Oeste study. These areas are most likely sand and gravel mines that have been created after 2002 when the Rio Salado Oeste study was completed.

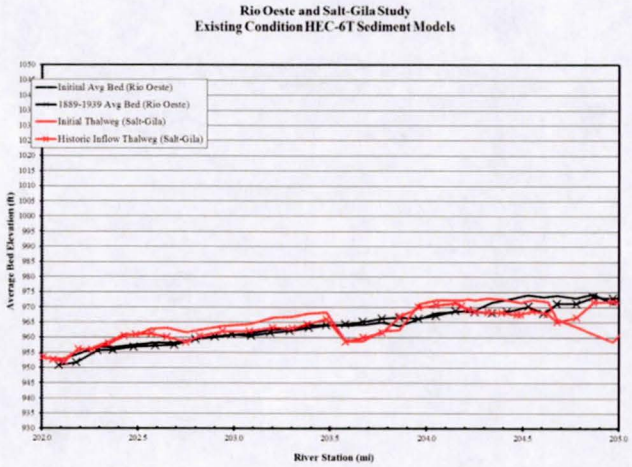

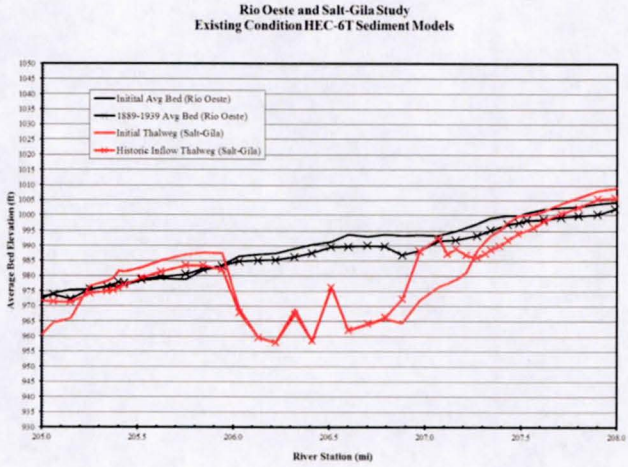

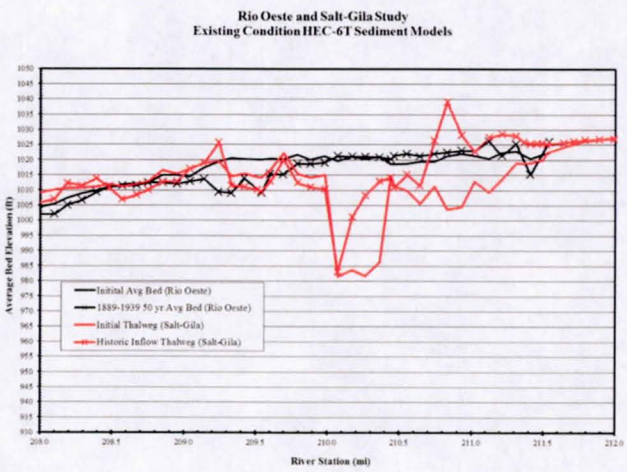

Figure 6-52. HEC-6T average bed elevations (main channel) for current study and the Rio Salado Oeste study

6.7.6.4 *Tres Rios North Levee PED Study*

The Tres Rios North Levee PED project ran from 91st Avenue to just upstream of Bullard Avenue. The sediment transport results in this area after a long term simulation indicate degradation in the entire study reach (WEST Consultants, Inc., 2002a). This agrees well with the HEC-RAS and HEC-6T results shown in Figure 6-17, Figure 6-18, Figure 6-19, and Figure 6-21. Plots showing the HEC-6T sediment transport results for both this current study and the Tres Rios North Levee PED study (WEST Consultants, Inc., 2002a) are shown in Figure 6-53 and Figure 6-54. This two study results show similar results. There are several different factors between the two sediment transport models such as different initial conditions geometry, different historic flow hydrographs, different sediment inflow hydrographs, etc. Despite these differences there are still similar patterns that can be observed.

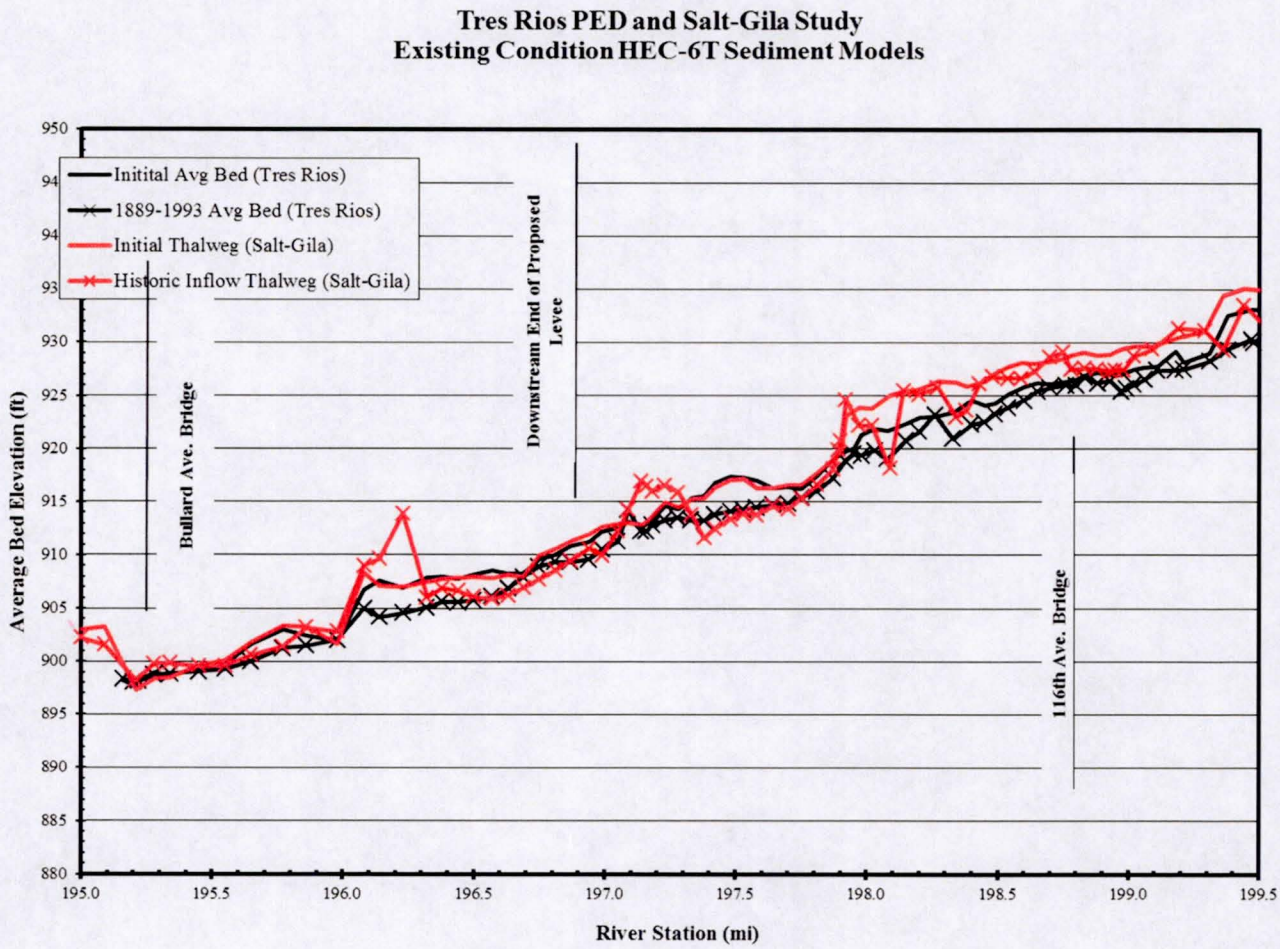

Figure 6-53. HEC-6T average bed elevations (main channel) for current study and the Tres Rios PED study (downstream end of the reach)

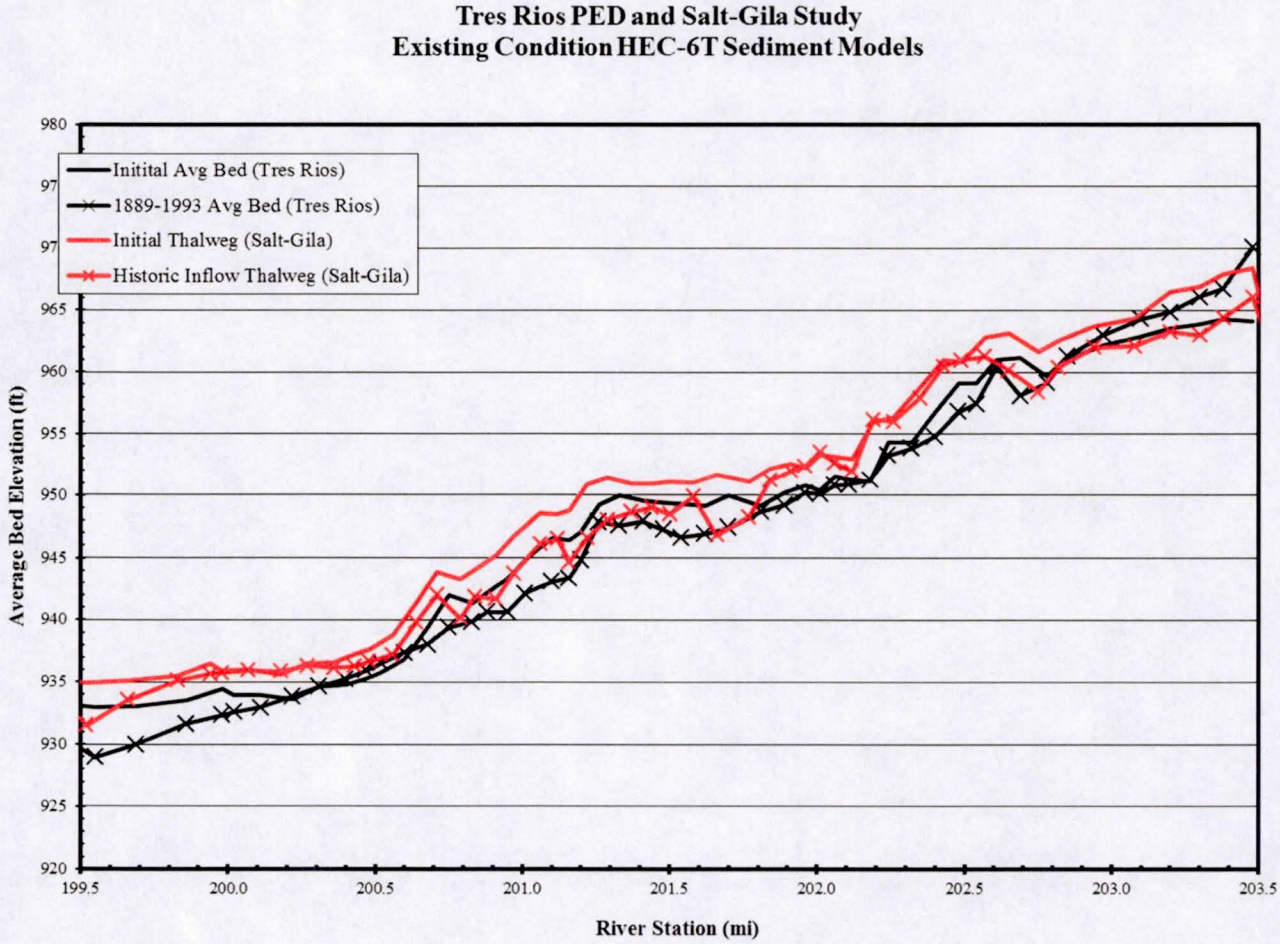

Figure 6-54. HEC-6T average bed elevations (main channel) for current study and the Tres Rios PED study (upstream end of the reach)

7 Draft FIS Data

Draft Flood Insurance Study data were not developed as part of this study.

8 References

Arizona Department of Water Resources. (2012). *Instructions for Organizing and Submitting Technical Documentation for Flood Studies.* Phoenix.

Flood Control District of Maricopa County. (2013). *Drainage Design Manaual for Maricopa County: Hydraulics.* Phoenix, AZ: Flood Control District of Maricopa County.

HNTB. (December 15, 2010). *Revised Draft Tres Rios Phase 3 Pre-Project Hydraulic Analysis Review Technical Memorandum.* Prepared for the US Army Corps of Engineers, Los Angeles District.

Hydrologic Engineering Center. (2010). *HEC-RAS River Analysis System Version 4.1.* Davis: U.S. Army Corps of Engineers.

Hydrologic Engineering Center. (2010). *HEC-RAS River Analysis System, Hydraulic Reference Manual, Version 4.1.* Davis: U.S. Army Corps of Engineers.

JE Fuller Hydrology and Geomorphology, Inc. (2010). *Tres Rios Phase 3 Environmental Restoration Project Design Documentation Report: Hydraulic Analyses Appendix.* Prepared for the US Army Corpos of Engineers, Los Angeles District.

Kimley-Horn and Associates. (2001). *Agua Fria Watercourse Master Plan: Sediment Trend Analysis.* Phoenix, AZ: Flood Control District of Maricopa County, FCD 99-24.

MBH Software. (2006). *Sedimentation in Stream Networks HEC-6T, v. 5.13.22.* Clinton, MS: MBH Software.

Michael Baker, Jr., Inc. (1999). *Salt-Gila River Floodplain Delineation Restudy.* Phoenix, AZ: For the Flood Control District of Maricopa County, FCD 90-59.

Simons Li and Associates. (1995). *19th Avenue Landfill Environmental Cleanup: 19th to 15th Avenue at the Salt River.* Phoenix, AZ: City of Phoenix.

Stantec. (2006). *El Rio Watercourse Master Plan and Area Drainage Master Plan: El Rio Sedimentation Analysis.* Phoenix, AZ: Flood Control District of Maricopa County, FCD 2001C024.

Stantec. (2009). *Gila River Sediment Program.* Phoenix, AZ: Flood Control District of Maricopa County, FCD 2007C017.

Stantec. (2013). *Gillespie Area Drainage Master Study.* Phoenix, AZ: Flood Control District of Maricopa County, FCD 2009C039.

Stantec. (2014). *Lower Gilia River Floodplain Delineation Study DRAFT.* Phoenix, AZ: Flood Control District of Maricopa County, FCD 2012C017.

TY Lin International. (2011a). *Salt River Letter of Map Revision.* Phoenix: FEMA Case No: 13-09-3108P, Phoenix Aviation Department.

TY Lin International. (2011b). *Levee Certification Report: Levee ID No. 41 & 42.* Phoenix: City of Phoenix, Aviation Department.

U.S. Army Corps of Engineers. (1996). *Section 7 Study for Modified Roosevelt Dam, Arizona (Theodore Roosevelt Dam): Hydrologic Evaluation of Water Control Plans, Salt River Project to Gila River at Gillespie Dam.* Los Angeles District.

URS. (2010). *Rainbow Valley Area Drainage Master Plan Technical Data Notebook: Hydrology Report.* Phoenix, AZ: Flood Control District of Maricopa County, FCD 2006C029.

URS. (2011). *RVADMP - Waterman Wash Sediment Trasnport Analysis.* Phoenix, AZ: Flood Control District of Maricopa County, FCD 2009C029.

US Army Corps of Engineers. (2012). *Tres Rios Environmental Restoration Project: Design Documentation Report (DDR) for the Tres Rios North Levee.* Los Angeles District.

WEST Consultants, Inc. (2000). *Low Flow Channel Design Analysis for Rio Salado (Salt River), Arizona.* Los Angels, CA: Prepared for the US Army Corps of Engineers, Los Angeles District.

WEST Consultants, Inc. (2002a). *PED Hydraulic Design for the Tres Rios North Levee.* Los Angeles, CA: US Army Corps of Enigneers, Los Angeles District.

WEST Consultants, Inc. (2002b). *Rio Salado Oeste Study: Without Project Final Hydraulic Analysis Report.* Tempe: Prepared for U.S. Army Corps of Engineers Los Angeles District: Contract Number DACW09-00-D-0021.

WEST Consultants, Inc. (2011). *Sediment Transport Tool: Sediment Transport Model Comparison.* Phoenix: Flood Control District of Maricopa County.

WEST Consultants, Inc. (2012). *Tres Rios North Levee Floodplain and Floodway Re-Delineation Study: Salt and Gila Rivers, Maricopa County, Arizona.* Phoenix, AZ: Flood Control District of Maricopa County, FCD 2010C027 WA6.

WEST Consultants, Inc. (2015). *Lower Salt River Floodplain Delineation Study.* Phoenix, AZ: Flood Control District of Maricopa County, FCD 2013C013.

Wood, Patel and Associates. (1997). *Maryvale Area Drainage Master Study.* Phoenix, AZ: Flood Control District of Maricopa County, FCD 93-29.

Appendix A

Date Collection Report

(included in DVD)

Appendix B

As-Built Drawings

(included in DVD)

Appendix C

CHECKRAS Results

(included in DVD)

Appendix D

General Correspondence

(included in DVD)

Appendix E

Comments and Responses

(included in DVD)